STUDY OF THE MITOCHONDRIA AS A NEW THERAPEUTIC TARGET AGAINST HEAD AND NECK CANCER: EVALUATION OF MELATONIN EFFECTS

RESEARCH GROUP CTS-101: INTERCELULAR COMUNICATION

BIOTECHNOLOGY INSTITUTE

CENTRO DE INVESTIGACIÓN BIOMÉDICA (CIBM)

PARQUE TECNOLÓGICO DE CIENCIAS DE LA SALUD

DEPARTAMENT OF PHYSIOLOGY

FACULTY OF MEDICINE, UNIVERSITY OF GRANADA

Biomedicine doctoral programme

Under the supervision of Dr. GERMAINE ESCAMES ROSA

JAVIER FLORIDO RUIZ

2022

Editor: Universidad de Granada. Tesis Doctorales
Autor: Javier Florido Ruiz
ISBN: 978-84-1117-690-3
URI: https://hdl.handle.net/10481/80009

This Doctoral Thesis work has been carried out in the Research Group CTS-101: Intercellular Communication, of the Institute of Biotechnology, at the Centro de Investigacion Biomédica (CIBM) of the University of Granada.

During the realization of the following work, the graduate Javier Florido Ruiz was financed by the following contracts:

- **Type:** FPU Contract, Ministry of Science and Innovation, Spain**.** Full time: 31/10/2017-30/03/2022.
- **Organismo.** Universidad de Granada.
- **Centro:** Centro de Investigación Biomédica y Facultad de Medicina.
- **Departamento:** Physiology.

Some of the results presented in this Doctoral Thesis have been published in international journals:

Florido J, Martínez-Ruiz L, Rodriguez-Santana C, López-Rodríguez A, Hidalgo-Gutierrez A, Cottet-Rousselle C, Lamarche F, Schlattner U, Guerra-Librero A, Aranda-Martínez P, López LC, Escames G. Melatonin drives apoptosis in head and neck cancer by increasing mitochondrial ROS generated via reverse electron transport. Journal of Pineal Research. 2022, doi: 10.1111/jpi.12824.

Oher publications:

Florido J, Rodríguez-Santana C, Martínez-Ruiz L, López-Rodríguez A, Acuña-Castroviejo D, Rusanova I, Escames G. Understanding the Mechanism of Action of Melatonin, Which Induces ROS Production in Cancer Cells. Antioxidants. 2022, doi: 10.3390/antiox11081621.

López-Armas GC, Yessenbekova A, González-Castañeda RE, Arellano-Arteaga KJ, Guerra-Librero A, Ablaikhanova N, Florido J, Escames G, Acuña-Castroviejo D, Rusanova I. Role of c-miR-21, c-miR-126, Redox Status, and Inflammatory Conditions as Potential Predictors of Vascular Damage in T2DM Patients. Antioxidants. 2022, doi: 10.3390/antiox11091675.

Fernandez-Ortiz M, Sayed RKA, Roman-Montoya Y, de Lama MA, Fernandez-Martinez J, Ramirez-Casas Y, Florido-Ruiz J, Rusanova I, Escames G, Acuña-Castroviejo D. Age and Chronodisruption in Mouse Heart: Effect of the NLRP3 Inflammasome and Melatonin Therapy. International Journal of Molecular Sciences. 2022, doi: 10.3390/ijms23126846.

Guerra-Librero A, Fernandez-Gil BI, Florido J, Martínez-Ruiz L, García-López S, Rodríguez-Santana C, Shen YQ, García-Verdugo JM, López-Rodríguez A, Rusanova I, Quiñones-Hinojosa A, Acuña-Castroviejo D, Marruecos J, De Haro T, Escames G. Melatonin targets metabolism in head and neck cancer cells by regulating mitocondrial structure and function. Antioxidants. 2021, doi: 10.3390/antiox10040603

Acuña-Fernández C, Marín J, Díaz-Casado ME, Rusanova I, Darias-Delbey B, Pérez-Guillama L, Florido-Ruiz J, Acuña-Castroviejo D. Daily Changes in The Expression of Clock Genes in Sepsis and Their Relation with Sepsis Outcome and Urinary Excretion of 6-Sulfatoximelatonin.Shock. 2020, doi: 10.1097/SHK.0000000000001433.

Rusanova I, Martínez-Ruiz L, Florido J, Rodríguez-Santana C, Guerra-Librero A, Acuña-Castroviejo D, Escames G. Protective effects of melatonin on the skin: future perspectives. International Journal of Molecular Sciences. 2019, doi: 10.3390/ijms20194948

Fernandez-Gil BI, Guerra-Librero A, Shen YQ, Florido J, Martínez-Ruiz L, García-López S, Adan C, Rodríguez-Santana C, Acuña-Castroviejo D, Quinones A, Fernández-Martínez J, Abdel Moneim AE, Lopez LC, Rodriguez-Ferrer JM, Escames G. Melatonin enhances cisplatin and radiation cytoxicity in head and neck squamous cell carcinoma by stimulating mitochondrial ROS generation, apoptosis and autophagy. Oxidative Medicine and Cellular Longevity. 2019, doi: 10.1155/2019/7187128

Shen YQ, Guerra-Librero A, Fernandez-Gil BI, Florido J, García-López S, Martínez-Ruiz L, Mendivil-Perez M, Soto-Mercado V, Acuña-Castroviejo D, Ortega-Arellano H, Carriel V, Díaz-Casado ME, Reiter RJ, Rusanova I, Nieto A, López LC, Escames G, Combination of melatonin and rapamycin for head and neck cancer therapy: Suppression of AKT/mTOR pathway activation, and activation of mitophagy and apoptosis via mitochondrial function regulation. J Pineal Res., 2018, doi: 10.1111/jpi.12461

Mendivil-Perez M, Soto-Mercado V, Guerra-Librero A, Fernandez-Gil BI, Florido J, Shen YQ, Tejada MA, Capilla-Gonzalez V, Rusanova I, Garcia-Verdugo JM, Acuña-Castroviejo D, López LC, Velez-Pardo C, Jimenez-Del-Rio M, Ferrer JM, Escames G. Melatonin enhances neural stem cell differentiation and engraftment by increasing mitochondrial function. J Pineal Res., 2017, doi: 10.1111/jpi.12415

Fernandez-Gil BI, Abdel Moneim AE, Ortiz F, Shen YQ, Soto-Mercado V, Mendivil-Perez M, Guerra-Librero A, Acuña-Castroviejo D, Molina-Navarro MM, Garcia-Verdugo JM, Sayed RKA, Florido J, Luna JD, López LC, Escames G. Melatonin protects rats from radiotherapy-induced small intestine toxicity. PONE, 2017, doi: 10.1371/journal.pone.0174474

Abdel Moneim AE, Guerra-Librero A, Florido J, Shen YQ, Fernandez-Gil BI, Acuña-Castroviejo D, Escames G, Oral mucositis: Melatonin gel an effective new treatment. International Journal of Molecular Sciences 2014, doi: 10.3390/ijms18051003

Cardinali D, Escames G, Acuña-Castroviejo D, Ortiz F, Fernandez-Gil BI, Guerra-Librero A, García-López S, Shen YQ, Florido J. Melatonin-Induced Oncostasis, Mechanisms and

Clinical Relevance Journal of Integrative Oncology, 2016, doi: 10.4172/2329-6771.S1-006

Participation in research projects:

Name of the project: Conexión entre desincronización de los genes reloj y disfunción mitocondrial en la resistencia a la quimioterapia: evaluación de los efectos de la melatonina. **Reference:** SAF2017-85903-P. **Principal Investigator:** Germaine Escames. **Agency:** Ministerio de Economía y Hacienda. **Date:** 01/01/2018 - 31/12/2020. **Founds:** 108.900 €

Name of the project: Estudio del mecanismo de acción oncostático de la melatonina a nivel mitocondrial: implicación de la vía AMPK, del poro de transición mitocondrial y del potencial de membrana. **Reference:** PPJIB2019-13. **Principal Investigator:** Javier Florido. **Agency:** Vicerrectorado de Investigación y transferencia. Universidad de Granada. **Date:** 01/05/2020 - 30/04/2021. **Founds:** 1.500 €

Name of the project: Estudio preclínico de diferentes formulaciones de melatonina dirigidas a reducir la resistencia a la quimioterapia asociada a la función mitocondrial. **Reference:** B-CTS-071-UGR18. **Principal Investigator:** Germaine Escames. **Agency:** Consejeria de Economía, innovación y ciencia. Junta de Andalucía. **Date:** 01/01/2020 - 31/12/2021. **Founds:** 25.400 €

Name of the project: Nueva estrategia terapéutica para evitar la resistencia a la quimio y/o radioterapia asociada a la función mitocondrial: evaluación de diferentes formulaciones de melatonina. **Reference:** P18-RT-3222. **Principal Investigator:** Germaine Escames. **Agency:** Consejería de conocimiento, investigación y universidad. Junta de Andalucía. **Date:** 01/01/2020 - 31/12/2022. **Founds:** 119.652 €

Contributions to conferences related to this Doctoral Thesis:

Orals Communications

II congreso de Investigación PTS. Nueva estrategia terapéutica para evitar la resistencia a la quimioterapia asociada a la función mitocondrial. 2022. Granada (Spain). Alba López-Rodríguez; Alejandro Fábrega-Puentes; César Rodríguez-Santana; Laura Martínez-Ruiz; **Javier Florido**; Andrés Oliver-Ramirez; Germaine Escames.

Jornadas Científicas anual CIBERFES 2021. Cáncer y envejecimiento: función mitocondrial y desincronización de los genes reloj. 2021. Madrid (Spain). **Javier Florido**; Germaine Escames.

21st International Conference on Oxidative Stress Reduction, Redox Homeostasis and Antioxidants- Paris Redox 2019. New formulations of melatonin to induce oxidative stress and cell death xenografts of head and neck cancer cells. 2019. Paris (France). Laura Martínez Ruiz; **Javier Florido;** César Rodríguez Santana; Ana Guerra-Librero; Jorge García Checa; Germaine Escames.

I Jornadas Científicas del Centro de Investigación Biomedica. Combination of melatonin and rapamycin as a potential therapeutic strategy for head and neck cancer: melatonin protects normal cells from rapamycin associated toxicity but acts as a prooxidant agent inducing cancer cells apoptosis. 2017. Granada (Spain). Ying-Qiang Shen; Ana Guerra-Librero; Beatriz Irene Fernández Gil; **Javier Florido**; Laura Martínez Ruiz; Héctor F Ortega Arellano; Germaine Escames.

I Jornadas Científicas del Centro de Investigación Biomedica. Enhancement of chemotherapy by high melatonin concentration in Head and Neck Cancer Cells. 2017. Granada (Spain). **Javier Florido**; Beatriz Irene Fernandez Gil; Ana Guerra-Librero; Ying-Qiang Shen; Laura Martínez Ruiz; Sergio García López; Miguel Ángel Mendívil Pérez; Viviana M Soto; Darío Acuña Castroviejo; Germaine Escames.

I Jornadas Científicas del Centro de Investigación Biomedica. Metabolic switch produced by melatonin at high concentration induces apoptosis in cancer. 2017. Granada (Spain). Ana Guerra-Librero; Beatriz Irene Fernández Gil; **Javier Florido**; Ying-Qiang Shen; Laura Martínez Ruiz; Sergio García López; María Micaela Molina-Navarro; José Manuel García-Verdugo; Darío Acuña-Castroviejo; Germaine Escames

I Jornadas Científicas del Centro de Investigación Biomedica. Toxicity of radiotherapy is enhanced by high concentration of melatonin in Head and Neck Cancer Cells. 2017. Granada (Spain). Beatriz Irene Fernández Gil; Ana Guerra-Librero; Ying-Qiang Shen; **Javier Florido**; Ramy K Sayed; Miguel Ángel Mendívil Pérez; Viviana M Soto; Laura Martínez Ruiz; Christian Adán; Manuel González Díez; Darío Acuña Castroviejo; Germaine Escames

IV Workshop de Jóvenes Biotecnólogos. Enhancement of radio- and chemotherapy by high melatonin concentration in head and neck cancer. 2017. Granada (Spain). **Javier**

Florido; Beatriz I Fernández Gil; Ana Guerra-Librero; Ying-Qiang Shen; Laura Martínez Ruiz; Sergio García López; Ramy K Sayed; Miguel Mendívil Pérez; Viviana Soto-Mercado; Manuel González Díez; Darío Acuña Castroviejo; Germaine Escames.

IV Workshop de Jóvenes Biotecnólogos. Metabolic switch produced by melatonin at high concentration induces apoptosis in cancer. 2017. Granada (Spain). Ana Guerra-Librero; Beatriz I Fernández Gil; Sergio García López; Ying-Qiang Shen; **Javier Florido**; Laura Martínez Ruiz; Ramy K Sayed; María Micaela Molina-Navarro; José Manuel García-Verdugo; Manuel González Díez; Luis Carlos López; Darío Acuña-Castroviejo; Germaine Escames.

III Congreso de Estudiantes de Investigación Biosanitaria. Efecto de la melatonina en ratones tratados con quimio-radioterapia. 2017. Granada (Spain). Christian Adán; Ana Guerra-Librero; Beatriz I Fernández Gil; **Javier Florido**; Laura Martínez Ruiz; Manuel González Díez; Ramy K Sayed; Germaine Escames.

7th European Conference on Head and Neck Oncology (ECHNO). High concentration of melatonin potentiates the toxicity of irradiation in head and neck cancer cells. 2016. Budapest (Hungary). Beatriz I Fernández Gil; Ana Guerra-Librero; Ying-Qiang Shen; Sergio García López; **Javier Florido**; Manuel González Díez; Darío Acuña-Castroviejo; José Expósito Hernández; Isabel Tovar-Martin; Germaine Escames.

7th European Conference on Head and Neck Oncology (ECHNO). Efficacy of a New Pharmaceutical Formulation of Melatonin in Preventing Radiotherapy-Induced Mucositis. 2016. Budapest (Hungary). Germaine Escames, Francisco Ortiz, Beatriz Irene Fernández Gil, Ana Guerra-Librero, Ying-Qiang Shen, Sergio García López, **Javier Florido**, Manuel González Díez, Darío Acuña Castroviejo, José Expósito Hernández, Isabel Tovar Martín, Antonio Martínez Única.

The 2016 Controlling Cancer Summit. Efficacy of a new pharmaceutical formulation of melatonin in preventing radiotherapy-induced mucositis. 2016. London (United Kingdom). Germaine Escames; Francis Ortiz; Ying Q Shen; Beatriz I Fernández Gil; Ana Guerra-Librero; Sergio García López; **Javier Florido**; Manuel González Diez; Darío Acuña Castroviejo.

The 2016 Controlling Cancer Summit. High concentration of melatonin potentiates the toxicity of radio- and chemotherapy in Head and Neck Cancer Cells in culture and in vivo. 2016. London (United Kingdom). Beatriz I Fernández Gil; Ana Guerra-Librero; Ying Q

Shen; Sergio García López; **Javier Florido**; Manuel González Diez; Ramy K Sayed; Luis Carlos López; Darío Acuña Castroviejo; Germaine Escames.

The 2016 Controlling Cancer Summit. Oncostatic effects of melatonin: role of mitochondrial function. 2016. London (United Kingdom). Ana Guerra-Librero; Beatriz I Fernández Gil; Sergio García López; Ying Q Shen; **Javier Florido**; Ramy K Sayed; Micaela Molina Navarro; José Manuel García Verdugo; Manuel González Diez; Luis Carlos López; Darío Acuña Castroviejo; Germaine Escames.

Posters

IV Congreso nacional jóvenes investigadores en biomedicina. Melatonin induces anti-cancer effects by targetin respiratory chain complexes in Head and Neck cancer cells. Granada (Spain). **Javier Florido**; Cesar Rodriguez-Santana; Laura Martinez Ruiz; Alba López-Rodríguez; Ana Guerra-Librero; Uwe Schlattner; Germaine Escames.

IV Congreso nacional jóvenes investigadores en biomedicina. New formulation of melatonin supresses head and neck cancer growth via induction of ROS. 2022. Granada (Spain). Laura Martinez Ruiz; **Javier Florido**; Cesar Rodriguez-Santana; Alba López-Rodríguez; Ana Guerra-Librero; Beatriz I. Fernandez-Gil; Victor S. Carriel; David Sanches-Porras; Germaine Escames.

IV Congreso nacional jóvenes investigadores en biomedicina. The uncopling of the mitochondria induces an alteration of apoptosis and necrosis in head and neck cancer cells. Granada (Spain). Cesar Rodriguez-Santana; Laura Martinez Ruiz; **Javier Florido**; Alba López-Rodríguez; Ana Guerra-Librero; Nazzareno Capitanio; Germaine Escames.

II congreso de Investigación PTS. Evaluación de los efectos de la melatonina sobre los diferentes componentes de la cadena de transporte electrónico y fosforilación oxidativa en células HNSCC. 2022. Granada (Spain). **Javier Florido**; César Rodríguez-Santana; Laura Martínez-Ruiz; Alba López-Rodríguez; Alejandro Fábrega-Puentes; Alberto Jesús Medina Martínez; Ana Guerra-Librero; Germaine Escames.

21st International Conference on Oxidative Stress Reduction, Redox Homeostasis and Antioxidants- Paris Redox 2019. Melatonin induces apoptosis in head and neck squamous cell carcinoma by increasing mitochondrial function. 2019. Paris (France). **Javier Florido**; César Rodríguez Santana; Laura Martínez Ruiz; Ana Guerra-Librero; Jorge García Checa; Germaine Escames.

21st International Conference on Oxidative Stress Reduction, Redox Homeostasis and Antioxidants- Paris Redox 2019. The uncoupling of the mitochondria induce an alteration of apoptosis and necrosis in head and neck cancer cells. 2019. Paris (France). César Rodríguez Santana; Laura Martínez Ruiz; **Javier Florido**; Ana Guerra-Librero; Jorge García Checa; Germaine Escames.

6th International Conference on Innovative Approaches in Head and Neck Oncology (ICHNO). Effects of melatonin oral gel to prevent radiation-induced mucositis model in rat. 2017. Barcelona (Spain). Germaine Escames; C Tarrago; Francisco Ortiz; Beatriz I Fernández-Gil; N Lluch; Ana Guerra-Librero; Ying-Qiang Shen; **Javier Florido**; Darío Acuña-Castroviejo; R Bosser.

6th International Conference on Innovative Approaches in Head and Neck Oncology (ICHNO). Melatonin enhances the toxicity of radio- and chemotherapy in head and neck cancer cells. 2017. Barcelona (Spain). Germaine Escames; Beatriz I Fernández-Gil; Ana Guerra-Librero; Ying-Qiang Shen; Sergio García-López; **Javier Florido**; Ramy K Sayed; Darío Acuña-Castroviejo; José Expósito-Hernández.

6th International Conference on Innovative Approaches in Head and Neck Oncology (ICHNO). Melatonin gel protects the mitochondria from radiation damage preventing mucositis. 2017. Barcelona (Spain). Germaine Escames; Francisco Ortiz; Beatriz I Fernández-Gil; Ana Guerra-Librero; Ying-Qiang Shen; **Javier Florido**; Darío Acuña-Castroviejo.

Translational research in cancer cell metabolism. Metabolic switch produced by melatonin in head and neck cancer cells. 2016. Bilbao (Spain). Ana Guerra-Librero; Beatriz I Fernández Gil; Sergio García López; Ying-Qiang Shen; **Javier Florido**; Ramy K Sayed; María Micaela Molina-Navarro; José Manuel García-Verdugo; Manuel González Díez; Luis Carlos López; Darío Acuña-Castroviejo; Isabel Tovar; Germaine Escames.

7th European Conference on Head and Neck Oncology (ECHNO). High concentration of melatonin potentiates the toxicity of irradiation in head and neck cancer cells. 2016. Budapest (Hungary). E-poster seleccionado entre los 7 mejores de 243. Beatriz I Fernández Gil; Ana Guerra-Librero; Ying-Qiang Shen; Sergio García López; **Javier Florido**; Manuel González Díez; Darío Acuña-Castroviejo; José Expósito Hernández; Isabel Tovar-Martin; Germaine Escames.

XI Reunión del Grupo Español de Investigación en Radicales Libres. Melatonin at high concentration enhances the toxicity of radio- and chemotherapy in tongue cancer cells. 2016. Granada (Spain). Beatriz I Fernández Gil; Ying-Qiang Shen**;** Ana Guerra-Librero; **Javier Florido**; Miguel Mendívil Pérez; Viviana Soto-Mercado; Ramy K Sayed; Manuel González Díez; Darío Acuña-Castroviejo; Germaine Escames.

Patents related to this Doctoral Thesis:

Escames-Rosa G, Acuña-Castroviejo D, Guerra-Librero A, Fernández-Gil BI, Florido-Ruiz J. Uso de melatonina para el tratamiento de tumores. *ES.* Identifier: WO/2018/178497. Date: 04/10/2018

ACKNOWLEDGEMENT

Difícilmente podré agradecer con tan pocas palabras todo el cariño y ayuda recibida durante esta etapa que tanto me han hecho crecer a nivel profesional y personalmente. Para mí la tesis doctoral ha sido un camino constante de aprendizaje de la que he ido de vuestra mano tanto en los buenos como en los malos momentos, así que por todo ello GRACIAS.

En primer lugar, agradecer a mi directora y guía de mi Tesis Doctoral, primero por darme la oportunidad de entrar en su grupo de investigación desde que estaba en cuarto de carrera, ya que esta fue mi primera experiencia investigadora y, por la cual, me hayo realizando esta emocionante carrera profesional. Germaine es quien me ha inculcado el espíritu y criterio científico y, sobretodo, las ganas de hacer verdadera ciencia y de saber que, con esfuerzo, todo se consigue. Además, no solo he aprendido con ella a nivel científico, si no también a nivel personal, convirtiendo el laboratorio en una gran familia científica en la que todos nos cuidamos. Gracias por enseñarme tanto.

A Darío, por esa disposición y ganas de enseñar y transmitir todo ese conocimiento científico que posee. Creo que no sólo yo, pero todos los miembros del CTS-101 tenemos mucho que agradecerle por conseguir haber potenciado a este grupo hasta el nivel que ha alcanzado.

A Ana, por enseñarme desde el primer día que llegue al laboratorio de ciencia y, sobretodo, de la vida. Gracias por enseñarme desde 0, cuando aun no sabia ni lo que era pipetear agua. Gracias por esa paciencia de la que a veces te desquiciaba. También gracias por los tantos momentos vividos fuera y dentro del laboratorio, por esas risas, confidencias, viajes, fiestas y congresos. Gracias por tu apoyo y, sobretodo, tus super-consejos.

A Laura. Eres el mejor ejemplo de que el aprendiz puede superar al maestro. Recuerdo haber empezado enseñándote, pero no recuerdo el momento exacto en el que te convertiste en esa super investigadora. Eres para mí, mi mayor orgullo. Juntos hemos aprendido todo lo que sabemos dentro del laboratorio, pero, sobre todo, hemos aprendido a ser compañeros, humanos y sobretodo amigos. Gracias por ser como eres. Sigue así que se que llegaras muy lejos y allí estaré para verlo.

A César. Gracias por alegrarme los días en el laboratorio. Gracias por esa picaresca canaria graciosa que tanto te caracteriza. Juntos hemos aprendido a escuchar, a comprender y a empatizar. Muchos han sido los buenos momentos que hemos pasados y las muchas risas que han hecho alegrar esta etapa de nuestra vida. Gracias por tu alegría.

A Alba, la peque del laboratorio. Entraste dando alegría al laboratorio y desde el primer minuto con ganas de aprender y de que te enseñásemos todo lo que sabemos. Creo que eres la persona con la que mas he reído en la vida. Incluso en los momentos mas duro de la tesis has sido el rayito de luz en los días nublados. Se que aun tienes mucho mas que dar, pero también se que eres súper inteligente y la mas luchadora que nadie (aunque a veces no te lo quieras creer). No tengo dudas de que conseguirás todo lo que te propongas.

Al resto del CaCe Team, que, aunque ya os hayáis ido seguís formando parte de esta bonita historia. A Bea, por tratarme como a su hermano menor desde que llegué al laboratorio. Por enseñarme, escucharme y también espabilarme. Por sus muchos consejos y las muchas horas que pasamos tanto dentro como fuera del laboratorio. A Ying, Sergio, Alberto, Erika, María, Natalia, Claudia y Andrés, gracias por que también

vosotros me habéis ayudado en esta etapa. No solo por los buenos momentos si no porque de vosotros he aprendido que los alumnos tienen mucho que enseñar.

Al resto del CTS-101. A Paula, separados al nacer. Gran compañera de este viaje llamado Tesis. Muchas gracias por estar ahí siempre, en los buenos y en los malos momentos; en las risas, pero también en los lloros; en las peleas, pero también en las reconciliaciones; en viajes, en ferias, en los bailes hasta el suelo, en TODO. Sin ti esta etapa no tendría nada que ver. Muchas gracias amiga. A Agus, el chamán. Muchas gracias por ser mi guía científico, y personal. Gracias por siempre tener algo inteligente y racional que decir. Gracias, por tantas noches de confesiones y por los tan buenos momentos y experiencias vividas juntos. A Jose y a Fernández, gracias por enseñarme que en la vida esta el día y la noche. Gracias por tu cordura pero también, por tu locura. Gracias por alegrarnos los días con tus bromas, pero también por saber escuchar. Gracias por ser Jose y a la vez Fernández. A Eli, por ser la "mami" del grupo, la que mas nos cuida y se preocupa por nosotros. Por que, aunque no le guste salir mucho, siempre estará en lo que necesitemos. Gracias por ser la vez tan racional, inteligente y, sobre todo, tan buena. A Julia, por transmitirme sus ganas de disfrutar de la vida, de que la vida no se vive en 2X si no en 1X. Por enseñarme a sacar lo mejor de cada momento, por sus risas, sus consejos y por, aunque no le gusta demostrarlo mucho, preocuparse siempre tanto por cada uno de nosotros. A Sergio, pues no sé bueno, por la gracia natural que tiene y ser el mas apañado, no del laboratorio si no del universo. A Yoli, por ser tan natural como la vida misma. Por su gracia, su simpatía y la facilidad que tienes de alegrar los días. A Iryna, por sus sabios consejos dentro del laboratorio de cómo funciona un laboratorio. Y sobre todo por nuestros bailes que tanto nos gustan y que

casi siempre tenga algo bonito que decirte. A Luis Carlos, por prestar su ayuda y conocimiento. A Elena, Laura, Sara, Juanma, por ser como nuestros hermanos mayores dentro del laboratorio a los que acudir cuando tenemos dudas. En definitiva, a esta gran familia llamada CTS-101: los magníficos.

A todos los compañeros del CIBM o que me han acompañado a hacer ciencia durante esta etapa predoctoral. Gracias a Chufy, por ser no solo mi amigo desde la carrera, si no el mejor compañero de piso del mundo. Gracias por ayudarme, por aconsejarme, por animarme, por esas comidas, esas noches de pelis, juegos, fiestas, por las múltiples confesiones y por esa confianza y complicidad tan bonita que tenemos. Polos opuestos se complementan y esa es la sensación que tengo siempre contigo. Muchas gracias por todo lo que hemos vivido y por lo que nos queda. Gracias a Laura Hidalgo, por emprender esta etapa conmigo tanto en el laboratorio como fuera de el. Gracias por tus risas, porque, aunque estés agobiada y estresada (casi siempre) siempre sacas un hueco para compartir conmigo. Gracias a Teresa, Antoñito, Mari y Patri por no solo por la cantidad de material de laboratorio que nos prestáis, si no también por lo divertidos y lo bien que me lo paso con vosotros.

También quiero agradecer al Dr. Schlattner y a su Grupo por darme la oportunidad de formarme allí durante unos meses.

Gracias a Everybody, Bioquímicos, Marina y cada uno de mis amigos que me han aguatado durante estos años. Gracias por animarme a seguir siempre dando un paso hacia delante y nunca hacia detrás. Sois la familia que se elige y eso no lo cambio por nada del mundo. Muchas gracias por ser como sois.

Por último, y mas importante, gracias a mi familia. Gracias a mis padres por animarme a ser lo que he querido ser desde que pude decidir. Gracias por inculcarme el

espíritu de sacrificio y constancia en los estudios y por los que ahora puedo estar escribiendo esta Tesis. Gracias por animarme apoyarme en este camino académico/científico tanto económico como personalmente. Gracias por crear el hogar al que pertenezco y gracias por el orgullo que tenéis hacia mi. Que sepáis que también es mutuo. Gracias a mi hermana por acompañarme en esta etapa llamada vida. Contigo he vivido todo lo que se y recuerdo. Gracias por haber podido contar contigo siempre para lo bueno y lo malo, gracias por escucharme, apoyarme, sacarme sonrisas, momentos únicos y por las infinitas cosas que no cabrían en esta tesis. Muchas gracias por ser como eres, esa bellísima persona y hermana.

ABBREVIATIONS

Δψm: mitochondrial membrane potential

Δp: proton motive force

AANAT: arylalkylamine N-acetyltransferase

ACC: Acetyl-CoA carboxylase

AFMK: N1-acetyl-N2-formyl-5-methoxykynurenamine

Akt: protein kinase B

AMK: N-acetyl-5-methoxykinurenamine

AMPK: Adenosine monophosphate protein kinase

aMT: 5 methoxy-N-acetyltryptamine, melatonin

Ant A: antimycin A

AOX: alternative oxidase

ASMT: N-acetylserotonin O-methyltransferase

ATP: Adenosine triphosphate

ADP: Adenosine diphosphate

BNGE: Blue native gel electrophoresis

c3OHM: cyclic 3-hydroxymelatonin

CI-V: Complex I-V

CB: carotid body

CIC: Scientific Instrumentation Center

CoQ: Coenzyme Q

CsA: cyclosporin A

DCF: 2',7'-dichlorofluorescein

DCFA: Dichlorodihydrofluorescein diacetate

DNA: Deoxyribonucleic acid

EHHADH: enoyl-CoA hydratase and 3-hydroxyacyl CoA dehydrogenase;

ETS: electron transfer system

FAD: Flavin adenine dinucleotide

FACS: Fluorescence-activated cell sorting

FAO: fatty acid oxidation

FCCP: Trifluorocarbonylcyanide Phenylhydrazone

FMN: flavin mononucleotide

G-6-PDH: glucose-6-phosphate dehydrogenase

GPx: glutatione peroxidase

GRd: glutathione reductase

GSH: reduced glutathione

GSSG: oxidized glutathione

HIF-1α: hypoxia-inducible factor-1α

HNC: Head and neck cancer

HNSCC: Head and neck squamous cell carcinoma

IQ: Q-binding site

IR: ischemia reperfusion

KCN: Potassium cyanide

Malo: malonate

MCAD: medium-chain acyl-CoA dehydrogenase

mPTP: mitochondrial permeability transition pore

mtDNA: mitochondrial DNA

mtROS: mitochondrial ROS

NAC: N-acetylcysteine

NAD/NADH: nicotinamide adenine dinucleotide

nDNA: nuclear DNA

NFκB: nuclear factor kappa light chain enhancer of activated B cells

OCR: Oxygen consumption rate

OXPHOS: Oxidative phosphorylation system

PACC: Phosphorylated ACC

PAMPK: Phosphorylated AMPK

PI3K: phosphatidylinositol 3-kinases

PKM2: pyruvate kinase M2

PPP: pentose phosphate pathway

QH·: Semiquinone

RET: reverse electron transport

RIRR: ROS-induced ROS release

RNA: ribonucleic acid

ROS: Reactive oxygen species

Rot: rotenone

rRNA: ribosomal RNA

SC: sumpercomplex

SOD: superoxide dismutase

TCA: tricarboxylic acid cycle

TME: tumour microenvironment

TMRE: tetramethylrhodamine ethyl ester

TTFA: 2-thenoyltrifluoroacetone

tRNA: transfer RNA

UCP: uncoupling protein

UPLC-MS/MS: ultraperformance liquid chromatography with tandem mass spectrometry

VDAC: Voltage-dependent anionic channel

VEGF: vascular endothelial growth factor

“Somewhere,
something incredible is waiting to be known.”

Carl Sagan

A mi familia

RESUMEN

Resumen

El carcinoma de células escamosas de cabeza y cuello (HNSCC) es uno de los cánceres más comunes a nivel mundial. Sin embargo, a pesar de los avances realizados en cuanto a tratamientos y técnicas de diagnóstico, la tasa de supervivencia continúa siendo del 50%. Una de las principales causas es la resistencia que acaban desarrollando los pacientes a los tratamientos ya existentes, lo que conlleva a un elevado porcentaje de recaídas. Por ello, sigue siendo necesaria la búsqueda de nuevos fármacos y dianas terapéuticas que potencien los efectos de los tratamientos ya existentes y reduzcan sus efectos adversos.

Una posible diana terapéutica serían las especies reactivas de oxígeno (ROS), un grupo de moléculas altamente reactivas que actúan en distintas rutas de señalización en las células sanas y que, a su vez, están implicadas en el desarrollo de ciertas patologías como el cáncer. En este sentido, las células tumorales presentan un balance redox alterado en comparación con las células normales. Por tanto, una posible estrategia antitumoral sería aumentar directamente los niveles de ROS, así como disminuir la capacidad antioxidante de las propias células tumorales, induciendo la muerte celular programada.

En este ámbito es donde destaca la melatonina ya que, además de poseer importantes propiedades oncostáticas, numerosos estudios han demostrado su capacidad para regular la producción de ROS, tanto en células sanas como en tumorales. En este sentido, se ha demostrado que la melatonina tiene un efecto dual, disminuyendo el estrés oxidativo en las células sanas y aumentándolo en las células tumorales. Sin embargo, aunque se conoce el mecanismo de acción de la melatonina para disminuir los ROS en las células sanas, al día de hoy se desconoce el mecanismo de

esta molécula para ejercer un efecto pro-oxidante en las células tumorales, lo que dificulta su uso como tratamiento oncostático.

Por tanto, el objetivo de este trabajo fue dilucidar el mecanismo de acción de la melatonina para inducir la producción de ROS en células de cáncer de cabeza y cuello.

Para ello, analizamos los efectos de la melatonina en las líneas celulares HNSCC (Cal-27 y SCC-9) tratadas con melatonina a 0,5 y 1 mM. Además, comprobamos los efectos pro-oxidantes y pro-apoptóticos de la melatonina *in vivo*, en ratones *nude* atímicos con xenoinfertos de células Cal-27.

Medimos la producción de ROS mediante métodos fluorométricos y los niveles de apoptosis mediante citometría de flujo en las células HNSCC, en presencia de N-acetilcisteína (NAC) y de inhibidores mitocondriales. Se analizaron diferentes parámetros mitocondriales tales como expresión de OXPHOS por western blot, actividad de los complejos mitocondriales (CI-CV) por análisis espectrofotométricos, respiración mitocondrial por SeaHorse y con electrodo de oxígeno Clark y niveles de ATP mediante técnicas espectofotométricas. Asimismo, se estudiaron los niveles de CoQ por cromatografía líquida acoplada a espectrómetro de masas (UPLC-MS/MS), el potencial de membrana mitocondrial por métodos fluorimétricos y las expresiones de las UCPs por western blot. También realizamos un estudio de metabolómica mediante UPLC-MS/MS, así como un análisis de la conformación de los supercomplejos mitocondriales mediante electroforesis en gel nativo azul. Finalmente, comprobamos los efectos apoptóticos y pro-oxidantes de melatonina *in vitro* en las células Cal-27 que tenían inducida la expresión de la proteína oxidasa alternativa (AOX), mediante el uso de lentivirus, así como *in vivo* en xenotrasplantes con las células que sobreexpresan la

proteína AOX. Esta proteína evita la producción de ROS a través del transporte inverso de electrones (RET).

En este trabajo demostramos que la melatonina, al inducir el transporte inverso de electrones que conlleva a un aumento de los niveles de ROS, tiene un efecto pro-apoptótico en células de cáncer de cabeza y cuello. Concretamente, la melatonina indujo un cambio en el metabolismo tumoral y un aumento de la actividad mitocondrial, provocando, en dichas células tumorales, un aumento de los niveles de ROS inducido por un desacoplamiento del sistema de transporte electrónico y de la fosforilación oxidativa. Sorprendentemente, los distintos inhibidores de los complejos mitocondriales, incluida la rotenona, bloquearon el efecto pro-oxidante de la melatonina, lo que indica que la melatonina aumenta los niveles de ROS a través del transporte inverso de electrones. En este sentido, la melatonina también aumentó el potencial de membrana y el coeficiente $CoQ_{10}H_2/CoQ_{10}$, que son dos condiciones imprescindibles para la generación de RET-ROS. Por último, demostramos que la manipulación genética de las células Cal-27 que expresan la oxidasa alternativa, la cual transfiere electrones de la coenzima QH_2 al oxígeno, inhibió la generación de ROS y apoptosis inducidos por el tratamiento con melatonina, destacando la importancia del RET como el causante de la producción de ROS. Estos resultados demuestran que la producción de RET-ROS es un factor crucial en los efectos de la melatonina en las células tumorales y establecen el efecto dual de la melatonina en la protección de las células normales y la inducción de la apoptosis en las células tumorales.

Nuestros resultados demuestran, por primera vez, que la melatonina a altas dosis induce un amento de los niveles de ROS, a través del transporte inverso de electrones, lo que conlleva a un aumento de la muerte celular programada en las células

Cal-27 y SCC-9. Por tanto, estos resultados dilucidan el mecanismo de acción pro-oxidante de la melatonina en células tumorales, lo que facilita su posible uso en futuras aplicaciones oncológicas.

SUMMARY

Summary

Head and neck squamous cell carcinoma (HNSCC) is one of the most common cancer by incidence worldwide. Despite therapeutic and diagnostic advances, survival rates are still only about 50%. Drug resistance and relapse are the principal limitations of clinical oncology for many patients. It is therefore crucial to find new therapeutic targets and drugs to enhance the cytotoxic effects of conventional treatments without potentiating the adverse effects.

Reactive oxygen species (ROS) constitute a group of highly reactive molecules that have involved as regulators of important signaling pathways, but they are also involved in some pathologies such as cancer. In this context, tumor cells have an altered redox balance compared to normal cells, which can be targeted as an antitumoral therapy by increasing ROS levels and by decreasing the capacity of the antioxidant system, leading to programmed cell death.

Regarding that, melatonin is of particular importance in the development of innovative cancer treatments due to the regulation of ROS production in both normal and cancer cells. It has been demonstrated that melatonin has a dual effect, reducing ROS production in normal cells but increasing them in tumoral cells. However, despite the antioxidant effect of melatonin in normal cells has been described, the pro-oxidant mechanism of action of melatonin in tumoral cells remains unclear, which has hindered its use in clinical treatments.

In the present study, we aimed to elucidate the mechanism of action of melatonin to induce ROS production in in head and neck squamous cancer cells.

We analyzed the effects of melatonin on HNSCC cell lines (Cal-27 and SCC-9), which were treated with 0.5 or 1mM melatonin. We further examined the potential effects of melatonin to induce ROS and apoptosis in Cal-27 xenograft mice.

We measured ROS production using fluorometric methods and apoptosis levels by flow cytometry in HNSCC cells alone or in presence of N-acetyl cysteine (NAC) and mitochondrial inhibitors. In addition, we analyzed some mitochondrial parameters, such as: OXPHOS expression by Western Blot, mitochondria complex (CI–CV) activity by spectrophotometric analysis, mitochondrial respiration by SeaHorse and with a Clark oxygen electrode, and ATP levels by spectrophotometric technics. Likewise, CoQ levels by liquid chromatography–mass spectrometer (UPLC-MS/MS), mitochondrial membrane potential by fluorimetric methods and UCPs expressions by western blot were studied. We also performed a metabolomics study by UPLC-MS/MS, as well as an analysis of mitochondrial supercomplexes conformation by blue native gel electrophoresis (BNGE). Finally, we tested melatonin pro-oxidant and apoptotic effects *in vivo* in Cal-27 expressing alternative oxidase (AOX) protein, which avoid reverse electron transport (RET) ROS production, and *in vivo* inducing Cal-27 wild type and Cal-27 expressing AOX xenograft mice.

We demonstrated that melatonin mediates apoptosis in head and neck cancer by driving mitochondrial reverse electron transport (RET) to induce ROS production. Melatonin-induced changes in tumoral metabolism and increased mitochondrial activity which, in turn, induced ROS-dependent mitochondrial uncoupling. Interestingly, mitochondrial complex inhibitors, including rotenone, abolished the ROS elevation indicating that melatonin increased ROS generation via RET. Melatonin also increased the membrane potential and $CoQ_{10}H_2/CoQ_{10}$ ratio to elevate mitochondrial ROS production, which are essential conditions for RET. We found that genetic manipulation of Cal-27 cells with alternative oxidase, which transfers electrons from QH_2 to oxygen, inhibited melatonin-induced ROS generation, and apoptosis, highlighting the

importance of RET as the site of ROS production. These results illustrate that RET and ROS production are crucial factors for melatonin's effects in cancer cells and establish the dual effect of melatonin, to protect normal cells and to induce apoptosis in cancer cells.

Our data show, for the first time, that melatonin induces ROS complex I RET and leads to apoptosis from excessive ROS production, only at high doses, in Cal-27 and SCC9 cells. This pathway clarifies the proposed mechanism of action of melatonin inducing ROS production in cancer cells in order to propose future anti-neoplastic clinical applications.

INDEX

INTRODUCTION

1. Head and neck cancer

Head and neck cancer (HNC) is the most common malignant neoplasm of the upper aerodigestive tract, and it is the sixth most common cancer worldwide, with more than 500,000 new cases each year and a 5-year survival rates fewer than 50% (Johnson et al. 2020; Pisani et al. 2020). This type of cancer develops in the craniofacial bones, as well as in the salivary glands, in the skin and in the mucous membranes of the oral cavity, in the oropharynx, larynx and hypopharynx (Leemans, Braakhuis, and Brakenhoff 2011). Principally, this kind of neoplasm develops squamous cell carcinomas, also called head and neck squamous cell carcinoma (HNSCC), which arise from the squamous cells located in the mucosal epithelium (Figure 1) (Pai and Westra 2009). This type of cancer has a higher incidence in men than in women, and it is more prevalent in the elderly people because it is associated with lifestyle habits, such as alcohol or tobacco consumption. However, recently, it has also increased in young people because HNC is also associated with infection by the human papilloma virus (Choe et al. 2021; Pezzuto et al. 2015). In addition, these types of tumors are characterized by local recurrences, distant metastases and second primary tumors (Leemans et al. 2011).

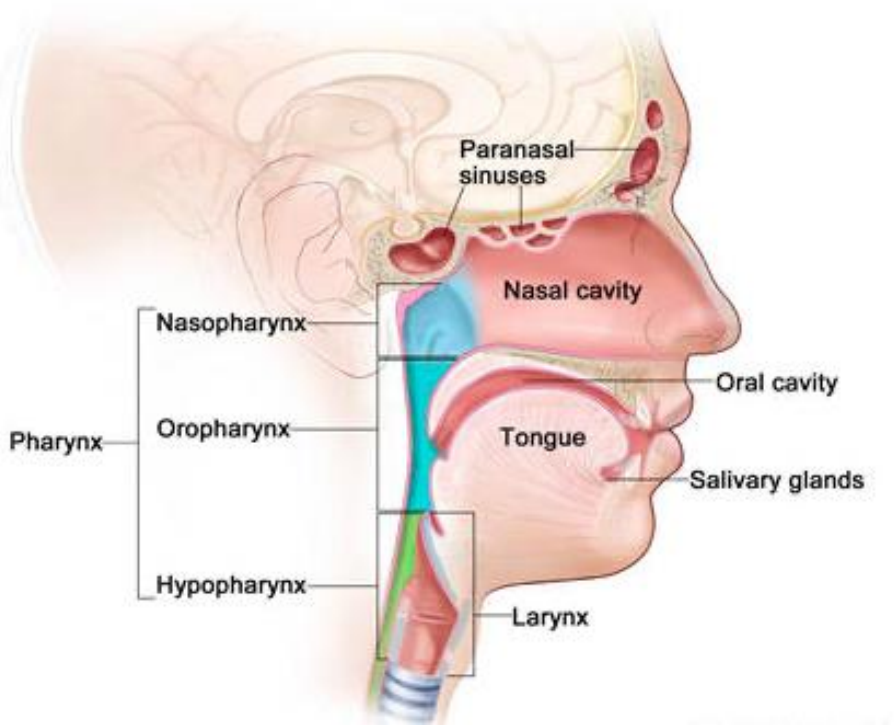

Figure 1. Head and neck regions. Illustrates location of paranasal sinuses, nasal cavity, oral cavity, tongue, salivary glands, larynx, and pharynx (including the nasopharynx, oropharynx, and hypopharynx). (https://www.cancer.gov/).

1.1 HNC treatments

HNC treatment is complex due to its large heterogeneity such as different location, etiology, molecular characteristic and clinical stage (Prystowsky 2015). From this perspective, at early stage, head and neck cancer is treated with local therapy, surgery, or radiation therapy. However, at advanced stage, it requires a combined therapy with surgery, radiation and chemotherapy (Puram and Bhattacharyya 2016), being the most used treatment the chemo- and radiotherapy combination (Pezzuto et al. 2015).

Surgery is used as standard treatment for HNSCC. However, to avoid damaging tissues, it is frequently limited by the anatomical extent of tumor (Argiris et al. 2008). Surgery remains the primary treatment strategy for head and neck cancers in oral cavity (Mody et al. 2021), which can be applied as a curative modality, at early stages, and as

a palliative treatment to reduce metastasis (Wang et al. 2018). Furthermore, developed in the early 2000s, TORS allows surgeons to use a surgical robot to view and access tumors in the head and neck without requiring any incisions through the neck, chin, or lip, which are typically needed in traditional open approaches (Mody et al. 2021).

Radiotherapy is an integral part of primary or adjuvant treatment in HNC. In the primary treatment setting, radiotherapy provides similar results to surgical resection in the treatment of certain early-stage head and neck cancers. For most locally advanced head and neck cancers, radiotherapy is a fundamental component of multimodality therapy and has a large variety of indications in the preoperative, primary, adjuvant, and palliative settings (Mody et al. 2021). Moreover, proton therapy represents a gradually emerging form of treatment that might have the potential to further improve outcomes for HNC patients. The major potential application of proton therapy is its role in re-irradiation for recurrent disease, resulting in an improvement of toxicity profile compared to traditional photon-based re-irradiation (Mody et al. 2021).

Regarding systemic therapy, in the past decade, the integration of immunotherapy into the management of head and neck cancers has substantially changed standard practices. Systemic therapies currently used in the treatment of head and neck cancers include cytotoxic chemotherapy, targeted therapies, and immunotherapy. For example, cisplatin-based regimen has long been a staple in the definitive management of locally advanced head and neck cancers, being the first-line treatment of choice for head and neck cancer (Mody et al. 2021). Cisplatin forms adducts with DNA, blocking the replication and transcription, thus exerting its cytotoxic effect (Tanida et al. 2012). On the other hand, the EGFR inhibitor, cetuximab, is gaining more importance as a new kind of treatment for HNC, considered its important role in the

tumorigenesis. Its combination also with other molecularly targeted agents (i.e., angiogenesis inhibitors) has surfaced as a novel strategy, whereas the combination of these novel agents with chemotherapy and radiotherapy is also under investigations (Argiris et al. 2008). However, given the results of a previous study (RTOG 1016), cetuximab is generally reserved for patients who are ineligible for cisplatin (Gillison et al. 2019).

1.2 Cancer treatment limitations

Despite the advances achieved in recent years, HNC treatments still have wide side effects:

- **Radiotherapy** is limited due to the resistance generated after continuous doses, and its side effects in healthy tissues adjacent to the tumor. Some examples of side effects are epidermitis and mucositis limiting the use of radiotherapy (Amable 2016; Maier et al. 2016).
- **Chemotherapy.** There are two main problems associated with cisplatin treatment: its toxicity and chemoresistance. The toxicity of the chemotherapy used generates numerous side effects since, being a systemic therapy, it not only acts on the tumor locally, but also affects many other organs, generating healthy tissue damage. In fact, its use is also associated with the appearance of mucositis. These side effects can be serious and even lead to treatment discontinuation in patients and, therefore, reducing treatment efficacy (Amable 2016).

The limitations of chemo and radiotherapy explain the poor prognosis and the low survival rate of patients with head and neck cancer. Moreover, a significant

proportion (69% of tumors of the oral cavity and pharynx and 45% of laryngeal carcinomas) are diagnosed at advanced stages (Mao et al. 2016). For all these reasons, HNC 5-year survival rates remain under 50%, being still necessary to develop new treatments or strategies that enhance the effects of existing treatments and reduce the side effects they produce or offer new therapeutic possibilities (Elicin et al. 2019; Johnson et al. 2020; Pisani et al. 2020; Rosenberg and Vokes 2021).

2. Mitochondria as a oncostatic target

Mitochondria are maternally inherited, cytoplasmic organelles that originated from symbiotic bacteria. They co-evolved with their host, such that most mitochondrial proteins are nuclear encoded. Mitochondria, however, retain a small 16Kb DNA genome (mtDNA) that encodes tRNAs (transfer RNA) and rRNAs (ribosomal RNA) and proteins essential for respiration. Cells have hundreds of mitochondria that can be wild type or can exist of mixtures of wild type and mutant forms, a state referred to as heteroplasmy (Zong, Rabinowitz, and White 2016). In healthy replicative eukaryotic cells, mitochondria regulate important cellular processes, such as proliferation, death, metabolic adaptation and Ca^{2+} homeostasis. Mitochondria are also the site of important reactions, including fatty acid oxidation (FAO), the tricarboxylic acid (TCA) cycle, oxidative phosphorylation (OXPHOS), the first step of gluconeogenesis, ketogenesis, heme biosynthesis and Fe/S cluster formation. They contain DNA that can vary with evolution, mutate or be partially deleted (Grasso et al. 2020). Moreover, the main source of free radicals in most cell types are the mitochondrial ROS (mtROS) produced by the respiratory system during oxidative phosphorylation (Brand 2010). Given the numerous functions of mitochondria, it is not surprising that mitochondrial dysfunctions participate in a series of diseases, including cancer (Grasso et al. 2020). Therefore, mitochondria have been proposed as a good therapeutic target against cancer.

2.1 Genomic integrity of mitochondrial DNA

As it is described above, mitochondria have their own genome (mtDNA). The mtDNA is continuously exposed to ROS produced by the mitochondria. Furthermore,

mtDNA is more susceptible to oxidative damage than nuclear DNA, for several reasons. First, the mtDNA is closer to the site of ROS generation. Second, this DNA is not protected by histones or chromatin structure, such as nuclear DNA. In addition, mtDNA has a very limited rate of damage repair (Yang et al. 2016) and therefore, has a higher rate of mutations. In fact, it has been shown that a wide variety of tumors have mutations in the proteins of the electron transport system encoded in mtDNA, such as breast, brain, colorectal, gastric, pancreatic, thyroid and ovarian. Given the high number of somatic mutations present in mtDNA, it appears that these mutations are related to carcinogenesis and the resistance to apoptosis exhibited by tumor cells, although it is unknown whether they are a cause or a consequence of cancer (Baysal 2006).

On the other hand, mutations in mtDNA can be deleterious, neutral, or beneficial (adaptive). Those mutations, that have a tumorigenic character, are usually related to an inhibition of the mitochondrial electron tranfer system (ETS) or an increase in the mitochondrial production of ROS. In addition, the increase in mitochondrial ROS, produced because of tumorigenic mtDNA mutations, also affects nuclear DNA (nDNA) which leads to increased cell proliferation. These mutations can be highly beneficial in early tumor stages, where cells are glycolytic and have reduced OXPHOS (Guo 2021). Mutations causing mitochondrial dysfunction are generally considered to be a cause of tumorigenesis (Li and Hong 2012).

However, not only mtDNA is mutated in tumor cells, but also some cancers are caused by mutations in the nuclear DNA that codes for mitochondrial enzymes, some of which are linked to altered ROS production. This would show that mitochondrial ROS production is the factor that links mitochondrial defects with neoplastic transformation (Brandon et al. 2006). Therefore, both nuclear and mitochondrial genome instability

cooperate in the tumorigenesis process. In addition, the genomic instability caused by the production of ROS also has an important implication in chemo and radioresistance (Srinivas et al. 2019). Thus, considering that genomic instability has an important role in tumor initiation and progression, combating genomic instability may be an important target in cancer therapies (Ferguson et al. 2015).

2.2 Mitochondrial ROS production

The main source of free radicals in most cell types are the mitochondrial ROS produced by the respiratory system during oxidative phosphorylation. In mitochondria isolated from rat skeletal muscle, 11 different sites at which electrons can lead to produce ROS have been described (Brand 2010). In this context, the respiratory system is the major source of ROS, being complexes I (NADH:ubiquinone oxidoreductase) and III (ubiquinol:cytochrome c oxidoreductase; cytochrome bc1 complex) generally regarded as the main source of ROS, while the contribution of intact complex II seems to be negligible (Brand 2010; Dröse 2013). However, recent studies highlighted the important role played by reverse electron transport (RET) producing mtROS (Dröse 2013; Jia et al. 2020; Onukwufor, Berry, and Wojtovich 2019).

2.2.1 Reverse electron transport (RET)

The electron flow in CI is described in two modes, forward and reverse. Under conditions of normal respiration, forward electron transfer is the energetically favored complex I-mediated transfer of electrons from nicotinamide adenine dinucleotide (NADH) to coenzyme Q (CoQ). However, and in some specific mitochondrial conditions, CI can reduce NAD+ to NADH with electrons received from $CoQH_2$ pool, generating a

high level of mtROS. This process is called RET and the requirements (Scialò, Fernández-Ayala, and Sanz 2017) are the following:

1. High $CoQH_2$/CoQ ratio due to high CII (or other enzymes) activity.
2. High mitochondrial membrane potential (Δψm).

In this way, to fully understand where RET-ROS is produced, it is necessary to describe the structure of the CI. CI is made up of 45 subunits and have an approximate size of 1 MDa. It has a hydrophobic domain responsible for proton pumping and a hydrophilic domain involved in electron transfer. Seven iron-sulfur centers transfer electrons between the flavin mononucleotide (FMN, site IF), where NADH is oxidized to NAD+, and the Q-binding site (IQ) where electrons are finally transferred to ubiquinone (Figure 2) (Lambert and Brand 2004). In this way, CI can produce ROS when electrons circulate in the forward or reverse direction. When CI-linked substrates (i.e., glutamate or malate) are used to feed the respiratory system, electrons circulate through CI in the forward direction. In these conditions, blocking the IQ site with rotenone causes over-reduction of the IF site, increasing superoxide production. However, when CII-linked substrates (i.e., succinate) are used and in presence of the conditions described above, a portion of the electrons can flow from CII to CI in a reverse direction. ROS produced in these conditions are blocked by rotenone indicating that ROS inhibition by rotenone is specific only for RET-ROS production. Moreover, it has been demonstrated that in the forward transport, superoxide is produced at IF site, while in the reverse flow, the IQ site is the responsible of RET-ROS production (Scialò et al. 2017). Therefore, one way to differentiate RET-ROS production is by using rotenone, which increases ROS production in the forward direction, but decreases it via RET (Lambert and Brand, 2004)

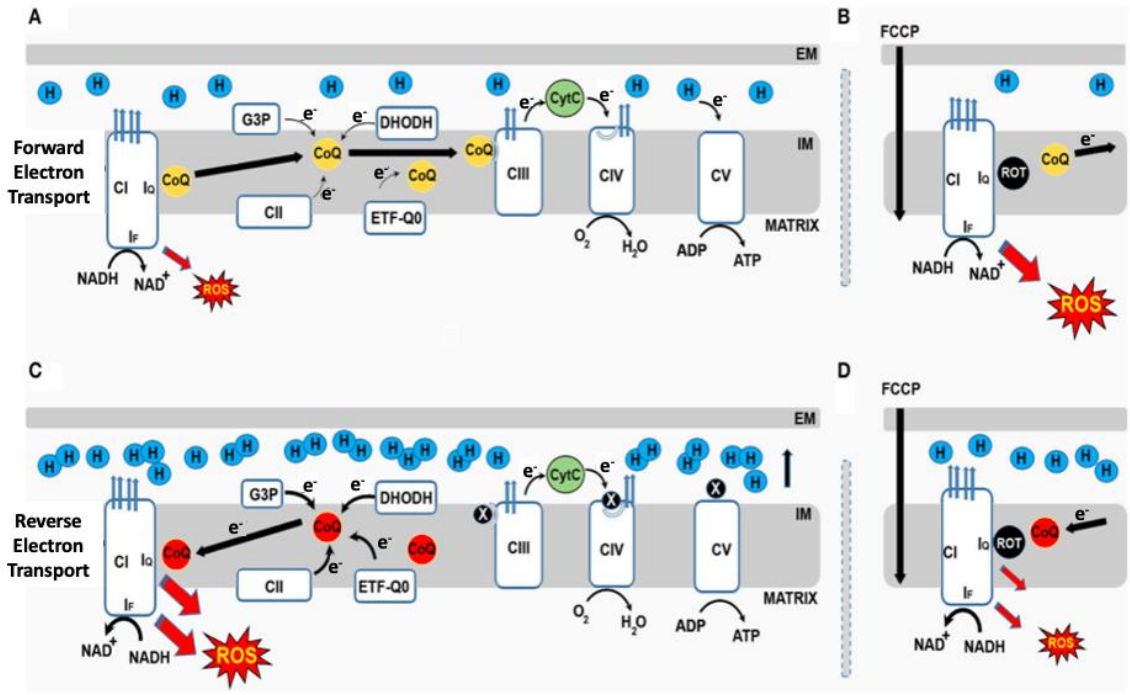

Figure 2. Respiratory CI produces ROS in both, forward and reverse direction. (A) During forward electron transfer (FET), CoQ receives electrons from complexes I and II, DHODH, G3P, ETFQO and other enzymes. During this process electrons mainly leak to produce superoxide from the IF site of CI during the oxidation of NADH to NAD+. (B) In these conditions, if rotenone blocks the IQ site, electrons cannot be transferred to CoQ, leak and generate ROS. FCCP also increases mtROS generation during FET. (C) When the CoQ pool becomes over-reduced, a high membrane potential favors the reverse transfer of electrons from ubiquinol to CI in a process called reverse electron transport (RET). During RET electrons leak at either IF or IQ generating a significant amount of superoxide. (D) Blocking the IQ site with rotenone during RET prevents CoQ from transferring electrons back to CI and reduces ROS production. Similarly, FCCP reduces ROS by dissipating membrane potential. (Scialò et al. 2017).

Moreover, RET-ROS production is not only inhibited by CI inhibitors but also for CII, CIII, CIV and uncouplers, as described below:

- **CII Inhibitors.** CII inhibitors also blocks RET-ROS production since a high CII activity is required for RET-ROS production. Specific inhibitors of CII can be divided into two subgroups (Fig 3): (i) inhibitors that bind to the carboxylate (succinate) binding site (i.e., oxaloacetate and malonate) and (ii) inhibitors that bind to the Q site (i.e., 2-thenoyltrifluoroacetone (TTFA), atpenins or diazoxide) (Dröse 2013).

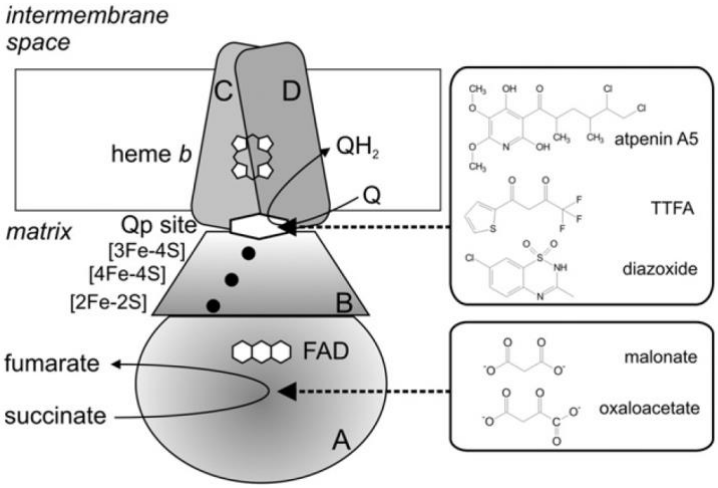

Figure 3. Structure of complex II. Composition and arrangement of redox centers. The four subunits (Sdh A-D) are indicated by capital letters, the relative positions of the prosthetic groups are indicated as black circles ([FeS]-clusters), a tricyclic structure (FAD), a stretched hexagon (Qp site) and a schematic porphyrin ring (heme b). The structures and binding sites of some inhibitors are also indicated. (Dröse 2013).

- **CIII, CIV Inhibitors and uncouplers.** Both CIII and CIV inhibitors also block RET-ROS production since they collapse mitochondrial membrane potential, and a high Δψm is another requirement for RET. Same situation happens with uncouplers as FCCP.

2.2.1.1 RET and metabolism

RET-ROS is particularly well suited to detecting metabolic changes which require metabolic adaptations. RET is sensitive to changes in: 1) the redox state of CoQ, which is directly related to electron flow through the ETS, and 2) variations in mitochondrial membrane potential, which correlated with the capacity to produce ATP.

It has been demonstrated that CI produces ROS in the forward or reverse direction depending on the substrates used to feed the respiratory system. Respiratory complexes are organized in larger superstructures called supercomplexes. In this way, depending on the source of energy available (e.g. sugars or fats), supercomplexes are present in different organizations (i.e. CI+CIII+CIV, CI+CIII and CIII+CIV, in addition to CIV

alone) (Scialò et al. 2017). The organization adopted will maximize the use of the available fuel. Fatty acids oxidation is more related, than glucose oxidation, with an over-reduction of CoQ pool and with an increase in RET-ROS production. In these conditions, RET-ROS promotes the degradation of CI, increasing the association between CIII and CIV, which is more efficient for the oxidation of fatty acids (Figure 4).

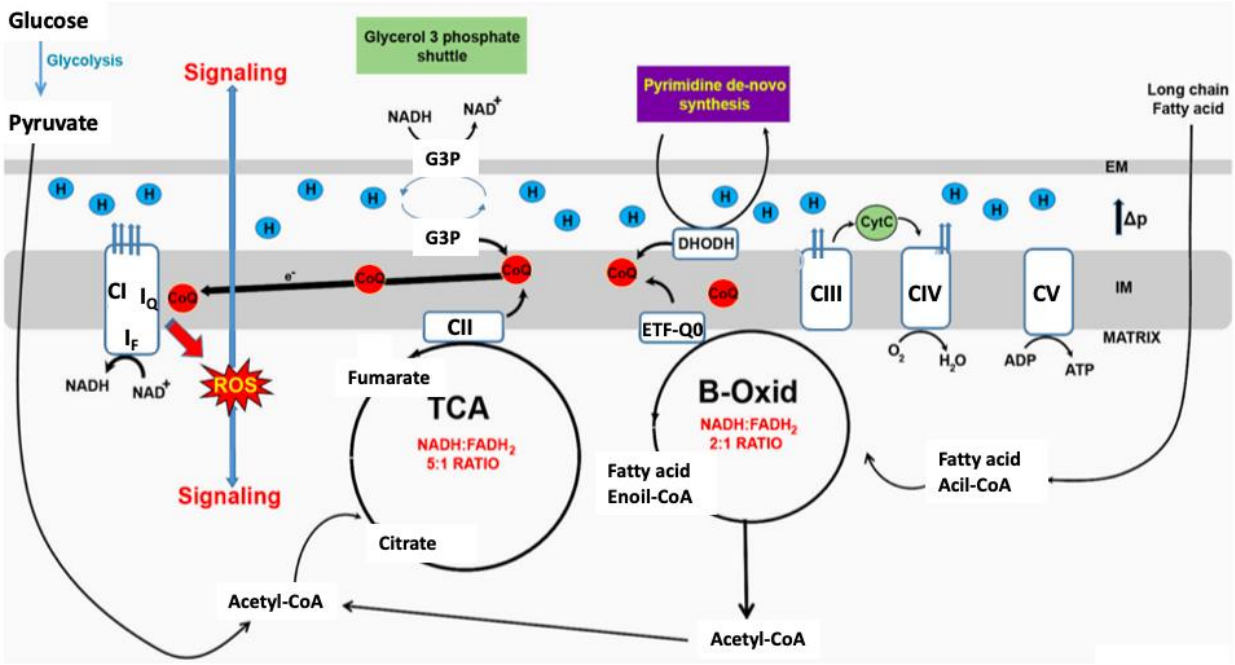

Figure 4. Reverse electron transfer (RET) regulation by cell metabolism. The redox state of the CoQ pool determines electron leak and superoxide production and can be used by mitochondria as a signaling mechanism. Since RET is sensitive to changes in electron flow and membrane potential, it can be used to detect changes in energy supply and fine-tune cell metabolism. For example, an increase in the availability fatty acid alters the NADH:$FADH_2$ ratio from 5:1 to 2:1 and in response levels of CI are reshuffled by ROS produced via RET (RET-ROS). (Guarás et al. 2016).

2.2.1.2 RET and physiology

In recent years, RET-ROS have been implicated in several physiological processes. Firstly, the differentiation of myoblasts into myotubes requires an increase in mtROS levels which is prevented with antioxidant treatment that inhibits differentiation (Lee et

al. 2011). Importantly, rotenone, which increases ROS production in the forward direction but decreases them via RET (Figure 2), also inhibits differentiation. Similarly, knockdown of CI subunits, which prevents the assembly of the full complex and decreases RET, also reduces myoblast differentiation (Scialo et al. 2016).

In response to bacterial infection, macrophages reorganize their ETS, decreasing the levels of CI and increasing the activity of CII. These changes are required to produce an inflammatory response characterized by production of pro-inflammatory cytokines such as interleukin 1β (IL-1β) and IL-10. This suggests that both, re-organization of the respiratory system and production of cytokines, are elicited via production of RET-ROS. Accordingly, Mills et al. have shown that macrophages alter the way of ROS are produced in response to lipopolysaccharide (Mills et al. 2016). To achieve this, macrophages interrupt ATP production via oxidative phosphorylation (switching to producing ATP via glycolysis), boost oxidation of succinate by CII and increase mitochondrial membrane potential, subsequently triggering the production of RET-ROS. Suppression of RET-ROS by preventing oxidation of succinate, blocking RET with rotenone or ectopically expressing an alternative oxidase from Ciona intestinalis (that prevents the over-reduction of CoQ) inhibits the generation of pro-inflammatory cytokines required to fight bacterial infection. These results indicate that RET-ROS signaling is instrumental for metabolic and immune reprogramming of macrophages and thus the initiation of an inflammatory response (Scialo et al. 2016).

Another important physiological phenomenon that seems to be regulated by RET-ROS signaling is the sensing of oxygen levels by the carotid body (CB) (Fernández-Agüera et al. 2015). The chemoreceptor cells of CB are responsible for inducing a response to hypoxia. Under normoxia, CB cells use NADH and CI produces low levels of

ROS in the forward direction. However, under hypoxia, cells undergo a metabolic shift characterized by increased utilization of succinate, which alters ROS production from CI from the forward to the reverse direction (Fernández-Agüera et al. 2015). In this model, not only ROS but also a boost in NADH levels is required to trigger the hypoxia response, suggesting that RET-ROS signaling may require other signals to elicit a physiological adaptation.

2.2.1.3 RET and disease

A clear example of RET and disease is the ischemia reperfusion (IR) injury (Figure 5). Loss of blood flow to tissue (ischemia) and subsequent reestablishment (reperfusion) results in IR injury. In mitochondria, depleted oxygen during ischemia combined with its rapid restoration at reperfusion cause oxidative damage to tissue. This damage can be produced by ROS generated in several places in mitochondria. At CI, metabolic substrates that accumulate during ischemia are rapidly oxidized at reperfusion, causing damage. Specifically, accumulated succinate drives RET and ROS production, implicating CI ROS in the oxidative damage from IR injury (Onukwufor et al. 2019).

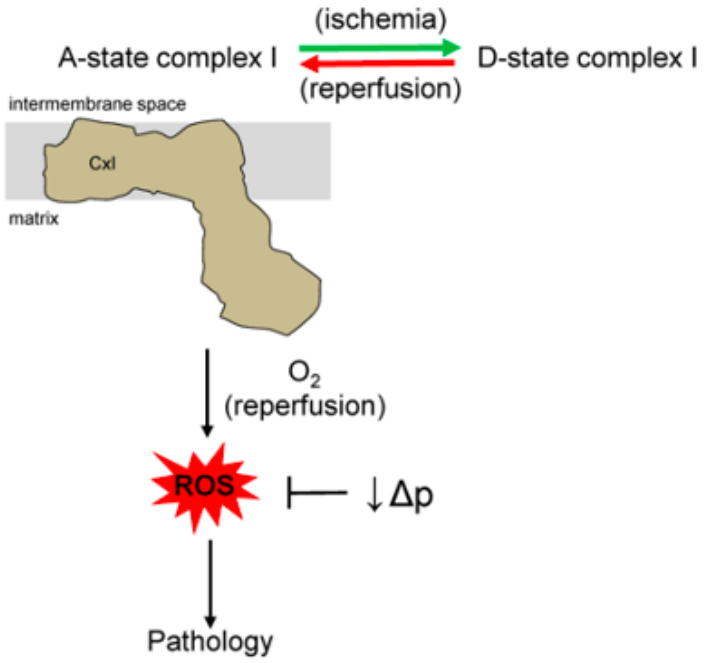

Figure 5. Factors that affect RET in ischemia reperfusion (IR) injury. During ischemia, succinate accumulation drives RET at complex II forcing electrons to CI, where ROS is subsequently overproduced. Complex I has two states, active (A) and dormant (D). Ischemia drives an A-form that transition to D-form. During reperfusion D-form transition back to A-form generating reactive oxygen species (ROS) that causes IR injury. The mitochondrial proton motive force (Δp) is a main driving force for RET. Therefore, decreasing the Δp removes a main driver of RET and ROS production at reperfusion. (Onukwufor et al. 2019).

CI has enzymatically active (A) and dormant (D) states under different conditions. The A state has catalytic NADH/Q oxidoreductase activity. However, the D state is inhibited and more susceptible to oxidative modification *in vitro*. During ischemia there is a reversible transition from the A to the D state. This transition is hypothesized to be a physiologic mechanism to limit ROS production at reperfusion, as the D state makes less ROS by RET than the A state. Oxidative damage at reperfusion is driven by RET succinate oxidation at functional CI in the A state. Ischemic transition of CI to the D state could be a preparation for reperfusion, serving to inhibit CI activity and RET (Onukwufor et al. 2019).

2.3 Mitochondria metabolism reprogramming in cancer cells (Warburg effect)

Tumor metabolism has been the subject of numerous studies as it is one of the main characteristics that differentiate normal cells from tumor cells. The Warburg effect has been described as the conversion of glucose to lactate in the presence of oxygen and functioning mitochondria. It is a crucial component of the malignant phenotype and a central feature of the 'selfish' metabolic reprogramming of cancer cells, which is considered a 'hallmark of cancer' (Vaupel and Multhoff 2021). The switch to aerobic glycolysis (i.e. the conversion of glucose to pyruvate) followed by lactate formation is acquired very early in carcinogenesis (oncogenesis), even before tumor cells are exposed to hypoxic conditions. The Warburg phenotype constitutes a metabolic signature of 70–80% of human cancers, which results from the interplay between the normoxic/hypoxic activation of the transcription factor hypoxia-inducible factor-1α (HIF-1α), oncogene activation, loss of function of tumor suppressors, altered signalling pathways and interaction with components of the tumor microenvironment (TME), sometimes working in concert with epigenetic mechanisms. The Warburg effect reflects a metabolic programme of cancer cells driving sustained proliferation and accelerating malignant progression (Vaupel, Schmidberger, and Mayer 2019).

2.3.1 Major biochemical steps of aerobic glycolysis

The glycolytic pathway involves the catabolism of glucose to pyruvate in 9–10 biochemical steps, which are schematically shown in Figure 6. First, there is an upregulation of 'high-affinity' glucose transporter GLUT1, which induces the enter of glucose inside the cancer cell. Then, key glycolytic enzymes, hexokinase 2,

phosphofructokinase 1, enolase 1, and the low-activity pyruvate kinase M2 (PKM2), metabolism glucose to 2 pyruvate molecules, the end product of aerobic glycolysis. In a following step, pyruvate is converted into lactate, which is exported via upregulated MCT4 transporters into the extracellular space, where it contributes to acidification (pH <6.8), which contributes to metastasis phenotype. Transcriptional activation also includes the mitochondrial pyruvate dehydrogenase kinase 1, which inactivates the 'bottleneck' or 'gatekeeper' enzyme pyruvate dehydrogenase and thus impedes the intra-mitochondrial conversion of pyruvate to acetyl-CoA into the mitochondria. As a result, pyruvate is shunted from the mitochondria and is converted to lactate in the cytosol. Lactate is exported into the extracellular space, where it is accumulated (up to 40 mm) (Vaupel and Multhoff 2021).

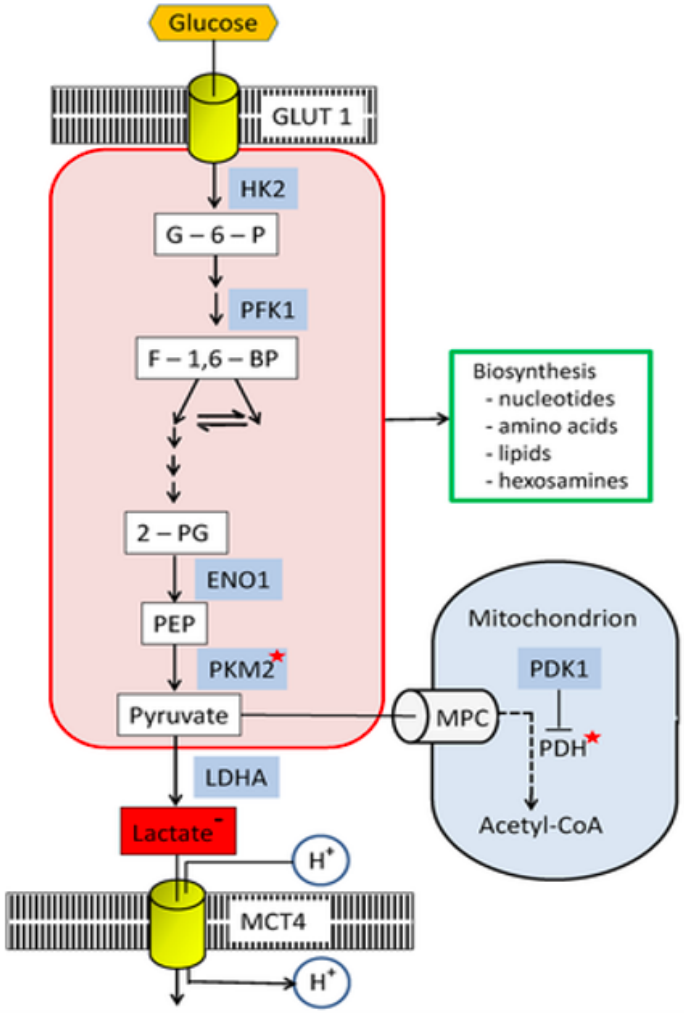

Figure 6. Key biochemical steps of the Warburg phenotype. Upon enhanced import through overexpressed GLUT1 transporters, glucose is converted into 2 pyruvate molecules, the final product of aerobic glycolysis. In a following step, pyruvate is converted into lactate, which is exported via upregulated MCT4 transporters into the extracellular space, where it contributes to acidification (pH <6.8). 'Gatekeeper' enzymes (marked with a red star) lead (a) to an accumulation of upstream glycolytic intermediates (PKM2*) utilized for the biosynthesis of nucleic acids, non-essential amino acids, lipids and hexosamines, and (b) to a diversion of pyruvate away from the mitochondria (TCA cycle, OXPHOS) by encoding PDK1, which in turn activates the 'gatekeeper' enzyme PDH*. Abbreviations: 2-PG, 2-phosphoglycerate; acetyl-CoA, acetyl-coenzyme A; F-1,6-BP, fructose-1,6-bisphosphate; G-6-P, glucose-6-phosphate; MPC, mitochondrial pyruvate carrier; PEP, phosphoenolpyruvate; PDK1, pyruvate dehydrogenase kinase 1. Red Box: 9(−10) biochemical steps of aerobic glycolysis in the cytosol. (Vaupel and Multhoff 2021).

The overexpression of the poorly active/nearly inactive (dimeric) pyruvate kinase M2 (PKM2), another 'gatekeeper' enzyme, limits the phosphoenolpyruvate-to-pyruvate conversion (i.e. the final, irreversible step of glycolysis, providing ATP and thus leads to a backup of upstream glycolytic phospho-intermediates ('glucose carbons above

pyruvate kinase), which are shuttled into biosynthesis pathways allowing for sustained proliferation and unlimited growth. Beyond this metabolic role in glycolysis, PKM2 regulates gene expression in the nucleus, and phosphorylates several proteins that regulate key signalling pathways and contribute to the redox homeostasis of cancer cells. In this way, it has been demonstrated that, due to the metabolic reprograming, cancer cells obtain 2 NADPHs per mole of glucose via the activation of pentose phosphate pathway (PPP), which maintains the antioxidative power of GSH, thus increasing the radioresistance of cancer cells, and can act as a directly operating antioxidant in the mitochondrial compartment (Vaupel and Multhoff 2021).

2.4 Mitochondrial permeability transition pore

The mitochondrial permeability transition pore is a multi-protein channel complex lying in the mitochondria, which is related with ROS production and cell apoptosis. Specifically, the redox homeostasis is determined by the balance between ROS generation and ROS depuration capacity. Undoubtedly, tipping the balance in favor of increased ROS production can severely alter the cellular redox equilibrium, potentially resulting in oxidative stress, which can cause oxidation of essential mitochondrial components. Finally, at high ROS level, it can irreversibly damage these components resulting in cell death. Within the great diversity of types of cell death, which to date comprise as much as 13 types, at least some of them could be associated with induction of the mPTP opening (Zorov et al. 2014).

In this way, mPTP opening represents a sudden change in the permeability of the inner mitochondrial membrane allowing not only protons, but also other ions and solutes of a size up to 1.5 kDa to go through this membrane. Moreover, this

phenomenon is related to homeostasis regulation, since, although mPTP induction is typically referred to as a pathological event, very often resulting in the degradation of aberrant mitochondria or damaged cell, regulating physiological homeostasis. Therefore, both physiological and pathological responses to oxidative stress may involve mPTP. In this context, it has been demonstrated that Ca^{2+} levels and ROS production can induce mPTP opening. As consequence, its activation causes intra- and inter-mitochondrial redox-environment changes leading to ROS release. This regenerative cycle of mitochondrial ROS formation and release was named ROS-induced ROS release (RIRR) (Zorov et al. 2014).

It has been proposed that RIRR may result in a cellular response that can be considered either physiological (i.e., promoting signaling resulting in the elevation of the tolerance to oxidative stress or the removal of unwanted organelles and cells) or pathological (i.e., the destruction of healthy mitochondria and cells). Adaptive cell elimination may involve cell death executed by necrotic or apoptotic mechanisms (for example, elimination of nonfunctional or damaged cells) (Zorov et al. 2014)

2.4.1 Pathophysiological function of mPTP

It has been proposed some models where mPTP may regulate pathophysiological process. The first role is to serve as a potential release valve which transiently opens a gate for controlled release of accumulated ions or newly formed low-molecular-weight toxic substances including elevated ROS and Ca^{2+}. This likely maintains mitochondrial (and cellular) redox homeostasis, which is a critical point in normal cell functioning. The characteristics of this mode include brief and reversible episodes of the mPTP pore opening. It serves as a housekeeping function and, at low energy demand, it is likely

relatively inactive. Specifically, this mode has been proposed for high stress/energy demand conditions (Zorov et al. 2014).

However, it has been demonstrated that, in some context, mPTP could induce a persistent and generally irreversible large conductance of the inner mitochondrial membrane sufficient to activate the mechanisms of destruction of mitochondria as we can see in the Figure 7.

This phenomenon would arise in response to the existence of impaired mitochondria and could be deleterious for the proper functioning of the whole mitochondrial population (connected in a functional network). Therefore, the opening of mPTP may lead to programmed mitochondrial elimination (mitophagy) (Vacek, Vacek, and Tyagi 2012). This point may correspond to the term mitochondrial criticality by reaching a redox crisis in an oxidatively stressed cell after which the behavior of mitochondrial energetics becomes unstable (Zorov et al. 2014).

Finally, it has been demonstrated that mPTP is not only related to mitophagy but also to the terminal destructive step resulting in cell death. As for mitochondria, impaired cells can be programmed for the destruction with the mPTP playing a critical role in that process. In general, this mechanism of cell elimination would encompass a large fraction of mitochondria, undergoing the process described above, involving significant releases of ROS from mitochondria undergoing mPTP (Juhaszova et al. 2004).

The cause of mitophagies and / or cell death process is the generation of the redox crisis, ROS levels higher that the threshold values. In this context, it has been demonstrated that the amount of ROS required to achieve the threshold for mPTP induction change depend on the ROS production and on the antioxidant defense of the cell. Furthermore, the mPTP threshold is highly dependent on ambient molecular

oxygen, since ROS production in the system is a reaction of the first order with respect to molecular oxygen (Zorov et al. 2014).

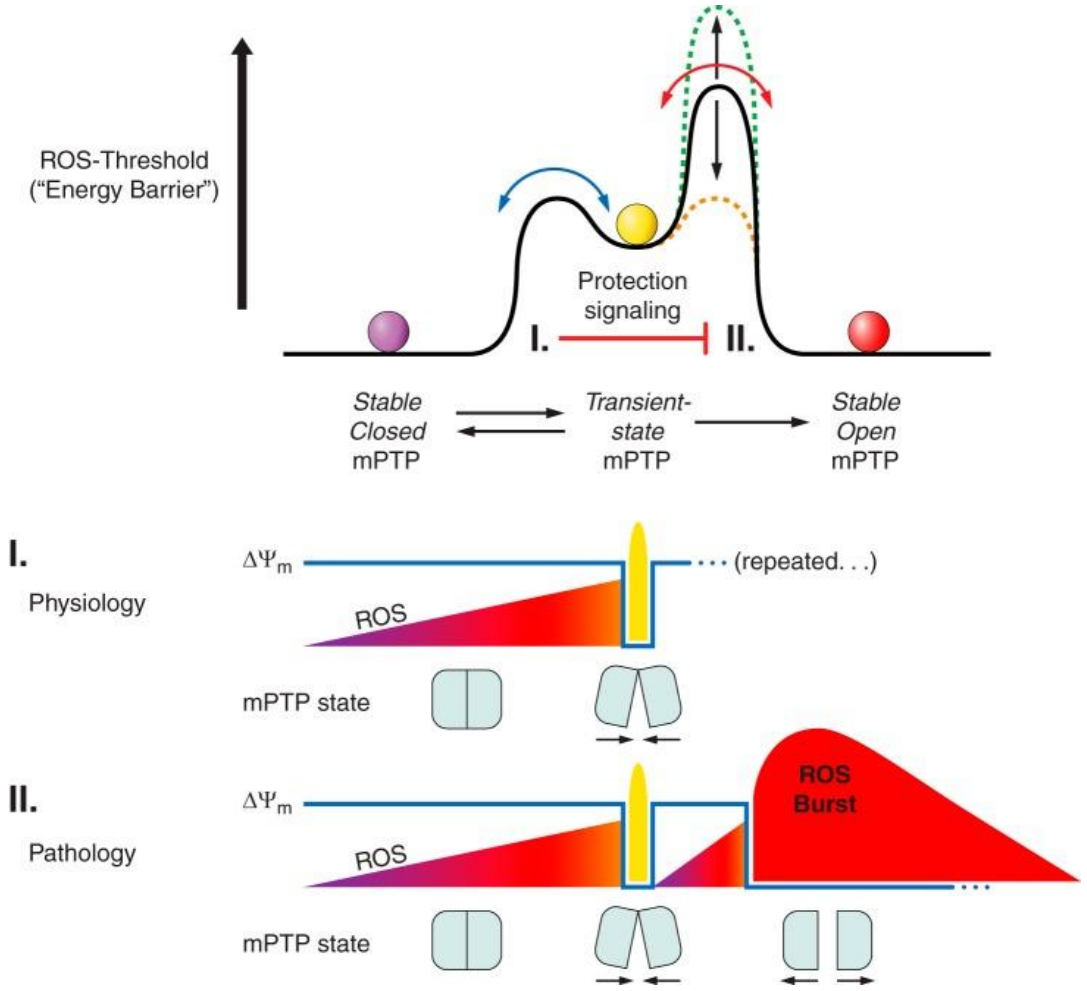

Figure 7. Schematical model of the pathophysiological roles of the mPTP. The stable state with the closed mPTP can undergo a transition to a metastable (transient) state of the mPTP. By analogy to an energy barrier (threshold) necessary to overcome in order to undergo a physico-chemical transition, the reaction probability and rate is determined by a redox threshold (process I) that normally is lower than the threshold of process II (pathology) determining the transition to the fully open, stable mPTP opening. (Zorov et al. 2014).

One example of described above was demonstrated in cardiac myocytes which were exposed to transient hypoxia, followed by a reoxygenation phase, demonstrated mitochondrial instability caused by the introduction of oxygen into the system. In these cells, it was shown that the induction of ischemia/reperfusion generated the mPTP opening and it was accompanying with a high ROS burst (Frank et al. 2012).

3. Melatonin

Melatonin or 5 methoxy-N-acetyltryptamine (aMT) (Figure 8) was discovered and isolated from bovine pineal in 1958 by Aaron Lerner (Tordjman et al. 2017). Melatonin not only has been found in mammals but also in a wide range of living systems (Hardeland 2008).

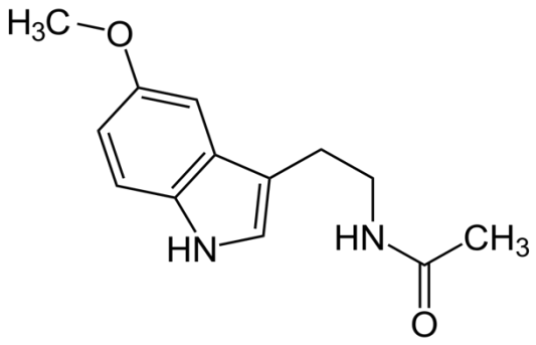

Figure 8. Schematic structure of melatonin**.**

3.1 Melatonin synthesis and metabolism

Because the discovery of melatonin was in pineal tissue (pineal melatonin), for many years the pineal was considered the exclusive source of melatonin in vertebrates. However, the presence of melatonin has been detected in multiple extrapineal tissues including the brain, retina, lens, cochlea, Harderian gland, airway epithelium, skin, gastrointestinal tract, liver, kidney, thyroid, pancreas, thymus, spleen, immune system cells, carotid body, reproductive tract, and endothelial cells, indicating that melatonin is synthesized in many other tissues (extrapineal melatonin). In all tissues, melatonin is produced from tryptophan via serotonin. In this context, tryptophan is converted into the neurotransmitter, serotonin by tryptophan hydroxylase and aromatic acid

decarboxylase enzymes. In the subsequent step, serotonin is converted into melatonin through the influence of arylalkylamine N-acetyltransferase (AANAT) and N-acetylserotonin O-methyltransferase (ASMT) enzymes (Talib et al. 2021).

The synthesis of pineal melatonin is controlled by the light-dark cycle through a polysynaptic pathway which connect the retina with the pinacocytes. Melatonin presents maximum levels in plasma (0.5 nM) at night between 2-3 am. However, the levels during the day are very low, because light inhibits its production. Once synthesized, melatonin is released into the bloodstream, accessing to cellular tissues and corporal fluids. Moreover, melatonin can easily cross through cell membranes because of its high lipophilicity and hydrophilicity what allows it to enter inside cells and its subcellular compartments (Venegas et al. 2013). Pineal melatonin is a synchronizer which is related to the circadian functions (Acuña-Castroviejo et al. 2014; Venegas et al. 2013).

Extrapineal melatonin is produced at higher concentration (micromolar range) than pineal melatonin (nanomolar pineal) (Venegas et al. 2013) in various tissues, fluids and organs other than the pineal gland. Its sinthesis is independent of the light-dark cycle, and this extrapineal melatonin is not released into the circulation, acting in an autocrine or paracrine manner, protecting cells from oxidative or inflammatory damage (Acuña-Castroviejo et al. 2014).

Regarding its metabolism, circulating melatonin is mainly metabolized in the liver, although it can also be metabolized in other organs. In extrahepatic tissues, melatonin is first converted to N1-acetyl-N2-formyl-5-methoxykynurenamine (AFMK), the main metabolite of melatonin, which is subsequently transformed into N-acetyl-5-methoxykinurenamine (AMK) (Fujiwara et al. 1978). Melatonin metabolites have

important antioxidant properties, being even greater than those of melatonin itself, as it is described below (Tan et al. 2015).

3.2 Melatonin proprieties in normal cells

3.2.1 Antioxidant properties of melatonin

The antioxidant effect of melatonin may be direct or indirect. Melatonin is a potent direct free radicals scavenger. Electron donation is the principal mechanism by which melatonin detoxifies the free radicals. Oxidation of melatonin by hydroxyl radicals leads to several hydroxylated products which can be explained by interaction of melatonin with two hydroxyl radicals, one acting by hydrogen abstraction and the other by combining with the reaction partner especially at the sides C2, C3, C6, and C7. After donating an electron to OH•, melatonin becomes a free radical itself, the indolyl radical cation. However, its reactivity is very low and, therefore, it is not toxic to cells (Hacışevki and Baba 2018). While melatonin has the capability of donating one or more electrons to free radicals resulting in their detoxification, the metabolites formed during this process, i.e., cyclic 3-hydroxymelatonin (c3OHM), AFMK, and AMK, also have similar capabilities (Figure 9). Moreover, these metabolites are even more potent than melatonin in scavenging free radicals. It is estimated that melatonin can eliminate up to 10 free radicals through a cascade reaction where a series of metabolites produced are also active (Talib et al. 2021).

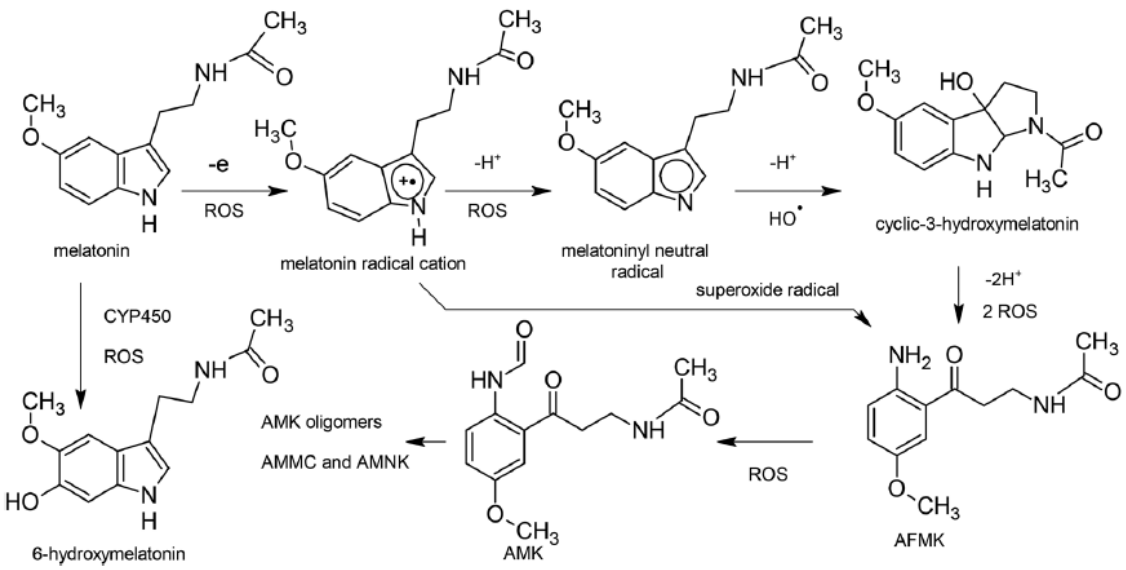

Figure 9. Structure of the melatonin metabolites. (Johns and Platts 2014).

Lipid peroxidation is a natural metabolic process under normal aerobic conditions, and it is one of the most investigated consequences of ROS action on membrane structure and function. Alterations in the fluidity of membranes result in negative effects on their functions, such as signal transduction processes, and are implicate in aging as well as in some diseases. Melatonin is known to be a stabilizer or protector of cell and organelle membranes because of its inhibitory effects on lipid peroxidation. Melatonin and its metabolites scavenge free radicals inhibiting the initiation and propagation of lipid peroxidation (Hevia et al. 2015). Moreover, when melatonin interacts with the inner mitochondrial membrane, it favors the flow of electrons and the production of ATP (Su et al. 2017). In this way, melatonin maintains the function and permeability of cell membranes (Escames et al. 1997). It has been demonstrated that melatonin is mainly concentrated in subcellular compartments where ROS concentration is higher, such as mitochondria where melatonin biosynthesis enzymes has been identified (Venegas et al. 2013; Tan et al. 2015).

In addition, cells are protected against oxidative stress by an interacting network of antioxidant enzymes. The activities of antioxidative enzymes depend on the duration and severity of oxidative stress. Under prolonged oxidative stress conditions, free radicals directly damage the antioxidant enzymes or reduce its activities (Hacışevki and Baba 2018). Melatonin, besides its ability to directly neutralize a number of free radicals and reactive oxygen and nitrogen species, also stimulates several antioxidative enzymes increasing its efficiency as an antioxidant (Acuña-Castroviejo et al. 2014). Melatonin increases the expression and activity of glutatione peroxidase (GPx), glutathione reductase (GRd), superoxide dismutase (SOD), catalase and glucose-6-phosphate dehydrogenase (G-6- PDH), as well as gamma-glutamylcysteine synthase (Tan et al. 2015). Therefore, melatonin regulates the oxidized glutathione (GSSG)/ reduced glutathione (GSH) balance under normal conditions and also in situations of increased oxidative stress (Acuña-Castroviejo et al. 2001).

3.2.2 Mitochondrial function

Melatonin has important actions in mitochondria. Due to its amphoteric property, melatonin can cross both cellular and subcellular membranes, concentrating in different compartments, including the mitochondria (Venegas et al. 2013). Melatonin plays a very important role in the mitochondria to preserve its integrity and functionality. Moreover, it has been described that melatonin is also synthesized in the mitochondria, which would be released into the cytoplasm by the MT1 transporter located in the outer mitochondrial membrane (Suofu et al. 2017).

Melatonin exhibits remarkable functional versatility to preserve the morphological and functional aspects of the cell membrane from free radical attack.

These include its ability to scavenge free radicals and to enhance the activity of the antioxidant enzymes. Furthermore, melatonin also increases the expression and activity of all the mictochondrial complexes and improves the transfer of electrons through the in the inner mitochondrial membrane. In this way, melatonin increases the efficiency of the ETS reducing electron leakage and free radical generation and increasing ATP production (Acuña et al. 2007). Moreover, AMK, a melatonin metabolite, also promotes mitochondrial complex I activity to elevate ATP production by lowering electron leakage and inhibiting the opening of the mitochondrial permeability transition pore (Hacışevki and Baba 2018).

Finally, melatonin regulates mitochondrial morphological changes, removing old and damaged mitochondria and preserving new and healthy mitochondria. Mitochondrial biogenesis, fusion and fission, as well as mitophagy have a circadian rhythm. This daily oscillation is due to the changes in the expression of clock genes, which are regulated by melatonin.

The processes of fission and fusion, that are been necessary to maintain cell homeostasis, regulate new mitochondria synthesis and remove old and damaged mitochondria that cannot be repaired, (Chang et al. 2019). In addition, melatonin also regulates mitophagy, which is essential to remove damaged mitochondria and preserve healthy ones. Moreover, it has been shown that melatonin increases mitophagy and mitochondrial biogenesis in cancer cells (Guerra-Librero et al. 2021; Proietti et al. 2017).

3.3 Melatonin properties in cancer cells

It has been widely demonstrated that melatonin has a dual effect, protecting normal cells and inducing cancer cell death (Fernandez-Gil et al. 2019; Guerra-Librero et

al. 2021; Moreira et al. 2015; Mortezaee, Najafi, et al. 2019; Y.-Q. Shen et al. 2018; Wölfler et al. 2001). Moreover, it also has been demonstrated that melatonin protects healthy tissues from oncostatic treatments reducing its side effects (Fernández-Gil et al. 2017; Ortiz, Acuña-Castroviejo, et al. 2015). However, although several mechanisms have been described, the underlying mechanism of action of melatonin has not yet elucidated (Cardinali and Escames 2016; Talib et al. 2021).

Antiproliferative and proapoptotic effect: One of the effects of melatonin that makes it useful in antitumor therapy is its ability to reduce neoplastic proliferation involving both cytostatic and cytotoxic effects. It has been shown, in some cancer cells, that melatonin downregulates some components involved in cell cycle progression from a mitotic stage to the next step, such as cyclin D1, cyclin B1, and cyclin-dependent kinases 4 and 1 (Talib et al. 2018). Moreover, melatonin inhibits proliferative ERK1/2 signaling pathway that controls gene expression and promotes cell cycle progression and cell division. Notably, melatonin activates ERK1/2 signaling in normal cells while it is inhibited in cancer cells, impeding their proliferation and, potentially, breaking their resistance to cytotoxic therapies. On the other hand, melatonin has also a cytostatic effect causing the accumulation of cells in the G0/G1 phase of the cell cycle or delaying the progression to the S phase of the cell cycle (Favero et al. 2018).

Moreover, melatonin also induces pro-apoptotic effects by altering the Bax/Bcl-2 ratio. Then, this signal induces the release of cytochrome c into the cytosol, leading to caspases activation and cell death. In this way, the induction of programmed cell death could be related to the melatonin capacity to alter oncostatic protein content such as, the inhibition of phosphatidylinositol 3-kinases/protein kinase B (PI3K/Akt), nuclear

factor kappa light chain enhancer of activated B cells (NFκB) or HIF-1 and / or the induction of the p53 pathway. However, the sensitivity of tumor cells to melatonin-induced apoptosis is different, depending on the cell lines (Talib et al. 2021) and on the dose, since this effect is related to a dose-dependent response (Farhood et al. 2019). In our Research Group, we have demonstrated that high-dose melatonin potentiates the cytotoxic effects of chemo and radiotherapy on tumor cells by increasing the expression of proapoptotic proteins as well as decreasing the antiapoptotic proteins of the Bcl-2 family (Fernandez-Gil et al. 2019; Guerra-Librero et al. 2021; Y.-Q. Shen et al. 2018).

Stimulation of the immune system: it has been demonstrated that melatonin regulates the immune system, an important factor in neoplastic diseases, where immune system function is compromised. In this context, melatonin has a close relation with immune cells, which is mediated through melatonin receptors. It has been suggested that ablation of the pineal gland is associated with loss of immune cells. Some cytokines and growth factors such as IFN-γ, granulocyte-macrophage colony-stimulating factor (GM-CSF) and granulocyte colony-stimulating factor (G-CSF) stimulate melatonin secretion, while IL-1 inhibits it. It has been reported that immune cells, such as CD4+ T helper cells and cytotoxic T lymphocytes, express melatonin receptors including MT1 and MT2 (Mortezaee et al. 2019). Melatonin also stimulates the release of IL-2 by upregulation of MT1 which, ultimately, leads to an increase in the number of NK cells. This would facilitate the recognition of tumor cells and their elimination by the immune system (Srinivasan et al. 2008). Melatonin also enhances the antigen presentation by macrophages to T-lymphocytes, leading to the activation and proliferation of CTLs. Melatonin may help the proliferation of CTLs and anti-cancer

activity of immune system by triggering the release of anti-tumor cytokines such as IFN-γ, TNF-α and IL-6 as well as suppression of IL-4 (Mortezaee et al. 2019).

Antiangiogenic effect: angiogenesis is an essential process in cancer progression as it provides solid tumors with the oxygen and nutrients that are necessary to maintain a high rate of cell division. Melatonin inhibits angiogenesis by inhibiting the proliferation of vascular endothelial cells and pro-angiogenic factors. Melatonin reduces the expression of vascular endothelial growth factor (VEGF), one of the main factors that stimulate angiogenesis, by destabilizing HIF-1α which induces VEGF expression (Su et al. 2017; Talib 2018).

Antimetastatic effect: melatonin also interfers with various steps necessary for the development of metastasis such as the loss of cell-cell contact, tissue invasion and extravasation. Melatonin increases the expression of E-cadherin, a protein necessary for the formation of tight junctions in cell-cell adhesion. Tumor cells have low levels of this protein, which favors the disruption of the junctions between cells, allowing cells to leave the primary tumor and invade adjacent tissues (Su et al. 2017). On the other hand, melatonin inhibits the epithelial-mesenchymal transition, a process by which tumor cells lose their adhesion to neighboring cells and become migratory. Melatonin inhibits this process by altering the signaling of the NF-kB pathway (Su et al. 2017).

There is highly credible evidence that melatonin mitigates cancer at the initiation, progression and metastasis phases. In many cases, the molecular mechanisms underpinning these inhibitory actions have been proposed. What is rather perplexing, however, is the large number of processes by which melatonin reportedly restrains

cancer development and growth. These diverse actions suggest that what is being observed are merely epiphenomena of an underlying more fundamental action of melatonin that remains to be disclosed.

3.3.1 Pro-oxidant effect

As it is described above, it has been demonstrated that melatonin has a dual effect. Melatonin reduces the adverse effects of cancer treatments by preventing ROS production, by improving mitochondrial function and by inhibiting apoptosis (Ortiz et al. 2015), while in tumor cells melatonin induces ROS production, leading to cell apoptosis (Proietti et al. 2017). It has been proposed several mechanisms which explain the pro-oxidant effect of melatonin in cancer cells (Florido et al. 2022).

3.3.1.1 Melatonin receptor

It has been widely demonstrated that high levels of melatonin are necessary to induce ROS production in tumor cells, thus highlighting the independent impact of low-affinity melatonin targets such as MT1, MT2 and ROR receptors (Reppert, Weaver, and Ebisawa 1994). This is confirmed by melatonin's pro-oxidant effect, which is unaffected by the MT1/MT2 antagonist luzindole and it is not altered by melatonin analogues with high affinity for MT1/MT2 receptors. On the other hand, it has been suggested that melatonin's pro-oxidant activity derives from binding to calmodulin, to which other enzymes such as phospholipase A2 (PLA2) associated with oxidative stress (Radogna et al. 2009 a).

The PLA2 enzyme cleaves membrane phospholipids, leading to the release of membrane bound arachidonic acid (AA), which is processed by cyclooxygenases (COXs)

and lipoxygenases (LOXs) to produce important inflammatory mediators, such as prostaglandins and leukotrienes, as well as to increase ROS production. However, Ca2+-independent phospholipase PLA2 (iPLA2) can bind to calmodulin that is inactivated. It has been demonstrated that melatonin, at high concentrations, binds to calmodulin, thus inducing the release of iPLA2 and, consequently, increasing ROS production in human tumor monocytes (Figure 10). The increase in ROS production by melatonin is inhibited by chlorpromazine, which prevents melatonin from binding to calmodulin. Finally, iPLA2 and 5-LOX inhibitors also abolish melatonin's ability to stimulate ROS production, indicating that these two enzymes are involved in melatonin's pro-oxidant activity. All these findings suggest that the binding of melatonin to calmodulin is required to induce ROS production (Radogna et al. 2009 b).

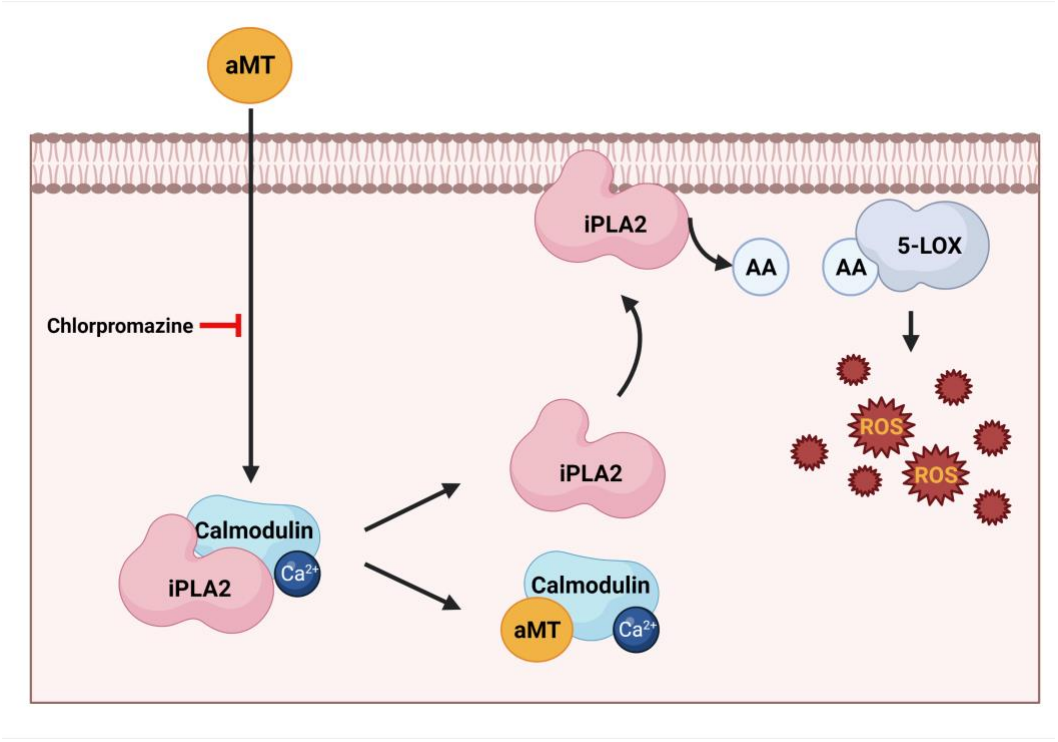

Figure 10. Melatonin induces ROS production in cancer cells through calmodulin binding. Melatonin binds to calmodulin, leading to the release of sequestered Ca2+-independent PLA2, which is then free to move to membranes and to release high doses of AA; in turn, liberated AA feeds 5-LOX to produce free radicals. (Florido et al. 2022).

3.3.1.2 Sirtuin pathway

Sirtuins, which are a class III histone deacetylase enzymes, are key molecular proteins involved in oxidative stress and play an important role in both, normal and cancer cells. Sirtuin-3 (SIRT3), which is located primarily in the mitochondrial matrix, regulates intracellular metabolism, mainly by modulating mitochondrial oxidative stress. It also regulates superoxide dismutase 2 (SOD2) by deacetylating and activating the SOD2 transcription factor FOXO3a, as well as by directly deacetylating and activating SOD2 dismutase activity. Furthermore, decreased SIRT3 expression increases ROS-mediated oxidative damage, suggesting that SIRT3 inhibitors could be therapeutically beneficial. It has been demonstrated that melatonin potentiates the cytotoxic effects of shikonin in HeLa cancer cells by inducing oxidative stress through the inhibition of SIRT3/SOD2 expression and activity. The combination of melatonin and shikonin, which increases ROS production in various cancer cell lines, promotes apoptosis. All these effects are reversed by ROS scavengers, thus suggesting that melatonin induces apoptosis in cancer cells by increasing ROS production. This is probably explained by the excessive levels of ROS induced by melatonin, which releases mitochondrial cytochrome C, leading to apoptosis in cancer cells (Lu et al. 2016).

On the other hand, other authors have reported that melatonin increases SIRT3 activity in lung cancer cells. This leads to the deacetylation of pyruvate dehydrogenase (PDH) which lead to an increase of complex I and IV activity which increases ROS production and reverses the Warburg effect. Thus, melatonin induces cancer cellular apoptosis by elevating ROS generation due to an increase in OXPHOS through the stimulation of SIRT3 activity (Chen et al. 2021). However, due to the different melatonin

effects on SIRT3, increasing or decreasing it, further research is required to clarify melatonin's mechanism of action via SIRT3.

3.3.1.3 Akt pathway

Akt, which is a serine/threonine kinase, plays a crucial role in major cellular functions such as cell size, cell cycle progression, genome stability, glucose metabolism regulation, transcription, and protein synthesis. Akt promotes cell survival by mediating cellular growth factors and by blocking apoptosis through the inactivation of pro-apoptotic proteins, as well as through the regulation of ROS balance. A wide range of proteins are sensitive to phosphorylation by AKT, such as glycogen synthase kinase-3 (GSK-3), a protein serine/threonine kinase involved in cell signaling that is phosphorylated on serine 9 and then inactivated (Florido et al. 2022).

Melatonin has been widely reported to modulate Akt, in both normal and tumor cells. For example, in human melanoma cells (SK-MEL-1), it has been demonstrated that, as melatonin promotes GSK-3 dephosphorylation at serine 9 via Akt pathway inhibition, the activation of GSK-3 by melatonin results in an increase in ROS production. This was confirmed by the use of the GSK-3 inhibitor BIO, which partially abrogates the generation of ROS in response to melatonin (Perdomo et al. 2020). It has also been reported that the pro-oxidative effects of GSK-3 are due to the degradation of NRF2, the master regulator of endogenous antioxidant responses. This pattern was also reported in the glioblastoma cell line U87MG, where the inhibition of Akt triggers GSK-3 activity which, in turn, switches off the antioxidant response of NRF2 (Ciotti et al. 2020).

3.3.1.4 Decreased antioxidant defenses

The pro-oxidant and oncostatic effects of melatonin can be explained by the increased levels of intracellular ROS as well as the decrease in antioxidant capacity, exhibited in the melatonin-treated cells, as described above. It has been demonstrated that melatonin decreases antioxidant enzymes such as catalase, glutathione peroxidase (GSH-Px) and SOD, and also increases lipid peroxidation in different cancer types (Abadi et al. 2018; Ammar et al. 2022; Fernandez-Gil et al. 2019; Guerra-Librero et al. 2021; Mihanfar et al. 2021). However, in nontumoral cells, melatonin reduces oxidative stress damage scavenging free radicals and increasing antioxidant enzyme activity.

3.3.2 Effect of melatonin on tumor metabolism (anti-Warburg effect)

Tumor metabolism has been the subject of numerous studies as it is one of the main characteristics that differentiate normal cells from tumor cells. The alteration of the metabolism in the tumor cell is related to the malignancy of these cells. In fact, tumor cells activate some metabolic pathways while inactivating others, increasing their proliferative capacity. Tumor cells undergo a metabolic reprogramming that allows them to meet the energy demand caused by the high rate of cell proliferation and maintain the redox balance inside the cell. Therefore, numerous studies have focused on studying tumor metabolism in recent years and it has even been proposed as a therapeutic target against cancer (DeBerardinis and Chandel 2016).

In 1956, Otto Warburg first described the mechanism by which tumor cells obtain energy. The metabolism of glucose, the central macronutrient, allows for energy to be

harnessed in the form of ATP through the oxidation of its carbon bonds. This process is essential for sustaining all mammalian life. In mammals, the end product can be lactate or, upon full oxidation of glucose via respiration in the mitochondria, CO_2. In tumors and other proliferating or developing cells, the rate of glucose uptake dramatically increases and lactate is produced (Liberti and Locasale 2016). Moreover, this characteristic makes tumor cells more susceptible to mitochondrial changes (Fulda, Galluzzi and Kroemer 2010).

The processes, collectively identified as the Warburg effect, are commonly associated with solid tumors and contribute significantly to their hardiness, invasiveness and their metastatic capability as well as rendering them resistant to radio and chemotherapies. Upregulation of glycolysis rate, as Warburg effect in cancer cell energy metabolism, could decrease the production of H_2O_2 and O_2^- by less reliance on mitochondrial OXPHOS (Ghanbari Movahed et al. 2019). Therefore, the inhibition of metabolic reprogramming could induce ROS production in tumor cells.

In this way, some authors suggest that melatonin can exert anti-Warburg effects. Specifically, it has been demonstrated that melatonin increases OXPHOS and inhibits glycolysis in cancer cells, resulting in increased ROS production (Chen et al. 2021; Guerra-Librero et al. 2021; He et al. 2020; Mao et al. 2016). Furthermore, it has been shown that melatonin inhibits HIF-1 in cancer cells, which is responsible for the overexpression of glycolytic enzymes, as well as the Myc oncogene in tumor cells, reversing metabolic reprogramming and increasing ROS production (Talib et al. 2021). However, the exact mechanism by which melatonin induces ROS production by inhibiting metabolic reprogramming in tumor cells is unknown.

Therefore, although it has been demonstrated the dual effect of melatonin, protecting normal cells from oxidative stress and inducing cancer cell death by increasing ROS production, the underlying mechanism for this difference is still unknown, being still necessary further investigation to understand the primitive mechanism by melatonin induce ROS production in cancer cells.

HYPOTHESIS AND OBJECTIVES

Considering tumor cells have an altered redox balance compared to normal cells, many antitumoral therapies are based on increasing ROS levels and decreasing antioxidant system capacity, leading to cancer cell apoptosis.

In this way, the ETS is the major source of ROS, and complexes I and III are generally regarded as the main ROS sources, whereas the contribution of intact complex II seems to be negligible. Recent studies have highlighted an important role for reverse electron transport in producing mtROS. RET occurs when the pool of CoQ is over-reduced with electrons from respiratory complex II. In the presence of a high proton motive force, complex I reduces NAD+ to NADH with electrons received from the ubiquinol pool, generating a high level of mtROS. All of these cellular alterations may lead to apoptosis. Moreover, complex I produces ROS in either the forward or reverse direction depending on the substrates used to feed the respiratory system, suggesting that a change in cell metabolism could induce RET in cancer cells.

In this way, previous studies by our Research Group have shown that melatonin increases apoptosis in HNSCC tumor cells and that, in turn, this effect is related to the inhibition of metabolic reprograming, which leads to an increase of mitochondrial function and ROS production. Moreover, various groups have reported, for many years, that high concentrations of melatonin can promote ROS generation, leading to cell death in a variety of cancers. However, it is still unclear the underlying mechanism by melatonin induces its oncostatic effects by increasing ROS production in tumor cells.

Based on the above, our hypothesis is that melatonin increases ROS production via RET on HNSCC tumor cells, leading to cancer cell death. Moreover, the increase in ROS production via RET could be induced by tumoral metabolic changes. The induction of metabolic change by melatonin treatment could produce an increase in bioenergetic

stress because of an uncoupling between ETS and oxidative phosphorylation, increasing the production of RET-ROS responsible, in turn, for activating cell death processes.

To verify this hypothesis, the objectives of this study were:

Principal objective:

To analyze the oncostatic mechanism of action of melatonin treatment in HNSCC Cal-27 and SCC-9 at the mitochondrial level.

Specifics Objectives:

- To analyze the correlation between melatonin pro-oxidant effects and the oncostatic effect of melatonin in Cal-27 and SCC-9 HNSCC cells.
- To study the capacity of melatonin to induce an uncoupling between mitochondrial respiration and oxidative phosphorylation in HNSCC cells.
- To analyze the implication of RET-ROS production on the oncostatic effect of melatonin.
- To analyze the influence of the metabolic changes produced by melatonin treatment on RET-ROS production in HNSCC cells.
- To verify the oncostatic mechanism of action of melatonin in Cal-27 cells expressing AOX *in vitro* and *in vivo*

MATERIALS AND METHODS

1. *In vitro* tests

1.1 Cells and treatments

Head and neck squamous cell lines have been used in this study. Two tongue cancer cell lines has been used, Cal-27 and SCC-9, obtained from the American Type Culture Collection (ATCC® CRL2095™ and CRL1629™ respectively) at the Cell Bank of the Scientific Instrumentation Center (CIC) of the University of Granada. The cells were cryopreserved in N_2 liquid in fetal bovine serum (FBS; 16000044, ThermoFisher Scientific, Madrid, Spain) at 5% DMSO.

Melatonin was prepared in a stock solution (aMT, 33457-24, Fagron Iberica S.A.U., Terrasa, Spain) at 40 mM in 15% propane-1,2-diol (24414.296, VWR, Radnor, PA, USA) in Dulbecco's phosphate buffer saline ([D]PBS, 14190094, ThermoFisher Scientific). This solution was sterilized by filtration (0.2 µm) and stored at room temperature (RT) protected from light.

1.1.1 Cell cultures

Cal-27 cells were cultured in Dulbeco's modified Eagle's medium (DMEM) with high glucose content and GlutaMAX™ supplement (41965039, ThermoFisher Scientific). The medium was supplemented with 10% FBS and 2% antibiotic/antimycotic solution (15240-062, LifeTechnologies, Carlsbad, California, USA).

SCC-9 cells were cultured in DMEM-F12 Nutrient Mixture Ham medium (1:1) supplemented with 10% FBS, 2% antibiotic/antimycotic, 0.4 µg/mL hydrocortisone (H6909, Sigma Aldrich, Madrid, Spain), L-glutamine 2 mM (25030081, ThermoFisher Scientific) and sodium pyruvate 0.5 mM.

Cells were kept in an incubator at 37°C with 5% CO_2 and 95% humidity. The medium was changed every 2-3 days until they reached 70-80% confluency, at which point subculture was performed. Moreover, mycoplasma test was performed to confirm that Cal-27 and SCC-9 cells using a PCR detection kit following the manufacturer's instructions (25235, LiliF Diagnostics, Burlington, MA, USA).

1.1.2 Melatonin treatment

When cells were at 60-70% of confluent, the culture medium was changed to FBS free medium. They were kept for 48 hours in serum deprivation and treated with different concentrations of melatonin (0, 500 and 1000 µM) for 48 hours. Vehicle was added to the control group. The experiments were carried out 24 and 48 hours after first melatonin treatment (Figure 11).

Figure 11. Melatonin treatment diagram.

Furthermore, to analyze the effect of melatonin in different mitochondrial parameters, specific compounds were used as melatonin pretreatment:

- To analyze the **prooxidant** effects of melatonin, N-acetylcysteine (NAC, A-8199, Sigma) was used at 5 mM, as a potent antioxidant.
- To analyze the effect of melatonin to regulate **mPTP opening**, cyclosporin A (CsA, SML1018, Sigma) was used at 1 µM, as a mPTP opening inhibitor.

- To analyze the effect of melatonin on the **mitochondrial function**, different inhibitors of mitochondrial respiration compounds were used (Table 1):

Table 1. Inhibitors of mitochondrial respiration compounds.

Compound	Function	Concentration	Reference
Rotenone (Rot)	CI inhibitor	Cal-27 (3 nM) and SCC-9 (9 nM)	R-8875, Sigma
Malonate (Malo)	CII inhibitor	Cal-27 and SCC-9 (10 mM)	M1296, Sigma
Thenoyltrifluoroacetone (TTFA)	CII inhibitor	Cal-27 and SCC-9 (50 μM)	T27006, Sigma
Antimycin A (Ant A)	CIII inhibitor	Cal-27 and SCC-9 (2 μM)	A-8674, Sigma
Potassium cyanide (KCN)	CIV inhibitor	Cal-27 (200 μM) and SCC-9 (300 μM)	207810, Sigma
Trifluorocarbonylcyanide Phenylhydrazone (FCCP)	mitochondrial oxidative phosphorylation uncoupler	Cal-27 and SCC-9 (200 nM)	C2920, Sigma

1.2 Measurement of ROS production and mitochondrial mass

1.2.1 Measurement of ROS production by fluorescence microscopy

Mitochondrial superoxide was detected using the fluorescent MitoSOX™ Red Reagent (M36008, ThermoFisher Scientific) and mitochondrial mass with the fluorescent MitoTracker™ Green FM (M7514, ThermoFisher Scientific). Superoxide production by mitochondria can be visualized under fluorescence microscopy using MitoSOX™ Red Reagent. The reagent penetrates in living cells, and in mitochondria it is

rapidly oxidized by superoxide. Other systems that generate ROS are enable to react with this reagent.

MitoTracker™ Green FM is a mitochondrial selective probe that binds covalently to mitochondrial proteins by reacting with cysteine residues and accumulates in the mitochondrial matrix. This reaction is independent of mitochondrial membrane potential and is used to represent mitochondrial mass.

Therefore, the combination of these two reagents gave us information about the colocalization of superoxides with the mitochondria.

Procedure

Cal-27 cells (6,000 cells) were seeded and treated in chamber slides (154534PK, ThermoFisher). After 48 hours of melatonin treatment the medium was removed, and cells were washed twice with DPBS. Then, they were incubated in complete medium with 5 µM MitoSox and 50 nM MitoTracker™ Green FM for 20 min at 37°C under 5% CO_2 and washed with DPBS. Fluorescence was assessed by fluorescence microscopy at 510/580 nm and at 488/30 nm (Nikon Eclipse Ni-U microscope).

1.2.2 Measurement of ROS production by fluorimetry

To verified results obtained with fluorescence microscopy, free radical levels were also measured using the 2',7'-dichlorohydrofluorescein diacetate probe (DCFH-DA; D6883, Sigma). DCFH is oxidized to 2',7'-dichlorofluorecein (DCF), which is a fluorescent compound. DCFH-DA enters cells through the cell membrane and, inside the cell, is deacetylated by intracellular esterases, producing DCFH. This molecule is oxidized by intracellular ROS, forming the highly fluorescent compound DCF (Figure 12).

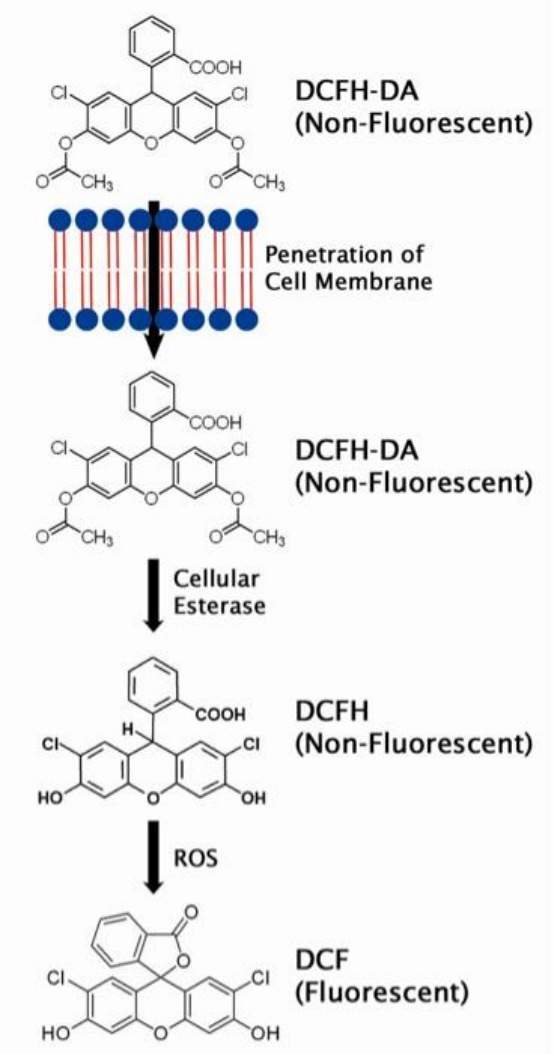

Figure 12. Mechanism of DCF Assay. (Cell Biolabs https://www.cellbiolabs.com/).

Procedure

Cells, already treated, were seeded the afternoon before the experiment in dark 96-well plates (236105, ThermoFisher Scientific) at a density of 10,000 cells per well. Each group was performed in triplicate. On the day of the experiment, the culture medium was replaced with phenol red free medium and DCFH-DA was added at 100 µM. Cells were then incubated for 30 minutes at 37°C. Subsequently, the cells were washed with PBS and Krebs-Ringer bicarbonate buffer was added. Fluorescence was measured with a FLx800 plate fluorimeter (Bio-Tek Instruments, Inc., Winooski, VT, USA) for 45

minutes in 5-minute intervals at 485 nm excitation and 530 nm emission.

1.3 Apoptosis analysis

Apoptosis is a process of programmed cell death. It was analyzed with an Annexin V-FICT/PI kit (ANXVKF-100T, Immunostep, Salamanca, Spain), following the manufacturer's instructions.

One of the ways to detect apoptosis in early stages is to check the localization of phosphatidylserine (PS) in the plasma membrane. PS is a type of phospholipid that in viable cells is maintained in the inner monolayer of the cell membrane. When the process of apoptosis begins to be triggered, PS is translocated to the outer layer of said membrane by means of flippases, offering a recognition mechanism for phagocytic cells. This localization can be easily detected since Annexin V specifically binds to PS in a calcium-dependent reaction. Annexin V molecules are labeled with different fluorophores such as fluorescein isothiocyanate (FITC). The samples are analyzed in the cytometer, providing an objective and rapid quantification. In late stages of apoptosis, when the plasma membrane has lost its integrity and DNA becomes accessible, large fluorescent molecules, such as propidium iodide (PI), binds to DNA by intercalating between the bases. With the data from both molecules, cells can be classified into non-apoptotic cells (annexin V-FICT negative/IP negative), cells in early apoptosis (annexin V-FICT positive/IP negative) and necrotic cells (annexin V-FICT positive/ PI positive).

Procedure

Cal-27 and SCC-9 cells were treated as described above. On the experiment day, cells (including dead cells) were harvested and washed twice with PBS at 37° C. Cells were then resuspended in 100 µL of 1X Annexin binding buffer. 5 µL of Annexin V-FITC and 5µL of PI were added, and the samples were incubated for 15 min at room temperature and protected from light. Finally, 400µL of Annexin 1X binding buffer was added. The cells were analyzed by flow cytometry in a Becton Dickinson FACSCanto II cytometer (Madrid, Spain) at the CIC of the University of Granada. Corresponding controls to determine flow cytometer compensation and quadrants were included in the assay (unlabeled cells, Annexin V-labeled cells only, and PI-labeled cells only).

1.4 Calcium retention capacity

The mPTP opening and its inhibition can be evaluated by determining the calcium retention capacity (CRC) of mitochondria to Calcium Green-5N, a low-affinity membrane impermeable dye that exhibits an increase in fluorescence emission intensity upon binding to calcium.

This assay is commonly performed by adding a fixed volume of calcium chloride to a mitochondrial sample at known intervals. Each addition causes a spike in signal that dissipates due to the uptake of calcium into the mitochondrial matrix. Opening of the mPTP collapses the mitochondrial membrane potential, which results in release of the accumulated calcium from the matrix, causing a sudden and sustained increase in fluorescence signal (Figure 13).

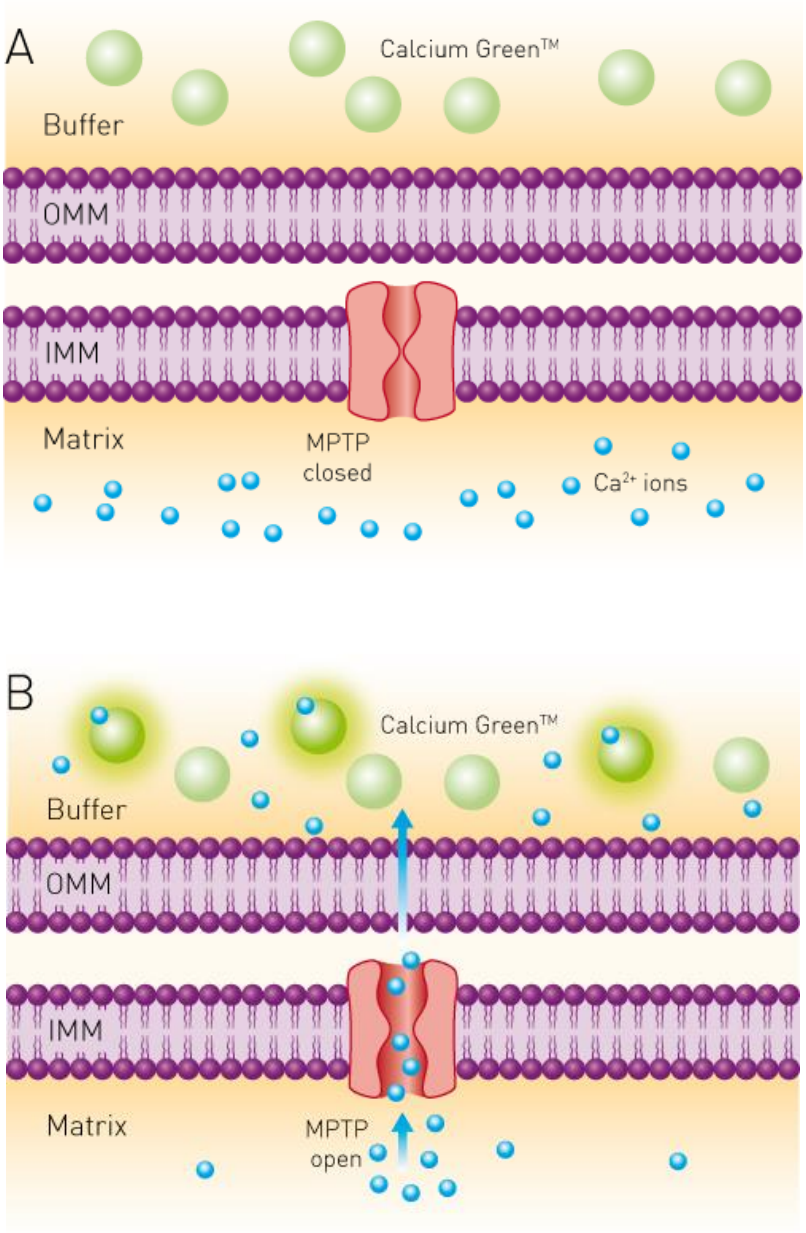

Figure 13. Principle of calcium retention assay. The membrane-impermeable Calcium Green reports on extra-mitochondrial Ca2+. (BMG Labtech https://www.bmglabtech.com/).

Procedure

First, $1 \cdot 10^6$ of trypan blue (15250-061, ThermoFisher Scientific) negative Cal-27 or SCC-9 cells were permeabilized by incubation under stirring for 2 min at 30°C in a medium containing 250 mM sucrose (S-0389, Sigma), 10 mM Tris-MOPS, 1 mM Pi-Tris supplemented with 100 µg/mL digitonin (D-145, Sigma). Then, to the permeabilized

cells, 0.25 µM of Calcium Green-5N (C3737, ThermoFisher Scientific) were added followed by 5 mM succinate in a final volume of 1 mL. The calcium retention capacity was measured by adding sequential 4 µM Ca^{2+} pulses until mPTP opening. Measurements of extramitochondrial Ca^{2+} were carried out fluorimetrically at 30°C using a PTI Quantamaster C61 spectrofluorimeter (excitation: 506 nm; emission: 530 nm) (Fontaine, Eriksson, et al. 1998; Fontaine, Ichas, and Bernardi 1998). Results were normalized by cells number whose viability was determined by trypan blue staining.

1.5 Determination of protein concentration

The protein concentration of the samples was determined by the Bradford method (Bradford, 1976) using Coomassie Blue G250 dye. The method consists of measuring the color conversion of the dye from brown to blue when its anionic groups interact with the amino groups of proteins.

Procedure

First, a standard line was prepared with BSA as standard, at increasing concentrations between 0.05 and 0.6 mg/mL. For the determination, 10 µL of each of the concentrations of the standard curve and of the samples were added to a 96-well plate. Each point of the curve and each sample were measured in duplicate. Subsequently, 200 µL of Bradford reagent (Bio-Rad, Hercules, CA, USA) were added. The mixture was incubated for 15 minutes at room temperature, with gentle agitation and protected from light. The absorbance measurement was performed with a plate spectrophotometer (Power Wave X-1, Bio-tek Instruments, VT, United States) at a wavelength of 595 nm. The results were expressed as mg of protein/mL.

1.6 Western blot analysis

Procedure

First, protein extraction was performed. For this, cell pellets were resuspended and sonicated in 60 µL of homogenization buffer, composed of Tris-HCl pH 7.6 50 nM, DTT (D0632, Sigma) 7.7 mg/mL, cocktail of protease and phosphatase inhibitors 100X and EDTA 100X (78429, ThermoFisher Scientific). Subsequently, it was centrifuged at a speed of 3,000 rpm for 20 minutes at 4ºC. Part of the supernatant was aliquoted for protein quantification, and the rest was transferred to a new tube. Then, loading buffer (10 mM Tris-HCl, 10% SDS, 20% 2-mercaptoethanol, 20% glycerol, 0.004% bromophenol blue) was added to this tube and the samples were incubated for 10 minutes at 99ºC and then kept at 4ºC for 5 minutes to denature proteins. Once the samples were prepared at the appropriate concentrations, the proteins were separated in 12 or 15% acrylamide/bis-acrylamide gels (1610159, BioRad, Hercules, California, USA), depending on the molecular weight of the protein of interest, by sodium dodecyl sulfate polyacrylamide gel electrophoresis (SDS-PAGE). After electrophoresis, the proteins were transferred to polyvinylidene difluoride membrane (PVDF, IPVH00010, Sigma).

Once the proteins were transferred to the membranes, they were incubated with blocking buffer containing 5% BSA in PBS with 0.1% Tween 20. They were then incubated with the primary antibody (Table 2) diluted in blocking buffer overnight at 4ºC. Following this incubation, the membranes were washed and incubated with the HRP-conjugated secondary antibodies at room temperature for 1 hour. Protein-antibody interaction was detected by chemiluminescence using the ECL™ Prime Western Blotting Detection Reagent (GERPN2232, GE Healthcare Life Sciences, Barcelona, Spain) following the manufacturer's instructions. The image was digitized with ChemiDoc MP Imaging System

(BioRad) and the bands were quantified using Image J software. The intensity of the bands obtained in the detection of the proteins of interest were normalized to GAPDH or β-tubulin for whole cells samples and to VDAC (voltage-dependent anion channel) for the mitochondrial fraction. Data were expressed relative to the control group.

Table 2: Antibodies reference.

Rabbit Phospho-Acetyl-CoA Carboxylase (Ser79) Antibody (anti-P-ACC), 1:1000	Cell signaling, MA, USA	3661S
Rabbit Acetyl-CoA Carboxylase Antibody (anti-ACC), 1:1000	Cell signaling	3662S
Rabbit Phospho-AMPKα (Thr172) Antibody (anti-P-AMPK), 1:1000	Cell signaling	2531S
Rabbit AMPKα Antibody (anti-AMPK), 1:1000	Cell signaling	2532S
Mouse Total OXPHOS Rodent WB Antibody Cocktail (anti-OXPHOS), 1:1000	Abcam	ab110413
Rabbit Anti-UCP1 antibody, (anti-UCP1), 1:1000	Sigma	U6382
Rabbit UCP2 Polyclonal Antibody (anti-UCP2), 1:250	Proteintech, Manchester, UK	11081-1-1AP
Rabbit UCP3 Polyclonal antibody (anti-UCP3), 1:2500	Proteintech	10750-1-AP
Mouse ACADM/MCAD antibody [3B7BH7] (anti-MCAD),	Abcam	ab110296
Mouse EHHADH (D-2) (anti-EHHADH), 1:500	Santa Cruz, Heidelberg, Germany	sc-393123
Mouse VDAC1/Porin antibody [20B12AF2] (anti-VDAC), 1:5000	Abcam	ab14734
Rabbit β-Tubulin Antibody (anti-B-tubulin), 1:1000	Cell signaling	2146
Mouse GAPDH Antibody (H-12) (anti-GAPDH), 1:500	Santa Cruz	sc-166574
HRP Goat Anti-Mouse Ig (anti-mouse), 1:1000	BD Pharmigenarticulo, San Jose, CA, USA	554002
Goat anti-Rabbit IgG (H+L) Secondary Antibody, HRP (anti-rabbit), 1:2000	ThermoFisher Scientific	31460

1.7 Electron transport system complex activity assays

Mitochondrial respiratory system activities for each complex were measured using kits from Abcam according to the manufacturers' instructions: complex I, II, II+III, IV and V (ab109721, ab109908, ab109905, ab109911 and ab109714, Abcam, Cambridge, UK). These protocols consist on target enzymes, which are first immunocaptured from cell samples before subsequent functional analysis (Figure 14). Moreover, these ELISA kits utilize highly validated monoclonal antibodies and proprietary buffers, which are able to capture even very large enzyme complexes in their fully-intact, functionally-active states. After the target has been immobilized in the well, substrate is added, and enzyme activity is analyzed by measuring the change in absorbance of either the substrate or the product of the reaction, depending upon which enzyme is being analyzed:

- **To complex I:** the production of oxidizes NAD+ by complex I is coupled with the oxidation of diaminobenzidine (DAB) to form a red-colored precipitate, increasing the absorbance at OD450 nm.
- **To complex II:** the production of ubiquinol by the enzyme is coupled to the reduction of the dye DCPIP (2,6- diclorophenolindophenol) and a decrease in its absorbance at OD600 nm which in turn recycles the substrate ubiquinone.
- **To complex II+III:** the rate of coupled complex II + III reaction is measured by monitoring the conversion of oxidized cytochrome c into reduced form, which can be observed as increase in absorbance at OD 550 nm.
- **To complex IV:** activity is determined colorimetricaly by following the oxidation of reduced cytochrome c as an absorbance decrease at 550 nm.
- **To complex V:** the conversion of ADP to ATP by ATP synthase is coupled to the

oxidation reaction of NADH to NAD+ with a reduction in absorbance at 340 nm.

By analyzing the enzyme's activity in an isolated context, outside of the cell and free from any other variables, an accurate measurement of the enzyme's functional state can be understood.

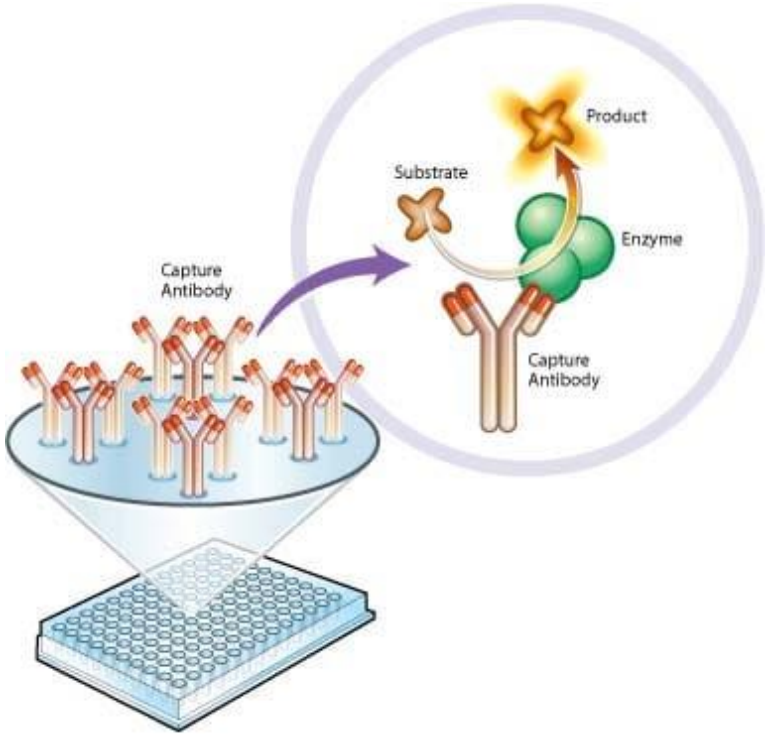

Figure 14. Principle of enzyme activity assay. Capture antibodies are pre-coated in the wells of microplates. After the target has been immobilized in the well, substrate is added, and enzyme activity is analyzed by measuring the change in absorbance of either the substrate or the product of the reaction (depending upon which enzyme is being analyzed). By analyzing the enzyme's activity in an isolated context, outside of the cell and free from any other variables, an accurate measurement of the enzyme's functional state can be understood. (Abcam https://www.abcam.com/).

Procedure

Cal-27 cells cultures were added to the microplate wells which have been precoated with capture antibodies specific for each mitochondrial respiratory system complex. After the target has been immobilized in the well, the complex activity was determined by following the oxidation and reduction of complex-specific substrates and

a dye. The absorbance (450 nm (complex I), 600 nm (complex II), 550 nm (complex II+III), 550 nm (complex IV) and 340 nm (complex V)) were measured at specific optical densities (OD) using a microplate reader spectrophotometer (Power Wave X-1; Bio-Tek Instruments, Inc., Winooski, VT, USA).

1.8 Measurement of mitochondrial respiration

Given that the mitochondrial respiration is more physiologically relevant than isolated mitochondria due to preserving their essential interactions with other intracellular systems, we decided to analyze mitochondrial respiration in Cal-27 cells using SeaHorse Analyzer and a Clark oxygen electrode. These different and complementary analyzers allowed us to achieve a precise information about the mitochondrial respiration.

1.8.1 Measurement of oxygen consumption rate by SeaHorse

First, the oxygen consumption rate (OCR) was measured with the XF24 Extracellular Flux Analyzer (Seahorse Bioscience, Copenhagen, Denmark), using a system that allows determining the mitochondrial bioenergetics of cells *in vitro*.

The oxygen consumed by the cell can be at the mitochondrial level (mitochondrial respiration) or it can be consumed without the participation of the mitochondria (non-mitochondrial respiration). Regarding to mitochondrial respiration, part of the oxygen consumed by the mitochondria is used for the production of ATP, through ATP-synthase, and another part is independent of oxidative phosphorylation (Proton Leak), as shown in Figure 15.

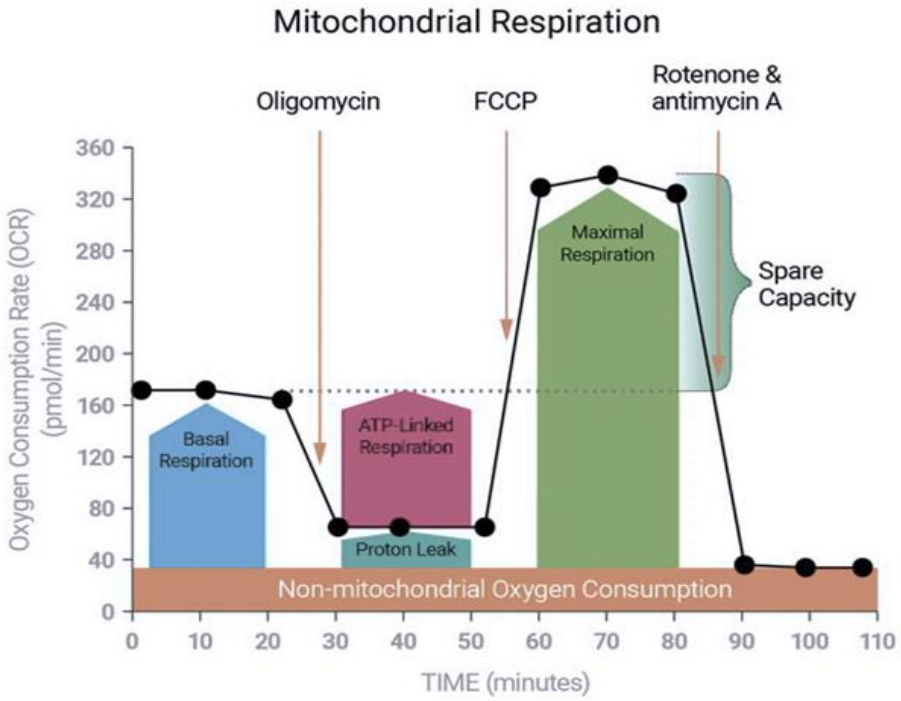

Figure 15. Representative schematic of the experimental design used in the breathing experiments. The fundamental parameters of mitochondrial function are shown: basal respiration, ATP production, proton escape, maximal respiration, and non-mitochondrial respiration. (Agilent Seahorse https://www.agilent.com/).

To analyze mitochondrial bioenergetics, it is necessary to determine a series of mitochondrial parameters. First, basal oxygen consumption is analyzed in the absence of inhibitors. Second, the Proton Leak is measured in presence of oligomycin, an ATP-synthase inhibitor. From the measurement of the electron escape, the production of ATP is estimated, and expressed as a percentage of the basal mitochondrial respiration that is not destined to maintain the proton escape. Third, the maximum respiratory capacity or capacity of the electron transfer system (ETS) is determined. To do this, FCCP, an oxidative phosphorylation uncoupler, is added. Finally, the oxygen consumption not dependent on the mitochondria is determined. For it, Antimycin A and rotenone, complex III and complex I inhibitors respectively, are injected (Figure 15).

Procedure

The day before the assay, cells were seeded in a 24-well Seahorse XF24 Cell Culture Microplates (Agilent, Santa Clara, CA, USA) at a density of 80,000 cells per well. Wells intended for internal SeaHorse corrections were left free without cells. Cells were incubated overnight in fresh culture medium. On the day of the assay, the cells medium was changed to base medium (103334-100, Seahorse Bioscience) supplemented with 10 mM glucose (D8375, Sigma), 5 mM pyruvate, and 2 mM glutamine. Cells were incubated for one hour at 37°C without CO_2.

For the analysis of mitochondrial respiration, three consecutive measurements of basal oxygen consumption were performed. The different inhibitors were then injected in the following order:

1. Port A: 75 µL of 8 µM oligomycin to obtain a final concentration in each well of 1 µM.
2. Port B: 75 µL of 4.5 µM FCCP to obtain a final concentration in each well of 0.5 µM.
3. Port C: 75 µL of 5 µM FCCP to obtain a final concentration in each well of 0.5 µM.
4. Port D: 75 µL of 11 µM antimycin A and 11 µM rotenone to obtain a final concentration in each well of 1 µM of both compounds.

The results are expressed as the rate of oxygen consumed normalized by protein content measured by Bradford assay (OCR, in pmol O_2/min/mg proteins).

1.8.2 Measurement of oxygen consumption rate by Clark oxygen electrode

Procedure

To further confirmation, OCR was also measured into a thermostatically controlled oxygraph vessel equipped with a Clark oxygen electrode at 37°C (Strathkelvin MS200A system). Cal-27 cells, at a density of $1 \cdot 10^7$, were added in the oxygraph chamber containing DMEM-F12 medium at a final volume of 500 µL. Results were normalized by cell number, and viability was determined using trypan blue staining.

1.8.3 Measurement of mitochondrial respiration in digitonin-permeabilized cells by Clark oxygen electrode

The measurement of OCR in intact cell has the inconvenient that you can lose information of what happens with CI and CII respiration by itself. By treating cells with specific detergents, such as digitonin, it is possible to produce membrane permeabilization by promoting loss of lipid content, although without losing important intracellular proteins; allowing to follow the state of mitochondrial respiration in the presence of different substrates (Gao et al. 2020):

- **State 2:** Mitochondrial respiration stimulated by the substrate of each specific complex: **glutamate/malate** as the subtract of complex I or **succinate** as the subtract of complex II.
- **State 3:** Mitochondrial respiration initiated by adding ADP in the presence of substrate.

- **State 4:** Mitochondrial respiration in the absence of ATP synthesis, which is uncoupled with the Oligmycin A.
- **Maximal respiration**: Mitochondrial respiration triggered by FCCP.

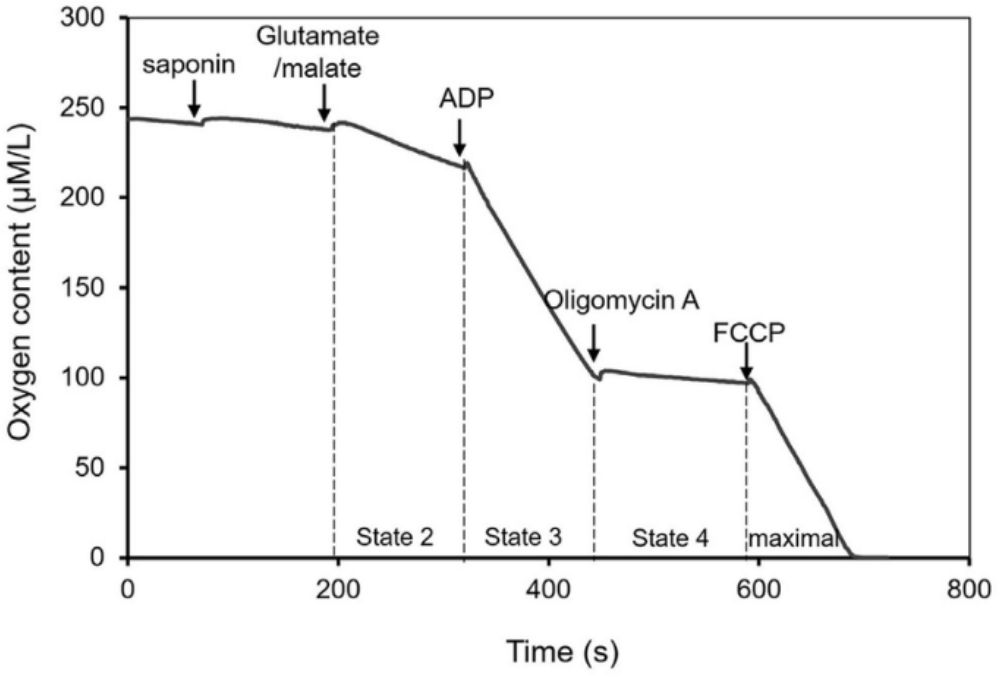

Figure 16. Representative trace of mitochondrial respiration in permeabilized cells. The slope of trace represents the different state of mitochondrial respiration. State 2: Mitochondrial respiration stimulated by the substrate in the absence of and added ADP; State 3: Mitochondrial respiration initiated by adding ADP in the presence of substrate; State 4: Mitochondrial respiration in the absence of ATP synthesis, which is uncoupled with the Oligmycin A. Maximal respiration: Mitochondrial respiration triggered by FCCP. (Gao, Li, Qin, Liu, & Gong, 2020).

Procedure

Oxygen consumption was measured in a thermostatically controlled oxygraph vessel equipped with a Clark oxygen electrode at 37°C. The Cal-27 cell suspension, which was prepared in respiration buffer (KET buffer: KCl 125 mM, EGTA 1 mM, Tris 20 mM). Cal-27 cells ($1 \cdot 10^7$), was added to the oxygraph chamber containing respiration buffer supplemented with 5 mM inorganic phosphate. The final volume was 500 µL. The experiment was begun with the addition of 100 µg/mL digitonin and either 5 mM

glutamate plus 2.5 mM malate or 5 mM succinate plus 1 µM rotenone, followed by the addition of 500 µM adenosine diphosphate (ADP; state 3) (Figure 16). Finally, 0.16 µg/mL oligomycin is added to determine the state 4. Results were normalized by cell number, with viability determined using trypan blue staining.

1.9 Determination of adenosine triphosphate levels

ATP concentration was determined using the ATP assay kit (ab83355, abcam) according to the manufacturer instructions. The assay is based on the phosphorylation of glycerol in order to generate a product that can be easily quantified fluorometrically (Ex/Em = 535/587 nm).

Procedure

First, 1 x 10^6 Cal-27 cells were harvested and washed with cold DPBS. Then cells were resuspending in an ATP Assay Buffer and homogenize by pipetting up and down a few times. Supernatants were collected after centrifugation for 5 minutes at 4°C at 13,000 *g*. Then samples were deproteinization using perchloric acid (PCA) 4 M and potassium hydroxide (KOH), 2 M.

At the time of the experiment, the ATP standard dilution (to generate the standard curve) and the reaction mix was added according to the manufacturer instructions. After 30 minutes of samples incubation, ATP levels were measured with a microplate fluorescence reader FLx800 (Bio-Tek Instruments, Inc., Winooski, VT, USA) at 535 nm to excitation and 587 nm to emission. Values of ATP levels were determined by using ATP standard curve. ATP concentration was normalized by protein content measured by Bradford assay.

1.10 Determination of CoQ_{10} and $CoQ_{10}H_2$ by liquid chromatography-mass spectrometer (UPLC-MS/MS)

Procedure

CoQ_{10} pools were extracted as previously described (Mao et al. 2021). After trypsinization, cells were quickly washed once in serum-free culture medium to remove serum-derived CoQ_{10} and $CoQ_{10}H_2$. We added freshly prepared ice-cold 1-propanol containing 100 µM tert-butyl-hydroquinone (112.941, Sigma) to the plates, which were then placed on a cold plate on ice. The cells were scraped with a cell lifter, vortexed and centrifuged. The supernatant extracts were stored on dry ice in the dark until analysis by liquid chromatography with mass spectrometry (UPLC–MS/MS). Samples were separated through a 30 min elution on an Acquity BEH C18, 10*2.1 mm, 1.7 µm particle size—Waters). Mobile phase A consisted of water with 0.1% formic acid with 10 mM ammonium acetate and 0.1% acetic acid; mobile phase B consisted of methanol with 2 mM ammonium acetate. The gradient was 0 min, 70% B; 8 min, 100% B; 26 min, 70% B; 30 min, 70% B. The injection volume was 20 µL. The column temperature was set to 45°C, and the flow rate was 300 µL/min. The UHPLC system was coupled online with a Q Exactive Focus mass spectrometer (Thermo, San Jose, CA, USA) as previously described (González-García et al. 2020). Scanning in Full MS mode (2 µscans) at 70,000 resolutions from 800 to 1000 m/z. Calibration was performed before each analysis using a positive calibration mix (Piercenet—Thermo Fisher, Rockford, IL, USA). Data were analyzed using Tracefinder 4.1 software (Thermo, San Jose, CA, USA). Analyte retention times were confirmed by comparison with external standard retention times.

1.11 Mitochondrial parameters analysis

1.11.1 Mitochondrial membrane potential analysis

Mitochondrial membrane potential was measured by fluorometric analysis using tetramethylrhodamine ethyl ester (TMRE, ab113852, Abcam), a cell permeant positively charged red-orange dye, that readily accumulates in active mitochondria because of their relative negative charge.

Procedure

Cells were seeded the night before in 96-well culture plates at $1 \cdot 10^4$ cells per well. Cells were incubated for 10 min at 37°C under 5% CO_2 with PBS for the experimental group or with 20 µM FCCP for positive control. Then, 400 nM of TMRE was added, and cells were incubated for 20 min at 37°C under 5% CO_2. Mitochondrial membrane potential was measured with the microplate fluorescence reader FLx800 (Bio-Tek Instruments) at 549 nm to excitation and 575 nm to emission.

1.11.2 Mitochondrial mass analysis by flow cytometry

After analyzed mitochondrial membrane potential and to discard that the effect in this parameter is due to a modification of mitochondrial mass we decided to quantified mitochondrial mass using MitoTracker™ Green FM. As it is described above, this compound is used to represent mitochondrial mass since it is a mitochondrial selective probe that accumulates in the mitochondrial matrix, independently of mitochondrial membrane potential.

Procedure

Cal-27 cell suspensions were incubated in the presence of 50 nM of MitoTracker™ Green FM for mitochondrial mass measurement for 15 min in a 5% CO_2 humidified atmosphere at 37°C and protected from light. Then, they were immediately analyzed by FACS (BD LSR FORTESSA, Becton Dickinson, Le Pont-de-Claix, France) at 488 nm to excitation and 530 nm to emission.

1.12 Determination of tricarboxylic acid (TCA) cycle intermediates by liquid chromatography–mass spectrometer (UPLC-MS/MS)

TCA intermediates were extracted as previously described (Al Kadhi et al. 2017). After trypsinization, cell suspensions were centrifuged. Once discarded the supernatant, cells were gently suspended by adding 10 ml of 0.9% sodium chloride before centrifugation. The supernatant was then removed and 0.5 ml of perchloric acid (0.3 mM) was added. The mixture was kept on ice for 10 minutes followed by further centrifugation at higher speed of 12,000 ×*g* for 10 minutes. Supernatant was then transferred to UPLC vials and kept at −20°C until analysis by liquid chromatography with mass spectrometry (UPLC-MS/MS). Samples were separated through 10 min elution on an Acquity UPLC BEH C18, 100 × 2.1 mm, 1.7µm particle size—Waters with an oven temperature of 40°C. Mobile phase A consisted of water with 0.1% formic acid; mobile phase B consisted of acetonitrile. The gradient was 0 min, 0% B; 8 min, 85% B; 8.1 min, 0% B. The injection volume was 10 µL. Separation was achieved using a gradient program at a flow rate was 400 µL/min. Data were acquired with MassLynx 4.0 software

and calibrated and quantified by QuanLynx software. Analyte retention times were confirmed by comparison with external standard retention times.

1.13 NAD/NADH quantification

NAD levels were measured using NAD/NADH assay kit (ab221821, Abcam) according to the instructions of the manufacturer. NAD/NADH Assay Kit II (Colorimetric) provides a sensitive and robust method to measure NAD+, NADH and their ratio in mammalian cell lysates. The assay is based on an ADH and diaphorase coupled-reaction that convers WST-1 to WST-1 formazan, which can be easily detected at OD 450 nm (Figure 17). As the reaction is not stopped, it is necessary to monitor the absorbance increase of WST-1 formazan at regular intervals after the reaction is initiated to determine the reaction velocity.

This assay requires purification of NAD+ and NADH from the cell lysates, which raises the efficiency of the reaction and increases the detection sensitivity.

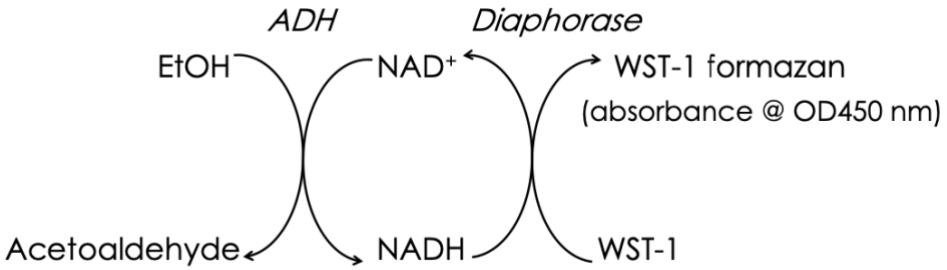

Figure 17. Basis of the method to determine NAD/NADH by WST-1 formazan. (Abcam https://www.abcam.com/).

Procedure

First, 1 x 10^6 Cal-27 cells were collected and washed with cold DPBS. Then, pellets were collected after centrifugation for 5 mins at 4°C at 2,000 rpm.

- For **NAD+ Acid extraction,** samples were incubated with 0.5 M perchloric acid (HClO4) for 30 minutes on ice. Then, 0.55 M K2CO3 for neutralization solution were used to extract NAD+.
- For **NADH alkaline extraction**, samples were incubated with 50 mM NaOH + 1 mM EDTA at 60°C for 30 minutes to reduce viscosity. Then, it was neutralized with 0.3 M Potassium Phosphate Buffer (pH 7.4).

At the time of the experiment, the NADH standard dilution (to generate the standard curve) and the reaction mix was added according to the manufacturer instructions.

NAD+ and NADH levels were measured with a microplate reader spectrophotometer (Power Wave X-1; Bio-Tek Instruments, Inc., Winooski, VT, USA) at 450 nm in kinetic mode for 30-90 mins at 10 mins intervals at room temperature, protected from light. Values of NAD+ and NADH levels were determined from a standard calibration curve according to the manufacturer's instructions. NAD+ and NADH concentration was normalized by protein content measured by Bradford assay.

1.14 Evaluation of supercomplexes (SCs) formation by BNGE

In contrast to sodium dodecyl sulfate (SDS)-PAGE, BN-PAGE allows protein separation under native conditions and preserves protein-protein interactions, which is

fundamental for studying SCs. Following solubilization of mitochondria and centrifugation, the anionic dye Coomassie G-250 sample additive was added to the supernatant. This dye is sufficiently soluble in water, but it can also bind to membrane proteins because of its hydrophobic properties. Binding a large number of dye molecules imposes a charge shift on the proteins that causes even basic proteins to migrate to the anode during the electrophoresis step of BN-PAGE. Here, proteins were not separated according to the charge/mass ratio but according to size in acrylamide gradient gels. Protein migration gradually decelerated with running distance and with decreasing pore size of the gradient gel. Individual proteins stopped migrating almost completely when they approach their size-dependent specific pore-size limit during BN-PAGE. Because negatively charged protein surfaces repel each other, the tendency of membrane proteins to aggregate was considerably reduced. Furthermore, membrane surfaces lost their hydrophobic character upon binding the dye, which converts membrane proteins into water-soluble proteins. This means that no detergent was required in the BN gels once Coomassie dye has occupied the protein surfaces. Therefore, the risk of denaturation of detergent-sensitive proteins was minimized during BN-PAGE (Jha, Wang, and Auwerx 2016).

Procedure

Blue native gel electrophoresis (BNGE) was performed on crude mitochondrial fraction from, approximately, 2 X 10^6 cells Cal-27 treated cells. One aliquot of mitochondrial fraction was used to protein determination by Bradford analyses. The remaining samples were then centrifuged at 13,000 x *g* for 3 min at 4ºC. The mitochondrial pellets were suspended in an appropriate volume of medium C (1 M

aminocaproic acid, 50 mM Bris-Tris-HCl, pH 7.0), and membrane proteins were solubilized with digitonin (4 g/g) and incubated for 10 min in ice. Then, the suspension was centrifugated at 13,000 x *g* for 30 min at 4ºC, and the supernatants were collected. 3 µL of 5% Brillant Blue G dye prepared in 1 M aminocaproic acids was added to the samples. Then, 100 µg of mitochondrial proteins were loaded and run on a 3-13 % gradient native gels as previously described (Hidalgo-Gutiérrez et al. 2019). After electrophoresis, the complexes were electroblotted onto PVDF membranes and sequentially tested with specific antibodies against CI, anti-NDUFA9 (ab14713, abcam), CIII, anti-ubiquinol-cytochrome c reductasa core protein I (ab14713, abcam), CIV, anti-COX IV (ab14744, abcam). Results were normalized by VDAC1.

1.15 Production of alternative oxidase (AOX) stable lines

In normal conditions, the AOX is inactive and, thus, does not interfere with the normal electron flow from complex I to complex IV. However, in some situations, when the quinone pool becomes highly reduced which activates the AOX, the activation of the AOX in these situations allows to prevent the over-reduction of the ubiquinone pool and, thus, ROS overproduction (Figure 18).

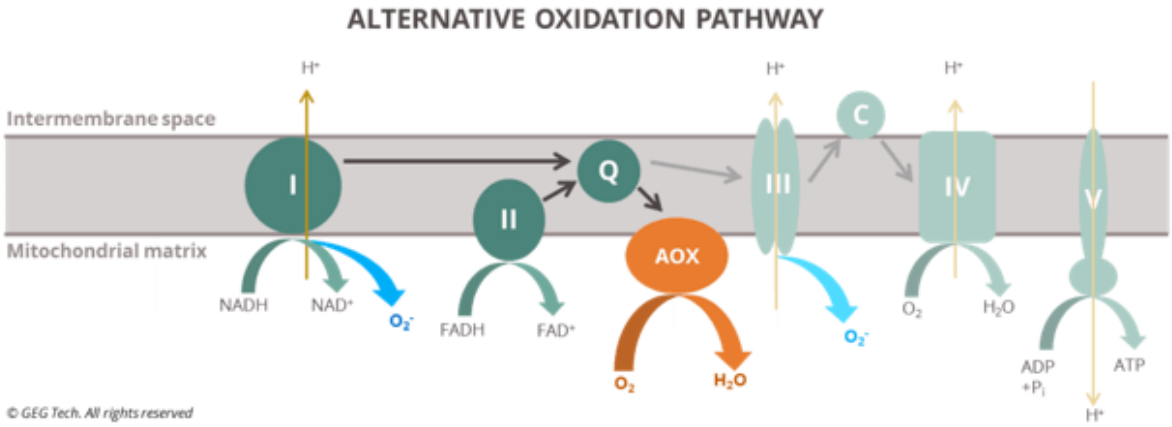

Figure 18. Representative scheme of the bypass of ETS by AOX. In the electro transport system electrons come from complex I and complex II to CoQ reducing it to $CoQH_2$. Then, $CoQH_2$ transfer electrons to complex III. However, AOX can oxidized $CoQH_2$ to CoQ by directly reducing O_2 to H_2O, bypassing of the complex III-IV-V segment of the respiratory and reducing $CoQH_2$ levels. (GEG Tech https://www.geg-tech.com/).

Procedure

Lentiviral vectors carrying the cDNA encoding AOX gene (sequence from Ciona intestinalis genome, DM193474.1, 1110 pb) were used to generate a Cal-27 cell line expressing AOX. Lentiviral vectors were purchased from GEG Tech. The AOX stable cell line was established by transducing Cal-27 cells with purified virus: $4 \cdot 10^5$ TU for $7.5 \cdot 10^5$ cells in 100 µL. Single cell colonies were established by adding 0.5 cells per well in a 96-culture plate. To confirm positive AOX cell lines, cellular mRNA was extracted from cultured cell samples using the RNA Purification Kit (74136, Qiagen, Barcelona, Spain) according to the manufacturer's instructions. The transmission of the AOX transgene was verified by qPCR on cDNA using AOXopt-F (GGATGAGCCCAATATCGAAG) and AOXopt-R (CTGAAACGAAAATGCCTTGG) primers (ThermoFisher Scientific). AOX protein expression also was confirmed by western blotting using anti-AOX antibody purchased from Carole Sellem (Institute for Integrative Biology of the Cell, University of Paris-Saclay, Paris).

1.16 Cell proliferation assay

The amount of DNA in each cell remains constant for a given cell line or cell type, so assays based on DNA content can be used to provide an accurate and simple measure of cell number.

Procedure

Cell proliferation was evaluated using the CyQuant assay (C7026, ThermoFisher Scientific). CyQUANT GR dye binds to cellular nucleic acids, allowing cell numbers to be calculated from a standard curve. CyQuant assay was performed following the manufacturer's instructions. Fluorescence was measured (excitation, 480 nm; emission, 520 nm) using a microplate fluorescence reader FLx800 (Bio-Tek Instruments, Inc., Winooski, VT, USA) and compared with a standard curve for cell number determination.

2. *In vivo* assays

All experiments were carried out following the protocol approved by the Institutional Committee for the Use and Care of Animals of the University of Granada (procedures 11-CEEA-OH-2013), developed in accordance with the European Convention for the Protection of Animals. Vertebrate animals used in experiments and other scientific purposes (CETS #123) and Spanish legislation (RD 53/2013).

2.1 Xenografts in mice

This study was conducted using 5- to 6-week-old athymic (nu/nu) nude mice (Janvier Labs, France) housed in appropriate sterile filter-capped cages and fed and given water *ad libitum*. Cell viability was assessed using the trypan blue exclusion test, and then suspensions of the HNSCC cell line Cal-27 as wild type or expressing AOX were subcutaneously (s.c.) transplanted into the left flanks of the mice at a $4x10^6$/0.2 mL in phenol red free DMEM.

Tumor size was measured twice a week with the help of a Vernier caliper, measuring two perpendicular diameters of each tumor in triplicate and its volume was calculated using the following formula:

$$\text{Tumor volume} = \text{length} \times \text{width}^2 / 2$$

Tumor length was the longest dimension and width the dimension perpendicular to length. When the tumors reached a volume of 100 mm^3, treatment was started (Y. Q. Shen et al. 2018).

2.2 Melatonin treatment

Mice were randomly divided into two groups, control group and mice treated with melatonin 3% administered by intratumorally injection 6 days per week for 35 days (Figure 19). Melatonin was dissolved in propane-1,2-diol and then diluted at 37.5% in saline solution.

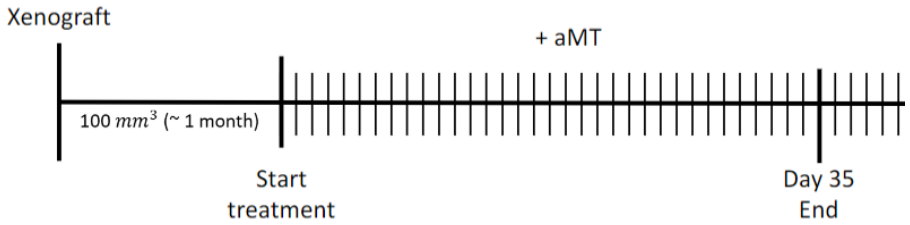

Figure 19. Melatonin treatment diagram.

2.3 Measurement of protein oxidation by western blot

Tumor ROS production was indirect measured by protein carbonyl assay kit (ab178020, Abcam), which is designed for the measurement of protein carbonyl groups that are created by the oxidation of proteins. This can be through reaction with ozone or oxides of nitrogen, or by metal catalyzed oxidation. In the protein carbonyl assay protocol, carbonyl groups in protein side chains are derivatized to 2,4-dinitrophenylhydrazone (DNP-hydrazone) by reaction with 2,4-dinitrophenylhydrazine (DNPH). The DNP moieties are detected by WB. The oxidative status of each protein can be compared between samples.

Procedure

Samples were prepared according to manufacturer´s instruction with all the reagents provided in oxidised protein western blot detection kit (ab178020, Abcam).

The DNP-derivatized protein samples were separated by polyacrylamide gel electrophoresis followed by Western blotting as explained in section 1.6. Then, the membranes were incubated with primary antibody, specific to the DNP moiety of the proteins. This step was followed by incubation with an HRP-conjugated secondary detector antibody specific for the primary antibody (which for this kit is a goat anti-rabbit IgG). Finally, the membranes are then treated with chemiluminescent reagents (luminol and enhancer). The image was digitized with ChemiDoc MP Imaging System (BioRad) and the bands were quantified using Image J software. The intensity of the bands obtained in the detection of the proteins of interest were normalized to GAPDH. Data were expressed relative to the control group.

2.4 TUNEL assay

First, the animals were perfused with saline solution and then with 3.7–4% neutral buffered paraformaldehyde (PFA, 252931-1215, Panreac AppliChem, Castellar del Vallès, Spain). Once perfused, the tumors were resected, and they were immersed in formaldehyde for 48 hours, ensuring that they maintained their original shape. After this incubation, tumors were dehydrated in 30% sucrose and embedded in OCT.

Apoptosis was evaluated using the DeadEnd Fluorometric TUNEL system (G3250, Promega, Madison, WI, USA) in tumor tissue sections following the manufacturer's indications. Hoechst (33342, Invitrogen, ThermoFisher Scientific, Waltham, MA, USA) was used to stain the nuclei. Image were acquired with a fluorescence microscopy (Nikon Eclipse Ni-U microscope). Quantification of TUNEL+ per field was done using 5 random fields per slide. Image were analyses with ImageJ software (Free Software Foundation Inc., Boston, MA, USA).

3. Statistical analysis

All statistical analyses were performed using Prism 8 scientific software (GraphPad Software Inc.). Unpaired Student's t tests were used to compare differences between experimental groups and their respective untreated controls. Data were expressed as the mean ± standard error of the mean of a minimum of three independent experiments. A $p < 0.05$ was considered statistically significant.

RESULTS

Part of the results shown in this section are included in the following article:

Florido J, Martínez-Ruiz L, Rodriguez-Santana C, López-Rodríguez A, Hidalgo-Gutierrez A, Cottet-Rousselle C, Lamarche F, Schlattner U, Guerra-Librero A, Aranda-Martínez P, López LC, Escames G. Melatonin drives apoptosis in head and neck cancer by increasing mitochondrial ROS generated via reverse electron transport.

Journal of Pineal Research, 2022

1. Melatonin induces apoptosis via ROS-dependent production

As the direct oncostatic effects of melatonin correlate with increased ROS levels and increased apoptosis in HNSCC (Guerra-Librero et al. 2021), we first analyzed ROS levels by MitoSox-Red and MitoTracker green fluorescent staining (Figure 20A) and fluorometric techniques (Figure 20B). Consistent with previous findings (Fernández-Gil et al. 2019; Guerra-Librero et al. 2021; Y. Q. Shen et al. 2018), melatonin treatment induced an increase in ROS production in Cal-27 cells, especially after 48 h at 500 or 1000 µM (Figure 20A,B), which correlated with a marked increase in apoptosis (Figure 20C). Similar results were obtained in SCC-9 cells (Figure 21A,B). Of note, pretreating cancer cells with N-acetylcysteine (NAC) at 5 mM to scavenge ROS (Figure 20D) inhibited melatonin induced apoptosis (Figure 20E).

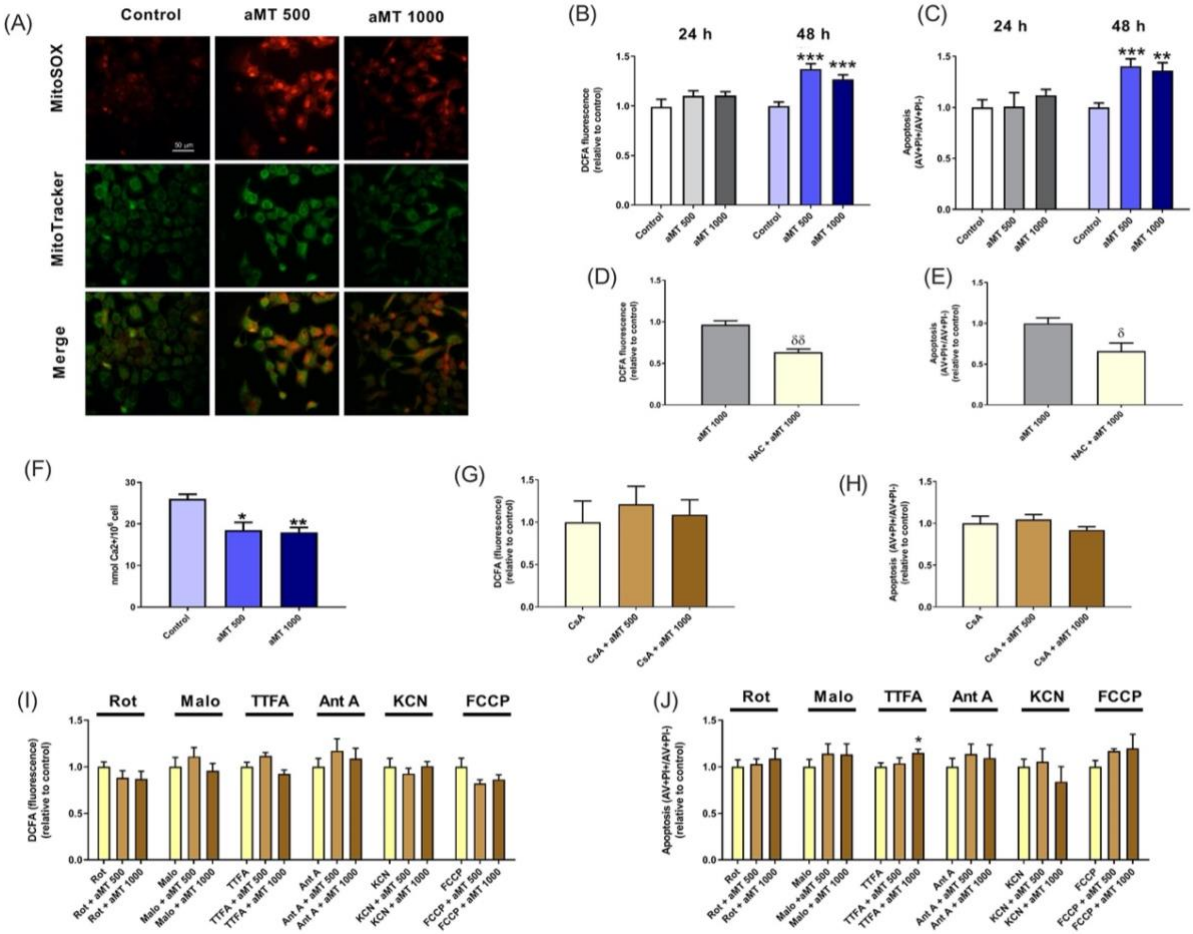

Figure 20. mtROS production drives melatonin-induced proapoptotic effects in Cal-27. (A) ROS (red) and mitochondria (green) detected by fluorescence microscopy after incubation with MitoSox-Red (5 µM) and MitoTracker (50 nM) for 20 min in Cal-27 cells treated with melatonin (aMT) for 48 h. Scale bar = 50 µm. (B) Measurements of intracellular ROS levels by fluorimetry after staining with the DCFA fluorescent probe after 24 and 48 h of melatonin treatment. (C) Apoptosis level (AV+/PI+ and AV+/PI−) analyzed by flow cytometry after 24 and 48 h of melatonin treatment. For (A–C), treatment groups included vehicle (control) and melatonin (aMT) at a concentration of 500 or 1000 µM for 24 h (gray range) or 48 h (blue range) in Cal-27 cells. (D) Measurements of intracellular ROS levels by fluorimetry after staining with the DCF fluorescent probe in Cal-27 cells treated with melatonin at 1000 µM alone and pretreated with NAC 5 mM. (E) Apoptosis level (AV+/PI+ and AV+/PI−) analyzed by flow cytometry in Cal-27 cells treated with melatonin at 1000 µM alone and pretreated with NAC 5 mM. (F) Calcium retention capacity detected by fluorometric assay in Cal-27 cells treated with melatonin at 500 or 1000 µM for 48 h. (G) Measurements of intracellular ROS levels by fluorimetry after staining with the DCF fluorescent probe in Cal-27 cells treated with melatonin at 500 or 1000 µM for 48 h and pretreated with CsA at 1 µM. (H) Apoptosis level (AV+/PI+and AV+/PI−) analyzed by flow cytometry in Cal-27 cells treated with melatonin at 500 or 1000 µM for 48 h and pretreated with CsA at 1 µM. (I) Measurements of intracellular ROS levels by fluorimetry after staining with the DCF fluorescent probe in Cal-27 cells treated with melatonin at 500 or 1000 µM for 48 h and pretreated with 3 nM rotenone, 10mM malonate, 50 µM TTFA, 2 µM ant A, 200 µM KCN, or 200 nM FCCP. (J) Apoptosis level (AV+/PI+ and AV+/PI−) analyzed by flow cytometry in Cal-27 cells treated with melatonin at 500 or 1000 µM for 48 h and pretreated with 3 nM rotenone, 10mM malonate, 50 µM TTFA, 2 µM antimycin A, 200 µM KCN, or 200 nM FCCP. Data are presented as mean ± standard error of the mean (n= 4–10 for each group; one-tailed unpaired t-test; *p < .05; **p < .01; ***p < .001 vs. control; δp < .05, δδp < .01 vs. aMT 1000 µM).

ROS production may trigger mPTP with further stimulation of ROS. Therefore, we measured the calcium retention capacity in Cal-27 cells treated with melatonin at 500 or 1000 μM after 48 h. Melatonin treatment decreased calcium retention capacity for both cell lines (Figures 20F and 21C), indicating that it increased the mPTP opening state in Cal-27 and SCC-9 cells. To corroborate whether the mPTP opening state induced apoptosis, cells were pretreated with an mPTP opening inhibitor, cyclosporin A (CsA) at 1 μM in both cell lines. As shown in Figure 20G and Figure 21D, CsA decreased melatonin-induced ROS production. Moreover, consistent with the above results, the reduced ROS production led to decreased apoptosis (Figures 20H and 21E). Overall, these findings suggest that the apoptotic effect of melatonin arises from ROS-induced mPTP opening. These data further support that melatonin-induced apoptosis requires sustained ROS production.

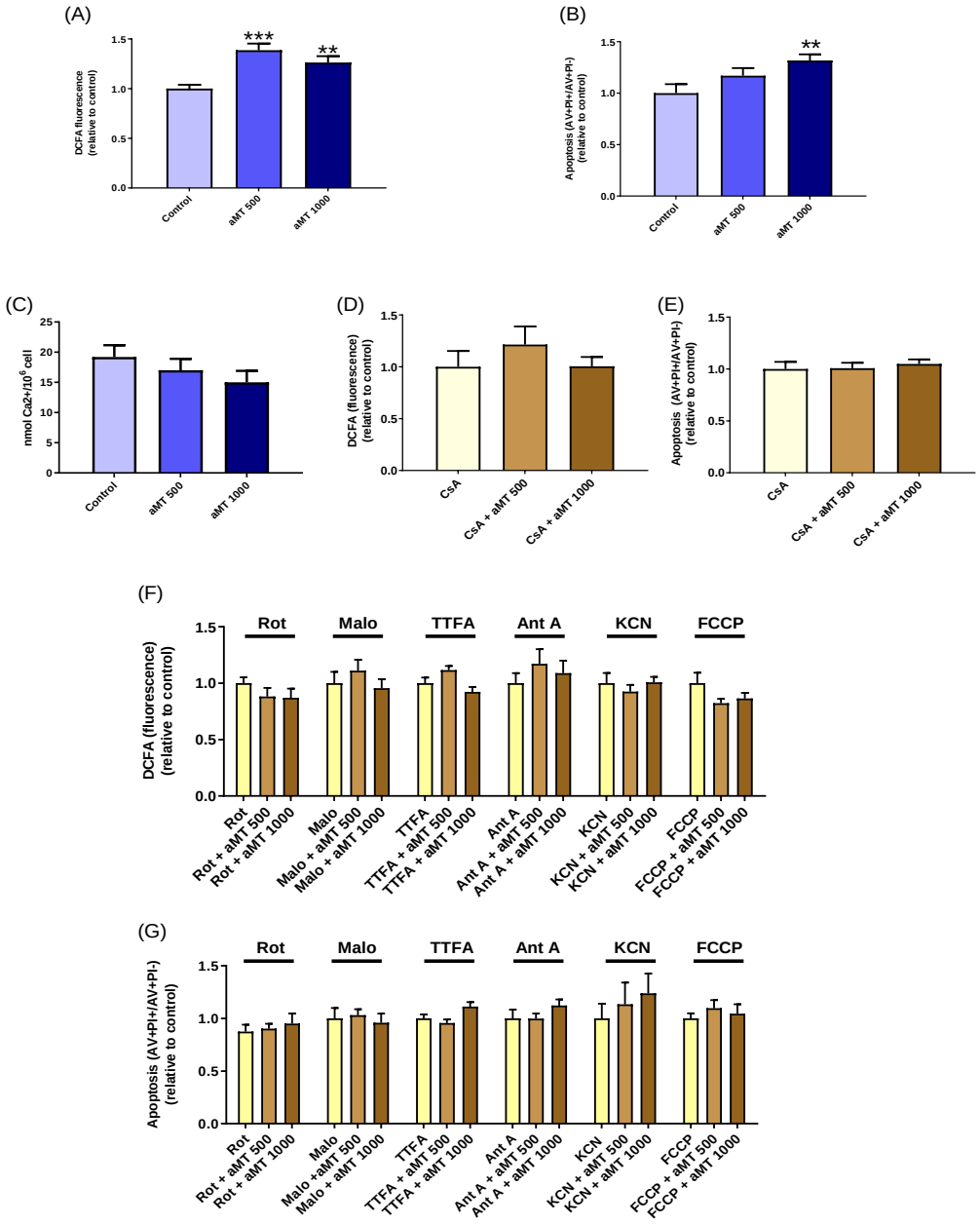

Figure 21. mtROS production drives melatonin-induced proapoptotic effects in SCC-9 cells. (A) Measurements of intracellular ROS levels by fluorimetry after staining with the DCF fluorescent probe. (B) Apoptosis level (annexin V+/PI+ and annexin V+/PI-) analyzed by flow cytometry. (C) Calcium retention capacity detected by fluorometric assay. For (A–C) treatment groups include vehicle (control) and melatonin (aMT) at 500 µM or 1000 µM for 48 h (blue range) in SCC9 cells. (D) Measurements of intracellular ROS levels by fluorimetry after staining with the DCF fluorescent probe in SCC-9 cells treated with 500 or 1000 µM for 48 h and pretreated with CsA at 1 µM. (E) Apoptosis level (AV+/PI+ and AV+/PI-) analyzed by flow cytometry in SCC-9 cells treated with 500 or 1000 µM for 48 h and pretreated with CsA at 1 µM. (F) Measurements of intracellular ROS levels by fluorimetry in SCC-9 cells treated with melatonin at 500 or 1000 µM for 48 h and pretreated with 9 nM rotenone, 10 mM malonate, 50 µM TTFA, 2 µM antimycin A (Ant A), 300 µM KCN, or 200 nM FCCP. (G) Apoptosis level (AV+/PI+ and AV+/PI-) analyzed by flow cytometry in SCC-9 cells treated with melatonin at 500 or 1000 µM for 48 h and pretreated with 9 nM rotenone, 10 mM malonate, 50 µM TTFA, 2 µM antimycin A, 300 µM KCN, or 200 nM FCCP.Data are presented as mean ± standard error of the mean (n = 4–9 for each group; one-tailed unpaired t test; ** $p < 0.01$, *** $p < 0.001$ vs. control).

To investigate whether the activity of ETS complexes is essential for ROS production, we applied different inhibitors of mitochondrial respiration. Of interest, pretreatment of Cal-27 and SCC-9 cells with rotenone, malonate, thenoyltrifluoroacetone, antimycin A, potassium cyanide, or carbonylcyanide-p-trifluoromethoxyphenylhydrazone (FCCP) inhibited melatonin-induced ROS production (Figures 20I and 21F). As expected, these results correlated with decreased melatonin-induced apoptosis (Figures 20J and 21G). These findings suggest that melatonin acts through high mitochondrial complex activities and high membrane potential to elevate mitochondrial ROS production and that all mitochondrial complex inhibitors, including rotenone, can abolish the ROS elevation (Figures 20I and 21F). Rotenone inhibits complex I RET (Chouchani et al. 2014; Scialò et al. 2017), so it is possible that melatonin alters mitochondrial respiration via RET.

2. Melatonin induces mitochondrial uncoupling in HNSCC cells

Mitochondrial ROS burst is a hallmark of complex I RET, and the activity of ETS complexes and the mitochondrial proton gradient is essential for RET (Dröse 2013). For these reasons, to elucidate the mechanism underlying the melatonin-induced ROS increase, we analyzed mitochondrial function in HNSCC cells. We evaluated OXPHOS protein levels by western blot analysis and OXPHOS activity by spectrophotometric analysis (Figure 22A–K). In agreement with the effects of melatonin in nontumor tissues (Acuña-Castroviejo et al. 2001; López et al. 2017; Martín et al. 2000; Ortiz, Acuña-Castroviejo, et al. 2015), melatonin increased the levels of complexes I and IV relative to control cells at 1000 μM after 48h of treatment (Figure 22A,D). This increase was

reflected primarily in increased complex I and IV activities after 24 h of treatment (Figure 22G,J). To our surprise and in contrast to results with the mitochondria of nontumor cells (López et al. 2017), melatonin at 48 h highly increased levels of complex II, and at 24 h increased its activity, at 1000 µM (Figure 22B,H). Complex III and complex V were unaffected (Figure 22C,E,I,K). Furthermore, we found a decrease in complex II and complex V activity after 48h of melatonin treatment at 1000 µM (Figure 22H,K), suggesting that the high concentration of melatonin during longer treatments decreased mitochondrial function.

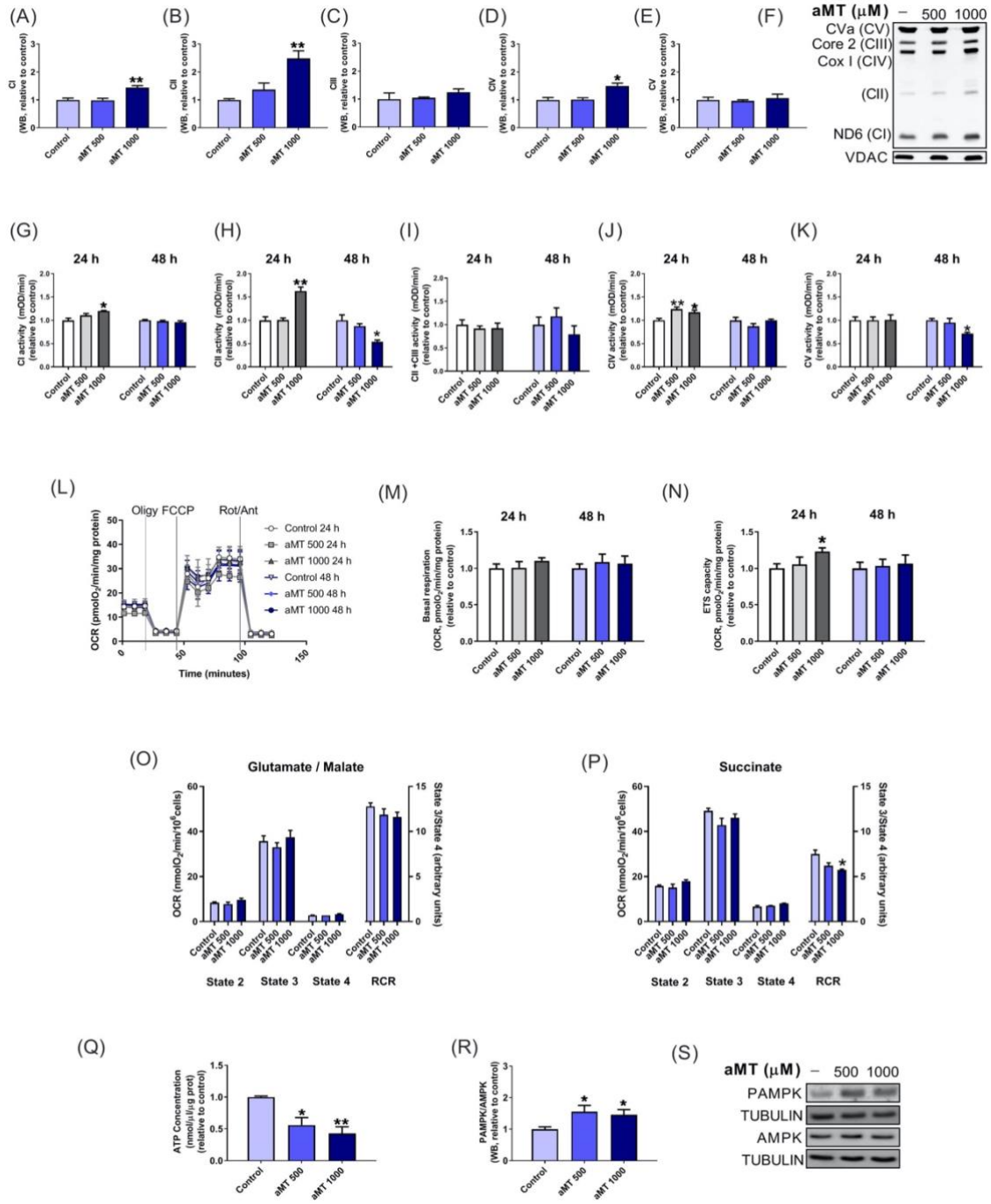

Figure 22. Effect of melatonin on mitochondrial function in the HNSCC Cal-27 cell line.
(A–F) Analysis of OXPHOS protein expression by western blot (WB). (G–K) Analysis of mitochondria complex (CI–CV) activity by spectrophotometric analysis. (L–N) OCR corresponding to (M) basal respiration and (N) ETS capacity, as analyzed by SeaHorse. (O) OCR in digitonin-permeabilized Cal-27 cells with glutamate/malate without ADP (state 2), in the presence of 500 µM ADP (state 3) or 0.16 µg/ml oligomycin A (state 4), and RCR calculation (state 3/state 4). (P) OCR in digitonin-permeabilized Cal-27 cells with succinate without ADP (state 2), in the presence of 500 µM ADP (state 3) or 0.16 µg/ml oligomycin A (state 4), and RCR calculation (state 3/state 4). (Q) Ratio of ATP levels measured by fluorometric test. (R,S) Ratio of PAMPK and AMPK expression analyzed by western blot. Treatment groups included vehicle (control) and melatonin (aMT) at 500 or 1000 µM for 24 h (gray range) or 48 h (blue range) in Cal-27 cells. Data are presented as mean ± standard error of the mean (n=3–8 for each group; one-tailed unpaired t-test; *p < .05; **p < .01 vs. control).

Next, using the Seahorse XF24 extracellular flux analyzer, we examined whether the change in mitochondrial complexes correlated with increased mitochondrial respiration. Again, to our surprise and in contrast to results observed for complex activities, melatonin did not modify the OCR corresponding to basal respiration (Figure 22L,M). However, melatonin induced increased electron transport system within 24 h in Cal-27 cells treated with 1000 μM melatonin, without any change at 48 h (Figure 22L,N).

To further confirm these results, we conducted experiments using oxygraph respiration in permeabilized Cal-27 cells. OCR was measured in the presence of glutamate/ malate (G/M) (Figure 22O) or succinate as substrates (state 2) (Figure 22P), after the addition of adenosine diphosphate (state 3) and followed by the addition of oligomycin (state 4). Melatonin at any dose did not modify the respiratory control ratio (RCR: state 3/state 4) with G/M, related to complex I-dependent respiration (Figure 22O). However, melatonin decreased the RCR with succinate, which is related to complex II dependent respiration (Figure 22P). These data suggest that melatonin induced an increase in some components of the ETS (complexes I, II, and IV) without increasing mitochondrial respiration, suggesting uncoupling between the ETS and phosphorylation in the mitochondria of Cal-27 cells.

To clarify the partial uncoupling between respiration and oxidative phosphorylation in mitochondria induced by melatonin, we analyzed steady-state levels of ATP by fluorometric assay (Figure 22Q) and adenosine monophosphate-activated protein kinase (AMPK) activation, which depends on the AMP/ATP ratio, by western blot analysis (Figure 22R,S). Melatonin reduced ATP levels after 48 h of treatment and activated AMPK (Figure 22Q–S), confirming that melatonin induced a mitochondrial uncoupling in Cal- 27 cells, increasing mtROS production.

3. Melatonin increases RET-ROS by modification of the CoQ redox state and mitochondrial membrane potential (Δψm)

Given that RET occurs when the pool of CoQ is overreduced with electrons from respiratory complex II (Jia et al. 2020; Murphy 2009) and that melatonin notably increased complex II activity and expression (Figure 22B,H), we analyzed the CoQ redox state by UPLC-MS/MS (Figure 3A,B). Consistent with our prediction, melatonin 1000 µM enhanced the $CoQ_{10}H_2/CoQ_{10}$ ratio after 24 h of treatment (Figure 23A), without increasing total CoQ (Figure 23B). We obtained similar results with melatonin after 48 h of treatment (Figure 23A,B).

The production of mitochondrial ROS via complex I RET tightly depends on high Δψm, and even a slight decrease in Δψm induced by FCCP reduces ROS generation via complex I RET (Robb et al. 2018). As we showed above, pretreatment of Cal-27 cells with FCCP abolished the melatonin-induced mitochondrial ROS burst (Figure 20I). Moreover, cell incubation with melatonin for 24 h significantly increased Δψm in Cal-27 cells (Figure 23C) without altering the mitochondrial mass, as measured by MitoTracker Green FM fluorescence (Figure 23D), further supporting melatonin-induced ROS generation via complex I RET. However, we observed a drop in Δψm after 48 h of melatonin treatment (Figure 23C), which could be explained by the fact that melatonin-induced sustained ROS production after 48 h may trigger mPTP opening (Figure 20F), inducing Δψm decline. Because uncoupling proteins (UCPs) are the direct downstream mediators of ROS-dependent mitochondrial production (Cadenas 2018) related to a drop in Δψm, we analyzed UCP protein levels by western blot analysis. As shown in Figure 23F,E, melatonin significantly increased UCP2 levels in a dose-dependent manner, explaining the steep reduction in Δψm.

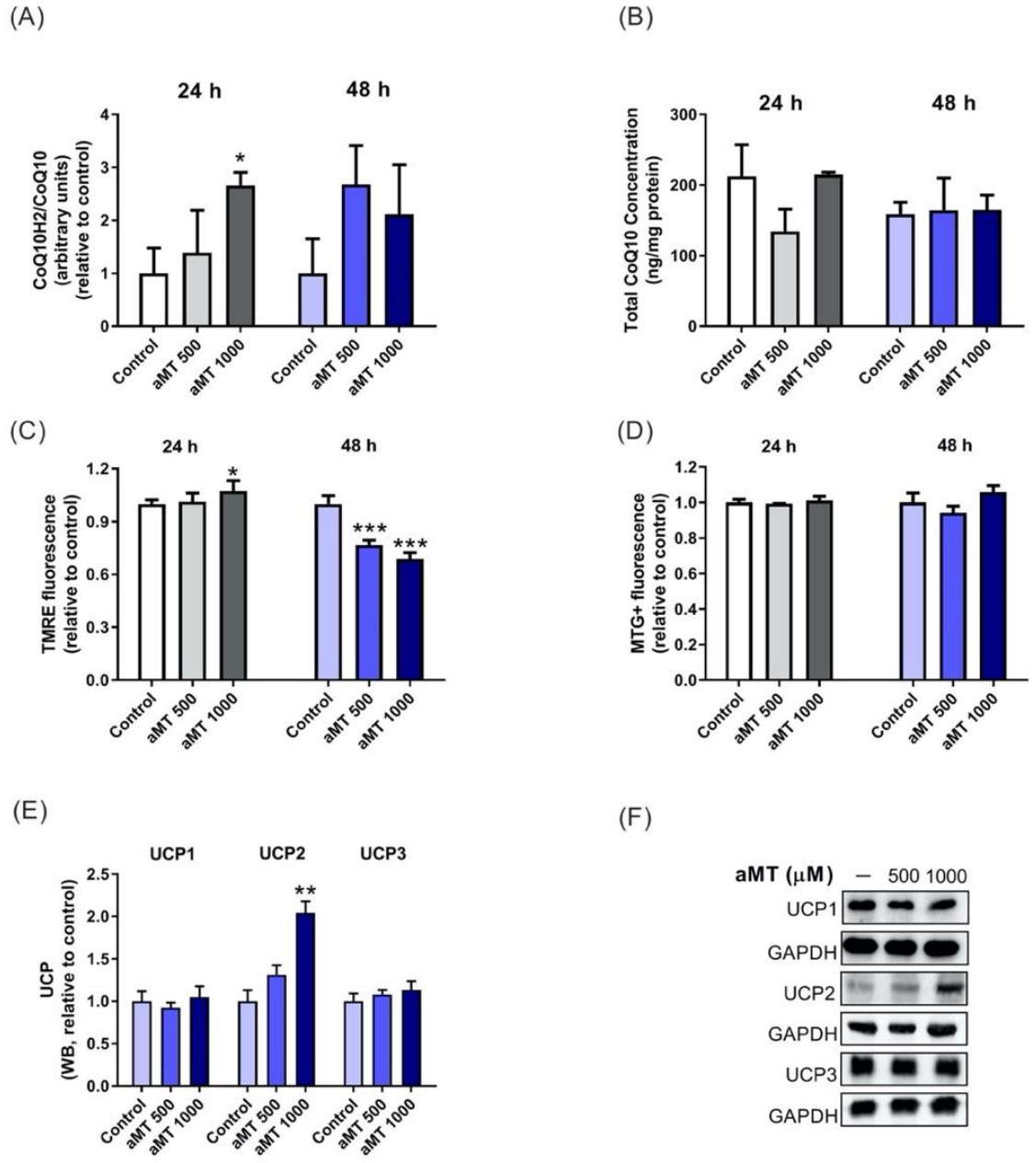

Figure 23. Increased RET-ROS by modification of CoQ redox and mitochondrial membrane potential in Cal-27 cells treated with melatonin. (A, B) CoQ10 and $CoQ_{10}H_2/CoQ_{10}$ ratio analyzed by UPLC-MS/MS. (C, D) (C) Mitochondrial membrane potential and (D) mitochondrial mass analyses by fluorimetry after staining with TMRE or MTG fluorescent probe, respectively. (E, F) Western blot analysis of UCP1, UCP2, and UCP3. Treatment groups included vehicle (control) and melatonin (aMT) at 500 or 1000 μM for 24 h (gray range) or 48 h (blue range) in Cal-27 cells. Data are presented as mean± standard error of the mean (n= 3–8 for each group; one-tailed unpaired t-test; *p < .05; **p <.01; ***p<.001 vs. control).

4. Melatonin increases RET-ROS by modification of metabolism

To examine how melatonin induces a modification of metabolism, we first carried out metabolomic analyses using UPLC-MS/MS and found that melatonin upregulated key TCA cycle metabolites in Cal-27 cells (Figure 24A–D), especially succinic acid, the principal substrate of RET (Figure 24A). This upregulation led to an increased NADH/NAD ratio (Figure 24E), further supporting that melatonin induced ROS generation via complex I RET.

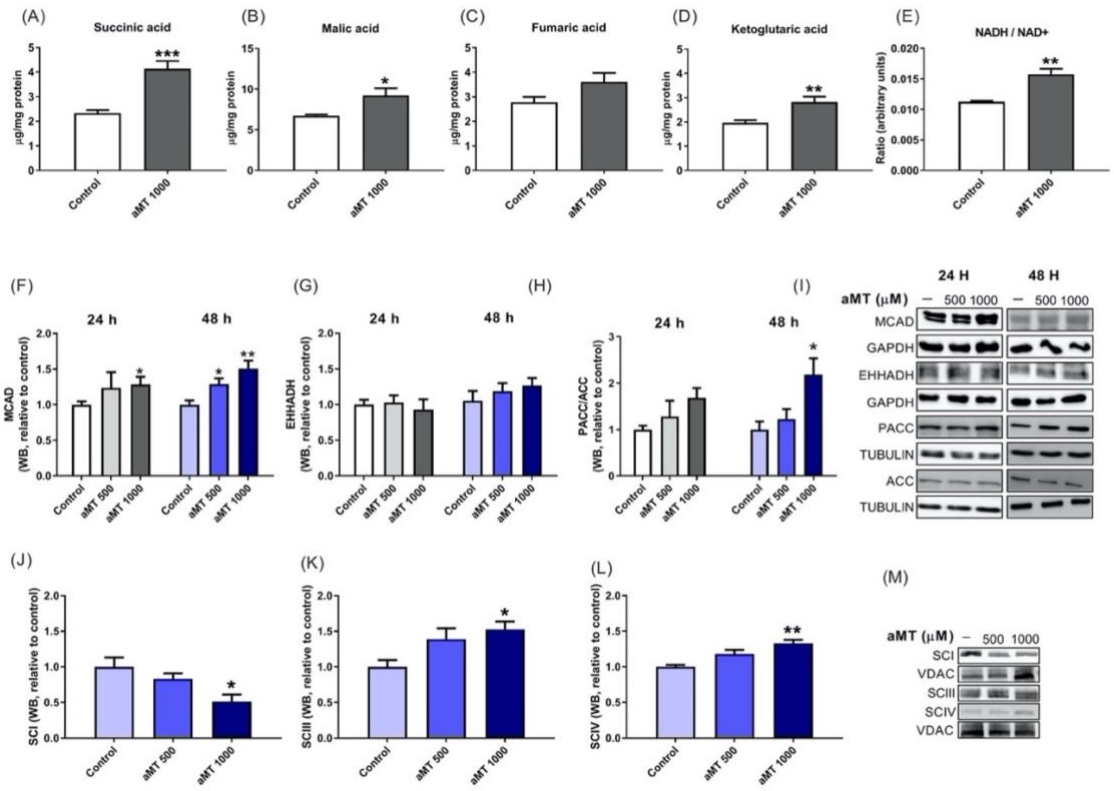

Figure 24. Melatonin-induced change in Cal-27 cell metabolism by upregulation of fatty acid oxidation and TCA metabolites. (A–D) Metabolomic study of intracellular levels of (A) succinic acid, (B) fumaric acid, (C) malic acid, and (D) ketoglutaric acid. (E) NADH and NAD+ levels measured using a colorimetric test and expressed as a ratio. (F–I) Western blot analysis of (F) MDAC, (G) EHHADH, and (H) PACC/ACC ratio. (J–M) Evaluation of SC formation by BNGE. Treatment groups included vehicle (control) and melatonin (aMT) at 500 or 1000 µM for 24 h (gray range) or 48 h (blue range) in Cal-27 cells. Data are presented as mean ± standard error of

the mean (n=3–7 for each group; one-tailed unpaired t-test; *p < .05; **p < .01; ***p < .001 vs. control).

When fatty acids are oxidized, NADH increases, resulting in an over-reduction of the CoQ pool and an increase in RET-ROS (Guarás et al. 2016). We analyzed medium-chain acyl-CoA dehydrogenase (MCAD) and enoyl-CoA hydratase and 3-hydroxyacyl CoA dehydrogenase (EHHADH), which regulate fatty acid oxidation, and acetyl-CoA carboxylase (ACC), which is involved in lipid biosynthesis. In a dose- and time-dependent manner, melatonin triggered increased levels of medium-chain acyl-CoA dehydrogenase (Figure 24F,I), with a tendency for EHHADH at 48 h (Figure 24G,I), and an increased phosphorylated/No- phosphorylated acetyl-CoA carboxylase ratio (Figure 24H,I), most likely due to the activated phosphorylated adenosine monophosphate protein kinase. Collectively, these results suggest that melatonin activated fatty acid oxidation as well as inhibiting lipid biosynthesis (Hidalgo-Gutiérrez et al. 2021).

The high $CoQ_{10}H_2/CoQ_{10}$ ratio during β-oxidation leads to RET-produced ROS and localized RET leads to changes in SC formation (Guarás et al. 2016). As expected, melatonin reduced the formation of SCs involving complex I (Figure 24J,M) but increased the formation of SCs involving complex III within 48 h in a dose-dependent manner (Figure 24K–M). These results indicate that melatonin rearranges the formation of SCs degrading CI and stimulating the formation of complexes III + IV SCs to favor the oxidation of fatty acids. These findings support the important role of melatonin in inducing changes in HNSCC cell metabolism, indicating that melatonin could be exerting its oncostatic effect via RET-ROS.

5. AOX expression reduces RET and inhibits melatonin's oncostatic effects *in vitro* and *in vivo*

To confirm whether RET underlies melatonin-induced ROS production in HNSCC cells, we used the AOX, a cyanide-insensitive oxidase that transfers electrons from QH_2 to oxygen, decreasing the $CoQH_2$/CoQ ratio (Onukwufor et al. 2019). For this reason, we expressed AOX in Cal-27 cells to examine whether reducing $CoQ_{10}H_2$ accumulation decreased ROS production and then apoptosis. AOX expression restored a normal $CoQ_{10}H_2/CoQ_{10}$ ratio (Figure 25B) without inducing significant changes in the total CoQ_{10} amount (Figure 25A). Moreover, the effects of melatonin in inducing ROS production and apoptosis were abolished in cells expressing AOX (Figure 25C,D). This result indicated that complex I RET induced by melatonin is also required for melatonin-induced sustained ROS production. Furthermore, to ensure AOX functionality, cells were treated with complex III inhibitor antimycin A. AOX cell line showed an increase in Cal-27 cell proliferation and mitochondrial respiration compared to WT in presence of antimycin A, indicating AOX functionality (Figure 26A-D).

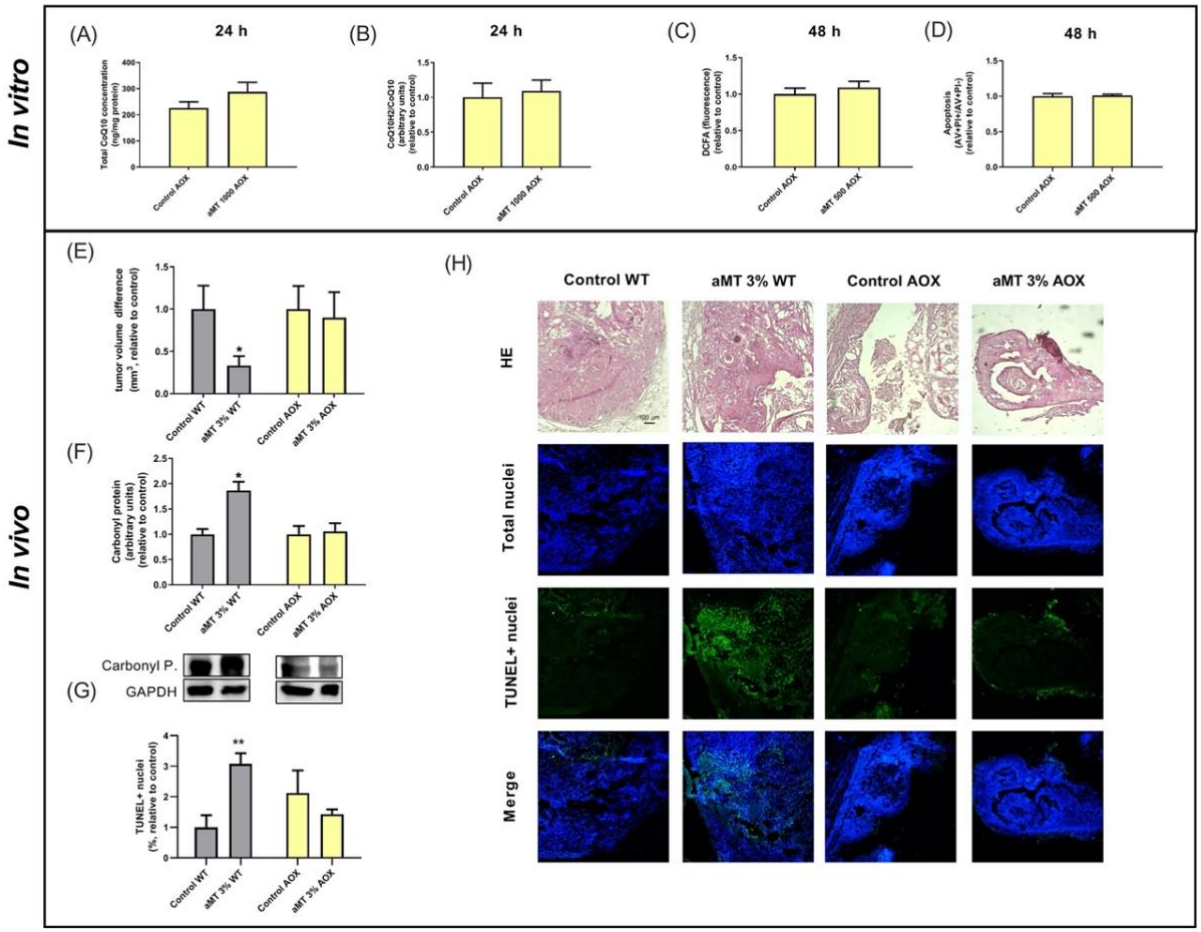

Figure 25. Melatonin-induced oncostatic effects are inhibited in Cal-27 expressing AOX *in vitro* and *in vivo*. (A,B) (A) Levels of total CoQ10 and (B) CoQ10H2/CoQ10 ratio in Cal-27 cells expressing AOX *in vitro*, analyzed by UPLC-MS/MS. Groups included vehicle (control) and melatonin (aMT) at 1000 µM for 24 h (treatment with the greatest difference vs. wild-type Cal-27). (C) Measurements in vitro of intracellular ROS levels by fluorimetry after staining with the DCF fluorescent probe in Cal-27 cells expressing AOX. Groups included vehicle (control) and melatonin (aMT) at 500 µM for 48 h (treatment with the greatest difference vs. wild-type Cal-27). (D) Apoptosis level (AV+/PI+ and AV+/PI−) analyzed in vitro by flow cytometry in Cal-27 cells expressing AOX. Groups included vehicle (control) and melatonin (aMT) at 500 µM for 48 h (treatment with the greatest difference vs. wild-type Cal-27). (E) Tumor volume difference analyzed *in vivo* with a caliper vernier. (F) Western blot analysis of carbonyl protein. (G,H) (H) TUNEL+ nuclei (apoptotic nuclei, green) and DAPI stained nuclei (total nuclei, blue). Scale bar = 100 µm. (G) The percentage of apoptotic cells was designated as the apoptotic index. For (E–G), treatment groups included WT Cal-27 xenograft treated intratumorally with vehicle (control WT) and melatonin at 3% (aMT 3% WT) or Cal-27–expressing AOX xenograft treated intratumorally with vehicle (control AOX) and melatonin at 3% (aMT 3% AOX). Data are presented as mean ± standard error of the mean (n=3–8 for each group; one-tailed unpaired t-test; *p < .05; **p < .01 vs. control).

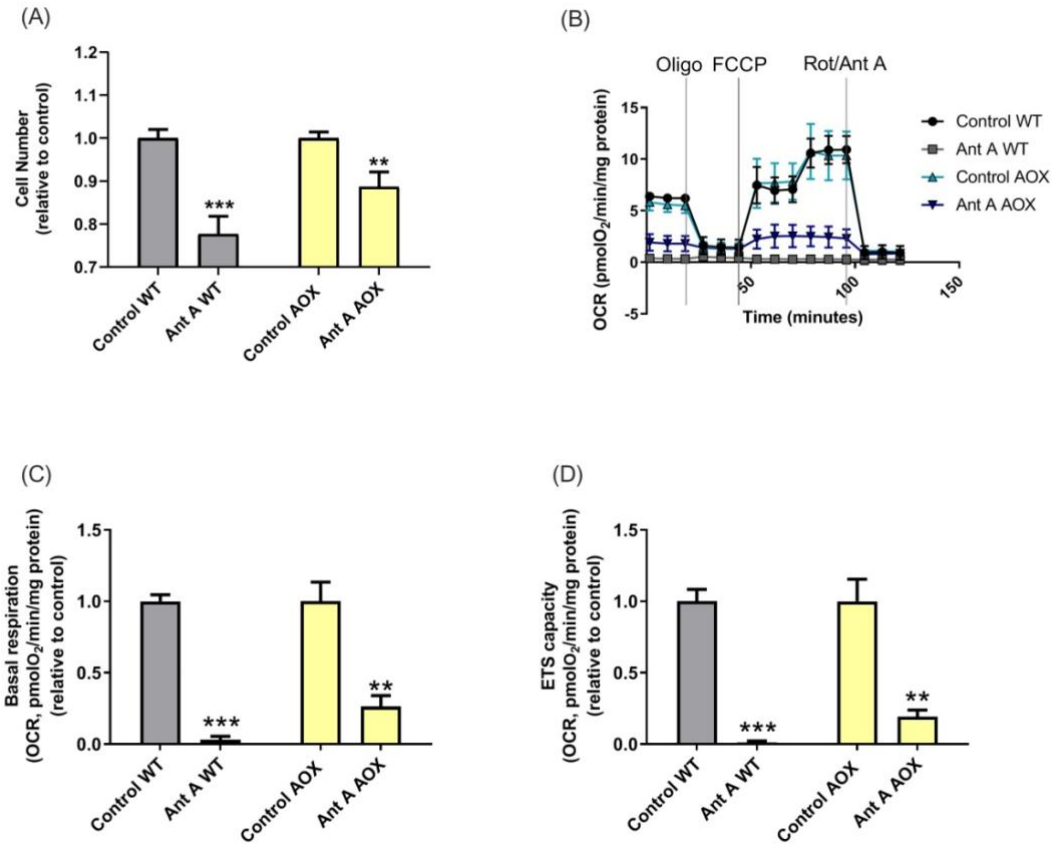

Figure 26. Validation of AOX functionality expression in Cal-27 cells. (A) Cell proliferation levels by fluorimetry analyzed after staining with the CyQuant-GR probe. (B–D) OCR corresponding to (C) basal respiration and (D) ETS capacity, as analyzed by SeaHorse in Cal-27 cells WT and Cal-27 expressing AOX. Groups included vehicle (control) and antymicin A (Ant A) at 2 µM for 48 h. Data are presented as mean ± standard error of the mean (n = 4–6 for each group; one-tailed unpaired t test; ** $p < 0.01$, *** $p < 0.001$ vs. control).

We further confirmed these results *in vivo*, using mice injected with wild-type Cal-27 cells or cells expressing AOX. Considering that our *in vivo* previous results suggested that melatonin administered intraperitoneally did not reach the mitochondria at a sufficient concentration (Y. Q. Shen et al. 2018), both groups were treated intratumorally with vehicle or with melatonin, which did not reach the plasma increasing melatonin level into the tumor. After 35 days of treatment, melatonin, which reduced greatly the tumor volume in wild-type Cal-27 cells, did not have any effect on volume in tumors containing cells expressing AOX (aMT 3% AOX) compared with its controls

(Figure 25E). To investigate whether melatonin induced complex I RET led to apoptosis, we analyzed carbonyl protein level and apoptosis using the TUNEL assay. As shown in Figure 25F–H, the effects of melatonin in increasing ROS production and apoptosis disappeared in tumors expressing AOX (aMT AOX) compared with controls. Overall, these findings support that melatonin induces ROS generation via complex I RET.

DISCUSSION

Melatonin has two seemingly opposing actions regarding its relationship with free radicals. Numerous studies have shown that it plays an effective role in maintaining mitochondrial homeostasis (Acuña-Castroviejo et al. 2001; López et al. 2017; Martín et al. 2000; Ortiz, Acuña-castroviejo, et al. 2015; Sun et al. 2020), but the mechanism by which melatonin induces ROS production in cancer cells is poorly understood. In this study, we provided evidence that melatonin mediates apoptosis in HNSCC cells by targeting mitochondria to induce ROS at complex I by RET (Figure 27).

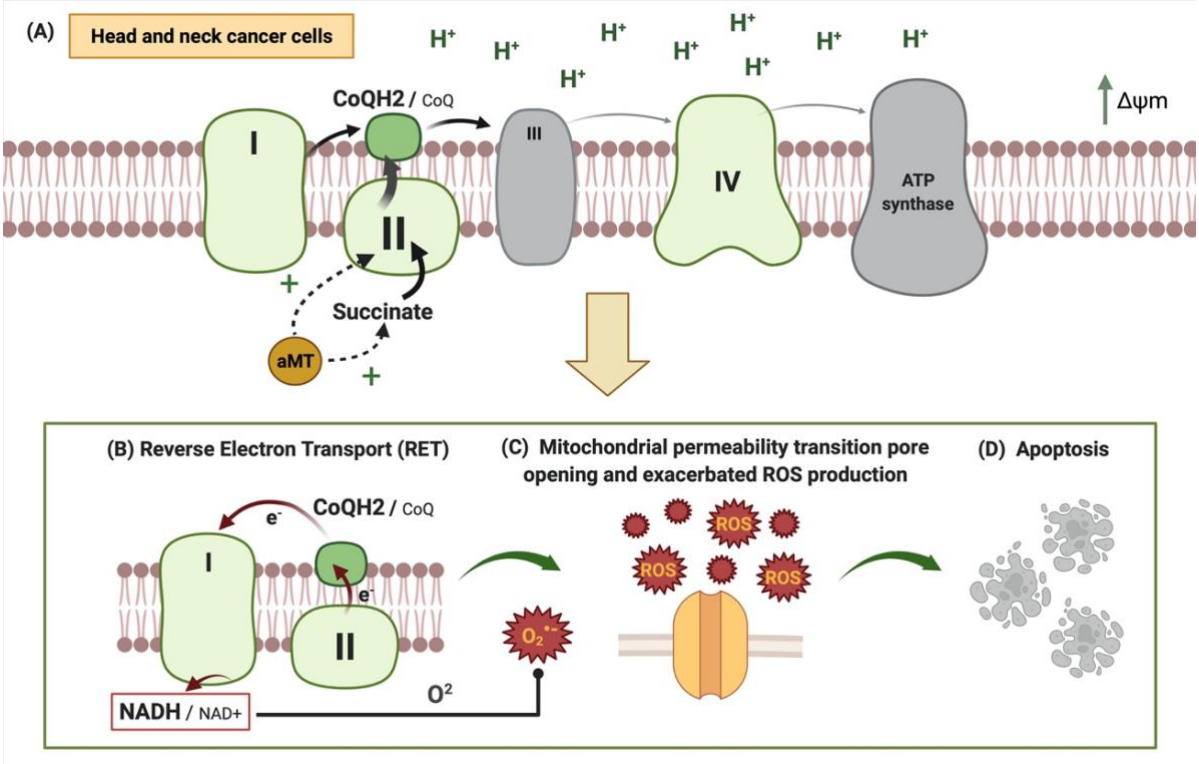

Figure 27. Melatonin mediates apoptosis in head and neck cancer by driving RET to induce ROS production. (A) Melatonin increases succinate levels, complex I, complex IV, and highly complex II activity and expression inducing an increase in CoQH2/CoQ ratio and Δψm. (B) As a consequence, melatonin induces RET-ROS. (C), which leads to mitochondrial transition pore opening and exacerbated ROS production. (D) Finally, a high amount of ROS produces cancer cell apoptosis. Image created with BioRender.com. CoQ, coenzyme Q; RET, reverse electron transport; ROS, reactive oxygen species.

The complex role of ROS in mediating tumor progression remains a subject of controversy. Cancer cells often exhibit altered mitochondrial function, including elevated ROS generation (Wallace 2012; Xu et al. 2020), which is involved in the initiation and progression of cancer (Sabharwal and Schumacker 2014; Szatrowski and Nathan 1991). However, high levels of ROS may induce anti-tumorigenic effects due to the increased oxidative damage, resulting in tumor cells death (Fernández-Gil et al. 2019; Guerra-Librero et al. 2021; Nogueira et al. 2008; Y. Q. Shen et al. 2018). The current findings show that melatonin-induced apoptosis was abolished by pretreatment of Cal-27 cells with the antioxidant NAC (Figure 20E), suggesting that ROS levels are increased by melatonin above a toxicity threshold that results in oxidative damage and cell death.

Moreover, ROS may trigger mPTP opening, which is a mitochondrial response to oxidative challenge that results in an amplified ROS signal and may cause perceptible mitochondrial and cellular injury (Zorov et al. 2014). The main sites of mtROS generation *in vivo* are respiratory complexes I and III (Chouchani et al. 2014; Scialò et al. 2017), although the relative contribution of these sites to total cellular ROS is unclear (Sullivan and Chandel 2014). Complex II is excluded from the list of potential candidates for important physiological contributors of ROS (Raha and Robinson 2000). However, under specific conditions, complex II subunits can lead to increased ROS generation via RET (Chouchani et al. 2014; Scialò et al. 2017). One way to differentiate RET-ROS production is by using rotenone, which increases ROS production in the forward direction, but decreases it via RET (Lambert and Brand 2004). Our current findings indicate that ROS production induced by melatonin was reduced under complex I inhibition with rotenone (Figure 20I), indicating that ROS production associated with forward electron transfer at

complex I is unlikely to contribute to cancer cells apoptosis. Moreover, ROS also decreased under inhibition of complexes II, III, and IV and with FCCP application (Figure 20I). Inhibition of complex II leads to a reduction in complex I–related ROS generation during RET (Dröse 2013). Moreover, FCCP dissipates mitochondrial proton motive force and decreases complex I ROS production (Onukwufor et al. 2019). Thus, we hypothesize that melatonin may mediate apoptosis in HNSCC cells by driving complex I RET to induce ROS-dependent mitochondrial uncoupling. Melatonin increased the expression and activities of complexes I, II, and IV, as well as ETS capacity (Figure 22A,B,D,G,H,J,N), and especially surprising to us was the increase in complex II with no effect on complex III. Complex II can adapt to different roles as a producer or modulator of mtROS depending on the activity of other complexes such as complex III (Dröse 2013). In contrast, we observed a lack of effect of melatonin on complex V expression and activity (Figure 22E,K) with a decrease in ATP production (Figure 22Q), which in part supports an earlier observation of melatonin-induced mitochondrial uncoupling (Bilska et al. 2021).

These results are in line with the observation that complex V stops producing ATP when RET occurs (Mills et al. 2016). In keeping with this observation, in the current work, melatonin activated AMPK (Figure 22R), which is a major mechanism downstream of mitochondrial uncoupling (Jia et al. 2020). These data further support that melatonin induced an uncoupling between mitochondrial electron transport activity and OXPHOS (Demine, Renard, and Arnould 2019). They also suggest that melatonin-induced uncoupling depends on complex II respiration, as melatonin-induced ROS production involved both complex I and complex II. Furthermore, these findings seem to confirm that melatonin-induced mitochondrial uncoupling depends on complex I RET (Scialò et al. 2017). When complex II–linked substrates, such as succinate, are used, a portion of

the electrons flow through complex I in the reverse direction. ROS produced under these conditions depend on the redox state of CoQ and Δp. With blocking of the Q binding site (I_Q) with rotenone or decreasing Δp with FCCP, there is a significant reduction in ROS production via RET (Murphy 2009; Onukwufor et al. 2019), as delineated above. Furthermore, our results showed that melatonin increased the $CoQ_{10}H_2/CoQ_{10}$ ratio and mitochondrial membrane potential (Figure 23A). These results appear to be congruent with the finding that ROS production via RET requires some essential features in the cell, such as certain activity of mitochondrial complexes to maintain a high Δp, especially high activity of complex II to over-reduce the CoQ pool (Dröse 2013).

Moreover, UCPs are the direct downstream mediators of ROS-dependent mitochondrial uncoupling (Bertholet et al. 2019). Other studies have shown that RET initiates generation of mtROS and that ROS-dependent activation of UCP2 in turn leads to mitochondrial uncoupling (Jia et al., 2020). As expected, in the current work, melatonin increased UCP2 (Figure 23E). Collectively, these results suggest that melatonin induces ROS generation by driving complex I RET, which in turn induces ROS-dependent mitochondrial uncoupling via UCP2 and mPTP opening, as described above.

On the other hand, under some specific situation such as cell metabolic reprogramming, cells undergo a metabolic shift characterized by increased use of succinate, which alters ROS production by complex I from the forward to the reverse direction (Fernández-Agüera et al. 2015). We showed here that in HNSCCs, melatonin increased all the intermediates of the Krebs cycle, especially succinate (Figure 24A-D). Moreover, respiratory complexes are organized in larger superstructures called SCs, depending on the source of energy available (Scialò et al. 2017). In fact, oxidation of fatty acids results in an over-reduction of the CoQ pool and in increased RET-ROS. Under

these conditions, ROS production by complex I RET leads to changes in SC formation (Guarás et al. 2016). Our results showed that melatonin increased β-oxidation (Figure 4F,G) and induced changes in the organization of SCs, reducing the formation of SCs involving Complex I, as well as increasing SCs involving complex III and complex IV (Figures 24J-L). These results indicate that melatonin rearranges the formation of SCs degrading CI and stimulating the formation of complexes III+IV SCs in order to favor the oxidation of fatty acids. These findings support the important role for melatonin in inducing changes in head and neck cancer cell metabolism. These findings further support that melatonin induces ROS generation via complex I RET.

Furthermore, our data suggest that there is a correlation between the cell content of melatonin and ROS production, thus supporting the notion that high concentrations of melatonin in cancer cells are required to it's the cytotoxic effect. Previously, we demonstrated that melatonin markedly decreases cell viability in the irradiated cells in a dose-dependent manner, especially at doses of 500 and 1500 μM. Surprisingly, 100 μM melatonin did not significantly reduce viability. Consistently, other authors found that melatonin at high concentrations (10–1000 μM) was able to promote ROS generation and induced apoptosis in human leukemic Jurkat cells. When tested at concentrations of <10 μM, melatonin did not induce significant ROS generation in these cancer cells. Moreover, we recently demonstrated that high doses of melatonin, such as those used in this study and elsewhere, significantly increased MT1 gene expression and led to a marked decrease in MT2 and RORα levels, suggesting that melatonin receptor expression may be involved, at least partly, in the indoleamine effect.

Finally, using AOX, a cyanide-insensitive oxidase that transfers electrons from QH_2 to oxygen and thus inhibits RET-ROS production, we confirmed the mechanism of

action of melatonin in inducing ROS production in cancer cells via complex I RET. Characterization of AOX in plants suggests that it is active only when the $CoQH_2$/CoQ ratio reaches a threshold, suggesting a regulatory switch (Onukwufor et al. 2019). *In vitro* results in the current work demonstrated that complex I RET mediated the pro-apoptotic effects of melatonin via ROS production (Figure 25C,D). Consistent with this finding, *in vivo* expression of AOX in a Cal-27 xenograft model abolished the therapeutic effects of melatonin (Figure 25E-H).

The question that arises is why melatonin produces large amounts of ROS by RET at complex I in HNSCC cells. It has been demonstrated that HNSCC cells present a metabolic reprograming. Specifically, HNSCC cells are mainly glycolytic (Li et al., 2020), since they preferentially use aerobic glycolysis for energy production, rather than mitochondrial metabolism (Hsieh et al., 2019). This metabolic change is regulated by an elevated expression of HIF-1α under normoxic conditions, so that glycolytic metabolism is also activated in the presence of oxygen (Wilkie et al., 2018). In cancer cells, HIF is activated and upregulates a variety of genes, including mitochondrial components (Chen et al. 2018). Specifically, HIF-1 activates the gene encoding pyruvate dehydrogenase (PDH) kinase 1 (PDK1), which phosphorylates and inactivates the catalytic subunit of PDH, the enzyme that converts pyruvate to acetyl coenzyme A for entry into the mitochondrial tricarboxylic acid cycle, increasing aerobic glycolysis and reducing mitochondrial metabolism. In this situation, HIF maintains ROS production at a physiologically low level and sustains integrity by decreasing respiratory activity (Fuhrmann and Brüne 2017). Moreover, it has been demonstrated that HIF inhibition in cancer cells results in increased ROS production and increased cell death. In this way, it also been demonstrated that melatonin can destabilize HIF-1α (Yang et al. 2014). We

previously have shown that melatonin inhibits tumor cells by reversing aerobic glycolysis (Guerra-Librero et al. 2021). Therefore, a key step in melatonin-based suppression of aerobic glycolysis is to destabilize HIF-1α (He et al. 2020). Melatonin destabilizes HIF-1α through different mechanisms, either by suppressing synthesis or promoting degradation (Vriend and Reiter 2016). These results align with the current observation that melatonin increased Krebs cycle intermediates (Figure 24A-E), including succinate and respiratory capacity (Figure 22N). Although deeper research is needed to confirm that HIF-1α is responsible for the induction of RET-ROS after melatonin treatment in HNSCC.

Our data show for the first time that melatonin induces ROS complex I RET after metabolism change in HNSCC and leads to apoptosis from excessive ROS production. This pathway likely represents a new mechanism underlying the oncostatic actions of melatonin in HNSCC cells and establish the dual effect of melatonin in protecting normal cells and inducing apoptosis in cancer cells.

CONCLUSIONS

First: Melatonin increases mitochondrial ROS production in HNSCC cells, resulting in mPTP opening and, finally, cancer cell apoptosis.

Second: Cells pretreatment with rotenone, malonate, TTFA, antimycin A, KCN or FCCP inhibits melatonin pro-oxidant effects and, therefore, melatonin oncostatic effects suggesting that high mitochondrial complex activities and high membrane potential are necessary to melatonin anti-tumoral effect.

Third: Melatonin increases complex I, II and IV expression and activity, but it is related to a decreased in the respiratory control ratio and ATP levels, indicating an uncoupling effect of the mitochondrial electron transport activity and phosphorylation.

Fourth: Melatonin increases $CoQ_{10}H_2/CoQ_{10}$ ratio and mitochondrial membrane potential in HNSCC cells, requirements for RET-ROS production.

Fifth: The uncoupling effects of melatonin in HNSCC are, at least partially, due to an increase of UCP-2 expression.

Sixth: Melatonin-induced change in HNSCC cells metabolism by upregulation of fatty acid oxidation and TCA metabolites. This metabolic change is linked to the rearrangement of SCs formation, degrading CI and stimulating the formation of complexes III + IV SCs to favor the oxidation of fatty acids.

Seventh: Melatonin-induced oncostatic effects are inhibited in Cal-27 expressing AOX *in vitro* and *in vivo*, confirming that melatonin oncostatic function is due to RET-ROS production.

BIBLIOGRAPHY

Abadi, Seyede Hadis Momeni Hasan, Alireza Shirazi, Ali Mohammad Alizadeh, Vahid Changizi, Masoud Najafi, Solmaz Khalighfard, and Hasan Nosrati. 2018. 'The Effect of Melatonin on Superoxide Dismutase and Glutathione Peroxidase Activity, and Malondialdehyde Levels in the Targeted and the Non-Targeted Lung and Heart Tissues after Irradiation in Xenograft Mice Colon Cancer'. *Current Molecular Pharmacology* 11:326–35. doi: 10.2174/1874467211666180830150154.

Acuña-Castroviejo, Darío, Germaine, Escames Carmen, María E. Díaz, Casado Elena, Lima Cabello, Luis C. López, Sergio Rosales, Corral Dun, et al. Reiter. 2014. 'Extrapineal Melatonin: Sources , Regulation , and Potential Functions'. *Cell. Mol. Life Sci.* 71:2997–3025. doi: 10.1007/s00018-014-1579-2.

Acuña-Castroviejo, Darío, Miguel Martín, Manuel Macías, Germaine Escames, Josefa León, Huda Khaldy, and Russel J. Reiter. 2001. 'Melatonin, Mitochondria, and Cellular Bioenergetics'. *Journal of Pineal Research* 30:65–74. doi: 10.1034/j.1600-079X.2001.300201.x.

Amable, Lauren. 2016. 'Cisplatin Resistance and Opportunities for Precision Medicine'. *Pharmacological Research* 106(1):27–36. doi: 10.1016/j.phrs.2016.01.001.

Ammar, Omar A., Mohamed A. El-Missiry, Azza I. Othman, and Maggie E. Amer. 2022. 'Melatonin Is a Potential Oncostatic Agent to Inhibit HepG2 Cell Proliferation through Multiple Pathways'. *Heliyon* 8:e08837. doi: 10.1016/j.heliyon.2022.e08837.

Argiris, Athanassios, Michalis V Karamouzis, David Raben, and Robert L. Ferris. 2008. 'Head and Neck Cancer'. *The Lancet* 371(9625):1695–1709. doi: 10.1016/S0140-6736(08)60728-X.

Baysal, Bora E. 2006. *Role of Mitochondrial Mutations in Cancer* 17(3):203-12. doi: 10.1385/ep:17:3:203.

Bertholet, Ambre M., Edward T. Chouchani, Lawrence Kazak, Alessia Angelin, Andriy Fedorenko, Jonathan Z. Long, Sara Vidoni, et al. 2019. 'H+ Transport Is an Integral Function of the Mitochondrial ADP/ATP Carrier'. *Nature* 571(7766):515–20. doi: 10.1038/s41586-019-1400-3.

Bilska, Bernadetta, Fiona Schedel, Anna Piotrowska, Joanna Stefan, Michal Zmijewski, Elżbieta Pyza, Russel J. Reiter, et al. 2021. 'Mitochondrial Function Is Controlled by Melatonin and Its Metabolites in Vitro in Human Melanoma Cells'. *Journal of Pineal Research* 70(3):1–19. doi: 10.1111/jpi.12728.

Brand, Martin D. 2010. 'The Sites and Topology of Mitochondrial Superoxide Production'. *Experimental Gerontology* 45:466–72. doi: 10.1016/j.exger.2010.01.003.

Brandon, M., P. Baldi, and D. C. Wallace. 2006. 'Mitochondrial Mutations in

Cancer'. *Oncogene* 25:4647–62. doi: 10.1038/sj.onc.1209607.

Cadenas, Susana. 2018. 'Mitochondrial Uncoupling, ROS Generation and Cardioprotection'. *Biochimica et Biophysica Acta - Bioenergetics* 1859:940–50. doi: 10.1016/j.bbabio.2018.05.019.

Cardinali, Daniel, and Germaine Escames. 2016. 'Melatonin-Induced Oncostasis, Mechanisms and Clinical Relevance'. *Journal of Integrative Oncology* 01(s1). doi: 10.4172/2329-6771.s1-006.

Chang, Janet Ya An, Fei Yu, Liheng Shi, Michael L. Ko, and Gladys Y. P. Ko. 2019. 'Melatonin Affects Mitochondrial Fission/Fusion Dynamics in the Diabetic Retina'. *Journal of Diabetes Research* 2019. doi: 10.1155/2019/8463125.

Chen, Ruoli, U. Hin Lai, Lingling Zhu, Ayesha Singh, Muhammad Ahmed, and Nicholas R. Forsyth. 2018. 'Reactive Oxygen Species Formation in the Brain at Different Oxygen Levels: The Role of Hypoxia Inducible Factors'. *Frontiers in Cell and Developmental Biology* 6:1–12. doi: 10.3389/fcell.2018.00132.

Chen, Xiangyun, Bingjie Hao, Dan Li, Russel J. Reiter, Yidong Bai, Baigenzhin Abay, Guojie Chen, et al. 2021. 'Melatonin Inhibits Lung Cancer Development by Reversing the Warburg Effect via Stimulating the SIRT3/PDH Axis'. *Journal of Pineal Research* 71:1–12. doi: 10.1111/jpi.12755.

Choe, Joshua H., Simbarashe Mazambani, Tae Hoon Kim, and Jung Whan Kim. 2021. 'Oxidative Stress and the Intersection of Oncogenic Signaling and Metabolism in Squamous Cell Carcinomas'. *Cells* 10(3):1–25. doi: 10.3390/cells10030606.

Chouchani, Edward T., Victoria R. Pell, Edoardo Gaude, Dunja Aksentijević, Stephanie Y. Sundier, Ellen L. Robb, Angela Logan, et al. 2014. 'Ischaemic Accumulation of Succinate Controls Reperfusion Injury through Mitochondrial ROS'. *Nature* 515:431–35. doi: 10.1038/nature13909.

Ciotti, Sonia, Luca Iuliano, Sebastiano Cefalù, Marina Comelli, Irene Mavelli, Eros di Giorgio, and Claudio Brancolini. 2020. 'GSK3β Is a Key Regulator of the ROS-Dependent Necrotic Death Induced by the Quinone DMNQ'. *Cell Death and Disease* 11. doi: 10.1038/s41419-019-2202-0.

DeBerardinis, Ralph J., and Navdeep S. Chandel. 2016. 'Fundamentals of Cancer Metabolism'. *Science Advances* 2(5):e1600200. doi: 10.1126/sciadv.1600200.

Demine, Renard, and Arnould. 2019. 'Mitochondrial Uncoupling: A Key Controller of Biological Processes in Physiology and Diseases'. *Cells* 8:795. doi: 10.3390/cells8080795.

Dröse, Stefan. 2013. 'Differential Effects of Complex II on Mitochondrial ROS Production and Their Relation to Cardioprotective Pre- and Postconditioning'. *Biochimica et Biophysica Acta - Bioenergetics* 1827:578–87. doi: 10.1016/j.bbabio.2013.01.004.

Elicin, Olgun, Nikola Cihoric, Eugenia Vlaskou Badra, and Mahmut Ozsahin. 2019. 'Emerging Patient-Specific Treatment Modalities in Head and Neck Cancer–a Systematic Review'. *Expert Opinion on Investigational Drugs* 28(4):365–76. doi: 10.1080/13543784.2019.1582642.

Escames, Germaine, Juan M. Guerrero, Russel J. Reiter, Joaquin J. Garcia, Antonio Munoz-Hoyos, Genaro G. Ortiz, and Chang S. Oh. 1997. 'Melatonin and Vitamin E Limit Nitric Oxide-Induced Lipid Peroxidation in Rat Brain Homogenates'. *Neuroscience Letters* 230(3):147–50. doi: 10.1016/S0304-3940(97)00498-9.

Farhood, Bagher, Nasser Hashemi Goradel, Keywan Mortezaee, Neda Khanlarkhani, Masoud Najafi, and Amirhossein Sahebkar. 2019. 'Melatonin and Cancer: From the Promotion of Genomic Stability to Use in Cancer Treatment'. *Journal of Cellular Physiology* 234(5):5613–27. doi: 10.1002/jcp.27391.

Favero, Gaia, Enrico Moretti, Francesca Bonomini, Russel J. Reiter, Luigi Fabrizio Rodella, and Rita Rezzani. 2018. 'Promising Antineoplastic Actions of Melatonin'. *Frontiers in Pharmacology* 9:1086. doi: 10.3389/fphar.2018.01086.

Ferguson, Lynnette R., Helen Chen, Andrew R. Collins, Marisa Connell, Giovanna Damia, Santanu Dasgupta, Meenakshi Malhotra, et al. 2015. 'Genomic Instability in Human Cancer: Molecular Insights and Opportunities for Therapeutic Attack and Prevention through Diet and Nutrition'. *Seminars in Cancer Biology* 35:S5–24. doi: 10.1016/j.semcancer.2015.03.005.

Fernández-Agüera, M. Carmen, Lin Gao, Patricia González-Rodríguez, C. Oscar Pintado, Ignacio Arias-Mayenco, Paula García-Flores, Antonio García-Pergañeda, et al. 2015. 'Oxygen Sensing by Arterial Chemoreceptors Depends on Mitochondrial Complex I Signaling'. *Cell Metabolism* 22:825–37. doi: 10.1016/j.cmet.2015.09.004.

Fernández-Gil, Beatriz, Ahmed E. Abdel Moneim, Francisco Ortiz, Ying-Qiang Shen, Viviana Soto-Mercado, Miguel Mendivil-Perez, Ana Guerra-Librero, et al. 2017. 'Melatonin Protects Rats from Radiotherapy- Induced Small Intestine Toxicity'. *Plos One* 12:e0174474. doi: 10.1371/journal.pone.0174474.

Fernández-Gil, Beatriz I., Ana Guerra-Librero, Ying-qiang Shen, Javier Florido, Laura Martínez-Ruiz, Sergio García-López, Christian Adan, et al. 2019. 'Melatonin Enhances Cisplatin and Radiation Cytotoxicity in Head and Neck Squamous Cell Carcinoma by Stimulating Mitochondrial ROS Generation, Apoptosis, and Autophagy'. *Oxidative Medicine and Cellular Longevity* 2019:7187128. doi: 10.1155/2019/7187128.

Florido, Javier, César Rodriguez-Santana, Laura Martinez-Ruiz, Alba López-Rodríguez, Darío Acuña-Castroviejo, Iryna Rusanova, and Germaine Escames. 2022.

'Understanding the Mechanism of Action of Melatonin, Which Induces ROS Production in Cancer Cells'. *Antioxidants* 11(8):1621. doi: 10.3390/antiox11081621.

Fontaine, Eric, Ove Eriksson, François Ichas, and Paolo Bernardi. 1998. 'Regulation of the Permeability Transition Pore in Skeletal Muscle Mitochondria Modulation by Electron Flow through the Respiratory Chain Complex I'. *Journal of Biological Chemistry* 273:12662–68. doi: 10.1074/jbc.273.20.12662.

Fontaine, Eric, François Ichas, and Paolo Bernardi. 1998. 'A Ubiquinone-Binding Site Regulates the Mitochondrial Permeability Transition Pore'. *Journal of Biological Chemistry* 273:25734–40. doi: 10.1074/jbc.273.40.25734.

Frank, Anja, Megan Bonney, Stephanie Bonney, Lindsay Weitzel, Michael Koeppen, and Tobias Eckle. 2012. 'Myocardial Ischemia Reperfusion Injury: From Basic Science to Clinical Bedside'. *Seminars in Cardiothoracic and Vascular Anesthesia* 16(3):123–32. doi: 10.1177/1089253211436350.

Fuhrmann, Dominik C., and Bernhard Brüne. 2017. 'Mitochondrial Composition and Function under the Control of Hypoxia'. *Redox Biology* 12:208–15. doi: 10.1016/j.redox.2017.02.012.

Fujiwara, M., M. Shibata, Y. Watanabe, T. Nukiwa, F. Hirata, Noboru Mizuno, and O. Hayaishi. 1978. 'Indoleamine 2,3-Dioxygenase. Formation of L-Kynurenine from L-Tryptophan in Cultured Rabbit Fineal Gland.' *Journal of Biological Chemistry* 253(17):6081–85. doi: 10.1016/S0021-9258(17)34582-9.

Fulda, Simone, Lorenzo Galluzzi, and Guido Kroemer. 2010. 'Targeting Mitochondria for Cancer Therapy'. *Nature Publishing Group* 9(6):447–64. doi: 10.1038/nrd3137.

Gao, Meng, Anqi Li, Yuan Qin, Bilin Liu, and Guohua Gong. 2020. 'Protocol for Measurement of Oxygen Consumption Rate In Situ in Permeabilized Cardiomyocytes'. *STAR Protocols* 1(2):100072. doi: 10.1016/j.xpro.2020.100072.

Ghanbari Movahed, Zahra, Mohsen Rastegari-Pouyani, Mohammad hossein Mohammadi, and Kamran Mansouri. 2019. 'Cancer Cells Change Their Glucose Metabolism to Overcome Increased ROS: One Step from Cancer Cell to Cancer Stem Cell?' *Biomedicine and Pharmacotherapy* 112:108690. doi: 10.1016/j.biopha.2019.108690.

Gillison, Maura L., Andy M. Trotti, Jonathan Harris, Avraham Eisbruch, Paul M. Harari, David J. Adelstein, Erich M. Sturgis, et al. 2019. 'Radiotherapy plus Cetuximab or Cisplatin in Human Papillomavirus-Positive Oropharyngeal Cancer (NRG Oncology RTOG 1016): A Randomised, Multicentre, Non-Inferiority Trial'. *The Lancet* 393(10166):40–50. doi: 10.1016/S0140-6736(18)32779-X.

González-García, Pilar, Agustín Hidalgo-Gutiérrez, Cristina Mascaraque, Eliana Barriocanal-Casado,

Mohammed Bakkali, Marcello Ziosi, Ussipbek Botagoz Abdihankyzy, et al. 2020. 'Coenzyme Q10 Modulates Sulfide Metabolism and Links the Mitochondrial Respiratory Chain to Pathways Associated to One Carbon Metabolism'. *Human Molecular Genetics* 29:3296–3311. doi: 10.1093/hmg/ddaa214.

Grasso, Debora, Luca X. Zampieri, Tânia Capelôa, Justine A. Van De Velde, and Pierre Sonveaux. 2020. 'Mitochondria in Cancer'. *Cell Stress* 4(6):114–46. doi: 10.15698/cst2020.06.221.

Guarás, Adela, Ester Perales-Clemente, Enrique Calvo, Rebeca Acín-Pérez, Marta Loureiro-Lopez, Claire Pujol, Isabel Martínez-Carrascoso, et al. 2016. 'The CoQH2/CoQ Ratio Serves as a Sensor of Respiratory Chain Efficiency'. *Cell Reports* 15:197–209. doi: 10.1016/j.celrep.2016.03.009.

Guerra-Librero, Ana, Beatriz I. Fernandez-Gil, Javier Florido, Laura Martinez-Ruiz, César Rodríguez-Santana, Ying Qiang Shen, José M. García-Verdugo, et al. 2021. 'Melatonin Targets Metabolism in Head and Neck Cancer Cells by Regulating Mitochondrial Structure and Function'. *Antioxidants* 10:1–20. doi: 10.3390/antiox10040603.

Guo, Lishu. 2021. 'Mitochondria and the Permeability Transition Pore in Cancer Metabolic Reprogramming'. *Biochemical Pharmacology* 188:114537. doi: 10.1016/j.bcp.2021.114537.

Hacışevki, Aysun, and Burcu Baba. 2018. 'An Overview of Melatonin as an Antioxidant Molecule: A Biochemical Approach'. *Molecular Biology, Clinical and Pharmaceutical Approaches*. Doi: 10.5772/intechopen.79421

Hardeland, R. 2008. 'Melatonin, Hormone of Darkness and More - Occurrence, Control Mechanisms, Actions and Bioactive Metabolites'. *Cellular and Molecular Life Sciences* 65(13):2001–18. doi: 10.1007/s00018-008-8001-x.

He, Mindi, Chao Zhou, Yonghui Lu, Ling Mao, Yu Xi, Xiang Mei, Xue Wang, Lei Zhang, Zhengping Yu, and Zhou Zhou. 2020. 'Melatonin Antagonizes Nickel-Induced Aerobic Glycolysis by Blocking ROS-Mediated HIF-1 α /MiR210/ISCU Axis Activation'. *Oxidative Medicine and Cellular Longevity* 2020:1–14. doi: 10.1155/2020/5406284.

Hevia, David, Pedro González-Menéndez, Isabel Quiros-González, Ana Miar, Aida Rodríguez-García, Dun Xian Tan, Russel J. Reiter, et al. 2015. 'Melatonin Uptake through Glucose Transporters: A New Target for Melatonin Inhibition of Cancer'. *Journal of Pineal Research* 58(2):234–50. doi: 10.1111/jpi.12210.

Hidalgo-Gutiérrez, Agustín, Eliana Barriocanal-Casado, Mohammed Bakkali, M. Elena Díaz-Casado, Laura Sánchez-Maldonado, Miguel Romero, Ramy K. Sayed, et al. 2019. 'B- RA Reduces DMQ /CoQ Ratio and Rescues the Encephalopathic Phenotype in

Coq9 R239X Mice'. *EMBO Molecular Medicine* 11:1–18. doi: 10.15252/emmm.201809466.

Hidalgo-Gutiérrez, Agustín, Eliana Barriocanal-Casado, María Elena Díaz-Casado, Pilar González-García, Riccardo Zenezini Chiozzi, Darío Acuña-Castroviejo, and Luis Carlos López. 2021. 'β-RA Targets Mitochondrial Metabolism and Adipogenesis, Leading to Therapeutic Benefits against CoQ Deficiency and Age-Related Overweight'. *Biomedicines* 9(10). doi: 10.3390/biomedicines9101457.

Jha, Pooja, Xu Wang, and Johan Auwerx. 2016. 'Analysis of Mitochondrial Respiratory Chain Supercomplexes Using Blue Native Polyacrylamide Gel Electrophoresis (BN-PAGE)'. *Current Protocols in Mouse Biology* 6(1):1–14. doi: 10.1002/9780470942390.mo150182.

Jia, Jia, Zichuang Wang, Minjie Zhang, Caiyun Huang, Yanmei Song, Fuyou Xu, Jingyu Zhang, Jie Li, et al. 2020. 'SQR Mediates Therapeutic Effects of H2S by Targeting Mitochondrial Electron Transport to Induce Mitochondrial Uncoupling'. *Science Advances* 6:eaaz5752. doi: 10.1126/sciadv.aaz5752.

Johns, Jeffrey R., and James A. Platts. 2014. 'Theoretical Insight into the Antioxidant Properties of Melatonin and Derivatives'. *Organic and Biomolecular Chemistry* 12(39):7820–27. doi: 10.1039/c4ob01396d.

Johnson, Daniel E., Barbara Burtness, C. René Leemans, Vivian Wai Yan Lui, Julie E. Bauman, and Jennifer R. Grandis. 2020. 'Head and Neck Squamous Cell Carcinoma'. *Nature Reviews Disease Primers* 6:92. doi: 10.1038/s41572-020-00224-3.

Juhaszova, Magdalena, Dmitry B. Zorov, Suhn-Hee Kim, Salvatore Pepe, Qin Fu, Kenneth W. Fishbein, Bruce D. Ziman, et al. 2004. 'Glycogen Synthase Kinase-3β Mediates Convergence of Protection Signaling to Inhibit the Mitochondrial Permeability Transition Pore'. *Journal of Clinical Investigation* 113(11):1535–49. doi: 10.1172/jci200419906.

Al Kadhi, Omar, Antonietta Melchini, Richard Mithen, and Shikha Saha. 2017. 'Development of a LC-MS/MS Method for the Simultaneous Detection of Tricarboxylic Acid Cycle Intermediates in a Range of Biological Matrices'. *Journal of Analytical Methods in Chemistry* 2017:1–12. doi: 10.1155/2017/5391832.

Lambert, Adrian J., and Martin D. Brand. 2004. 'Inhibitors of the Quinone-Binding Site Allow Rapid Superoxide Production from Mitochondrial NADH:Ubiquinone Oxidoreductase (Complex I)'. *Journal of Biological Chemistry* 279:39414–20. doi: 10.1074/jbc.M406576200.

Lee, Seonmin, Eunyoung Tak, Jisun Lee, Ma Rashid, Michael P. Murphy, Joohun Ha, and Sung Soo Kim. 2011. 'Mitochondrial H2 O2 Generated from Electron Transport

Chain Complex i Stimulates Muscle Differentiation'. *Cell Research* 21(5):817–34. doi: 10.1038/cr.2011.55.

Leemans, C. René, Boudewijn J. M. Braakhuis, and Ruud H. Brakenhoff. 2011. 'The Molecular Biology of Head and Neck Cancer'. *Nature Reviews Cancer* 11:9–22. doi: 10.1038/nrc2982.

Li, Hui, and Ze Hui Hong. 2012. 'Mitochondrial DNA Mutations in Human Tumor Cells (Review)'. *Oncology Letters* 4(5):868–72. doi: 10.3892/ol.2012.874.

Liberti, Maria V, and Jason W. Locasale. 2016. 'The Warburg Effect: How Does It Benefit Cancer Cells? (Vol 41, Pg 211, 2016)'. *Trends in Biochemical Sciences* 41(3):211. doi: 10.1016/j.tibs.2015.12.001.

López, Ana, Francisco Ortiz, Carolina Doerrier, Carmen Venegas, Marisol Fernández-Ortiz, Paula Aranda, María E. Díaz-Casado, et al. 2017. 'Mitochondrial Impairment and Melatonin Protection in Parkinsonian Mice Do Not Depend of Inducible or Neuronal Nitric Oxide Synthases'. *PLoS ONE* 12:1–22. doi: 10.1371/journal.pone.0183090.

Lu, Jian-jun, Lingyi Fu, Zhipeng Tang, Changlin Zhang, Lijun Qin, Jingshu Wang, Zhenlong Yu, Dingbo Shi, et al. 2016. 'Melatonin Inhibits AP-2β/HTERT, NF-KB/COX-2 and Akt/ERK and Activates Caspase/Cyto C Signaling to Enhance the Antitumor Activity of Berberine in Lung Cancer Cells'. *Oncotarget* 7:2985–3001. doi: 10.18632/oncotarget.6407.

Maier, Patrick, Linda Hartmann, Frederik Wenz, and Carsten Herskind. 2016. 'Cellular Pathways in Response to Ionizing Radiation and Their Targetability for Tumor Radiosensitization'. *International Journal of Molecular Sciences* 17(1). doi: 10.3390/ijms17010102.

Mao, Chao, Xiaoguang Liu, Yilei Zhang, Guang Lei, Yuelong Yan, Hyemin Lee, Pranavi Koppula, et al. 2021. 'DHODH-Mediated Ferroptosis Defence Is a Targetable Vulnerability in Cancer'. *Nature* 593:586–90. doi: 10.1038/s41586-021-03539-7.

Mao, Lulu, Robert T. Dauchy, David E. Blask, Erin M. Dauchy, Lauren M. Slakey, Samantha Brimer, Lin Yuan, et al. 2016. 'Melatonin Suppression of Aerobic Glycolysis (Warburg Effect), Survival Signalling and Metastasis in Human Leiomyosarcoma'. *Journal of Pineal Research* 60(2):167–77. doi: 10.1111/jpi.12298.

Martín, Miguel, Manuel Macías, Germaine Escames, Josefa León, and Darío Acuña-Castroviejo. 2000. 'Melatonin but Not Vitamins C and E Maintains Glutathione Homeostasis in T-butyl Hydroperoxide-induced Mitochondrial Oxidative Stress'. *The FASEB Journal* 14:1677–79. doi: 10.1096/fj.99-0865fje.

Mihanfar, Ainaz, Bahman Yousefi, Saber Ghazizadeh Darband, Shirin Sadighparvar, Mojtaba Kaviani, and Maryam Majidinia. 2021.

'Melatonin Increases 5-Flurouracil-Mediated Apoptosis of Colorectal Cancer Cells through Enhancing Oxidative Stress and Downregulating Survivin and XIAP'. *BioImpacts* 11:253–61. doi: 10.34172/bi.2021.36.

Mills, Evanna L., Beth Kelly, Angela Logan, Ana S. H. Costa, Mukund Varma, Clare E. Bryant, Panagiotis Tourlomousis, et al. 2016. 'Repurposing Mitochondria from ATP Production to ROS Generation Drives a Pro-Inflammatory Phenotype in Macrophages That Depends on Succinate Oxidation by Complex II'. *Cell* 167:457-470.e13. doi: 10.1016/j.cell.2016.08.064.Repurposing.

Mody, Mayur D., James W. Rocco, Sue S. Yom, Robert I. Haddad, and Nabil F. Saba. 2021. 'Head and Neck Cancer'. *The Lancet* 398(10318):2289–99. doi: 10.1016/S0140-6736(21)01550-6.

Moreira, Andrea Janz, Raquel Ordoñez, Carlos Thadeu Cerski, Jaqueline Nascimento Picada, Andrés García-Palomo, Norma Possa Marroni, Jose L. Mauriz, et al. 2015. 'Melatonin Activates Endoplasmic Reticulum Stress and Apoptosis in Rats with Diethylnitrosamine-Induced Hepatocarcinogenesis'. *PLoS ONE* 10:e0144517. doi: 10.1371/journal.pone.0144517.

Mortezaee, Keywan, Masoud Najafi, Bagher Farhood, Amirhossein Ahmadi, Yaiza Potes, Dheyauldeen Shabeeb, and Ahmed Eleojo Musa. 2019. 'Modulation of Apoptosis by Melatonin for Improving Cancer Treatment Efficiency: An Updated Review'. *Life Sciences* 228(March):228–41. doi: 10.1016/j.lfs.2019.05.009.

Mortezaee, Keywan, Yaiza Potes, Hanifeh Mirtavoos-Mahyari, Elahe Motevaseli, Dheyauldeen Shabeeb, Ahmed Eleojo Musa, Masoud Najafi, and Bagher Farhood. 2019. 'Boosting Immune System against Cancer by Melatonin: A Mechanistic Viewpoint'. *Life Sciences* 238:116960. doi: 10.1016/j.lfs.2019.116960.

Murphy, Michael P. 2009. 'How Mitochondria Produce Reactive Oxygen Species'. *Biochemical Journal* 417:1–13. doi: 10.1042/BJ20081386.

Nogueira, Veronique, Youngkyu Park, Chia-Chen Chen, Pei-Zhang Xu, Mei-Ling Chen, Ivana Tonic, Terry Unterman, and Nissim Hay. 2008. 'Akt Determines Replicative Senescence and Oxidative or Oncogenic Premature Senescence and Sensitizes Cells to Oxidative Apoptosis'. *Cancer Cell* 14:458–70. doi: 10.1016/j.ccr.2008.11.003.

Onukwufor, John O., Brandon J. Berry, and Andrew P. Wojtovich. 2019. 'Physiologic Implications of Reactive Oxygen Species Production by Mitochondrial Complex I Reverse Electron Transport'. *Antioxidants* 8:20–24. doi: 10.3390/antiox8080285.

Ortiz, Francisco, Darío Acuña-castroviejo, Carolina Doerrier, José C. Dayoub, L. C. López, Carmen Venegas, José Antonio García, et al. 2015. 'Melatonin Blunts the

Mitochondrial / NLRP3 Connection and Protects against Radiation-Induced Oral Mucositis'. *J. Pineal Res.* 58:34–49. doi: 10.1111/jpi.12191.

Pai, S. I., and W. H. Westra. 2009. 'Moleccular Pathology of Head and Neck Cancer: Implications for Diagnosis, Prognosis and Treatment'. *Annu. Rev. Pathol.* 4:49–70. doi: 10.1146/annurev.pathol.4.110807.092158.Molecular.

Perdomo, Juan, Carlos Quintana, Ignacio González, Inmaculada Hernández, Sara Rubio, Juan F. Loro, Russel J. Reiter, et al. 2020. 'Melatonin Induces Melanogenesis in Human SK-MEL-1 Melanoma Cells Involving Glycogen Synthase Kinase-3 and Reactive Oxygen Species'. *International Journal of Molecular Sciences* 21:1–16. doi: 10.3390/ijms21144970.

Pezzuto, Francesca, Luigi Buonaguro, Francesco Caponigro, Franco Ionna, Noemy Starita, Clorinda Annunziata, Franco M. Buonaguro, et al. 2015. 'Update on Head and Neck Cancer: Current Knowledge on Epidemiology, Risk Factors, Molecular Features and Novel Therapies'. *Oncology* 89(3):125–36. doi: 10.1159/000381717.

Pisani, Paolo, Mario Airoldi, Anastasia Allais, Paolo Aluffi Valletti, Mariapina Battista, Marco Benazzo, Roberto Briatore, et al. 2020. 'Metastatic Disease in Head & Neck Oncology'. *Acta Otorhinolaryngologica Italica* 40:S1–86. doi: 10.14639/0392-100X-suppl.1-40-2020.

Proietti, Sara, Alessandra Cucina, Mirko Minini, and Mariano Bizzarri. 2017. 'Melatonin, Mitochondria, and the Cancer Cell'. *Cellular and Molecular Life Sciences* 74(21):4015–25. doi: 10.1007/s00018-017-2612-z.

Prystowsky, Michael B. 2015. 'Emerging Concepts in Head and Neck Squamous Cell Carcinoma'. *Archives of Pathology and Laboratory Medicine* 139:1332–33. doi: 10.5858/arpa.2015-0269-ED.

Puram, Sidharth V., and Neil Bhattacharyya. 2016. 'Quality Indicators for Head and Neck Oncologic Surgery: Academic versus Nonacademic Outcomes'. *Otolaryngology - Head and Neck Surgery (United States)* 155(5):733–39. doi: 10.1177/0194599816654689.

Radogna, Flavia, P. Sestili, C. Martinelli, M. Paolillo, L. Paternoster, M. C. Albertini, A. Accorsi, et al. 2009. 'Lipoxygenase-Mediated pro-Radical Effect of Melatonin via Stimulation of Arachidonic Acid Metabolism'. *Toxicology and Applied Pharmacology* 238:170–77. doi: 10.1016/j.taap.2009.05.011.

Radogna, Flavia, Laura Paternoster, Milena de Nicola, Claudia Cerella, Sergio Ammendola, Annalida Bedini, Giorgio Tarzia, et al. 2009. 'Rapid and Transient Stimulation of Intracellular Reactive Oxygen Species by Melatonin in Normal and Tumor Leukocytes'. *Toxicology and Applied Pharmacology* 239:37–45. doi: 10.1016/j.taap.2009.05.012.

Raha, Sandeep, and Brian H. Robinson. 2000. 'Mitochondria, Oxygen Free Radicals, Disease and Ageing'. *Trends in Biochemical Sciences* 25:502–8. doi: 10.1016/S0968-0004(00)01674-1.

Reppert, Steven M., David R. Weaver, and Takashi Ebisawa. 1994. 'Cloning and Characterization of a Mammalian Melatonin Receptor That Mediates Reproductive and Circadian Responses'. *Neuron* 13:1177–85. doi: 10.1016/0896-6273(94)90055-8.

Robb, Ellen L., Andrew R. Hall, Tracy A. Prime, Simon Eaton, Marten Szibor, Carlo Viscomi, Andrew M. James, and Michael P. Murphy. 2018. 'Control of Mitochondrial Superoxide Production by Reverse Electron Transport at Complex I'. *Journal of Biological Chemistry* 293:9869–79. doi: 10.1002/ajmg.1398.

Rosenberg, Ari J., and Everett E. Vokes. 2021. 'Optimizing Treatment De-Escalation in Head and Neck Cancer: Current and Future Perspectives'. *The Oncologist* 26(1):40–48. Doi: 10.1634/theoncologist.2020-0303.

Sabharwal, Simran S., and Paul T. Schumacker. 2014. 'Mitochondrial ROS in Cancer: Initiators, Amplifiers or an Achilles' Heel?' *Nature Reviews Cancer* 14:709–21. doi: 10.1038/nrc3803.

Scialò, Filippo, Daniel J. Fernández-Ayala, and Alberto Sanz. 2017. 'Role of Mitochondrial Reverse Electron Transport in ROS Signaling: Potential Roles in Health and Disease'. *Frontiers in Physiology* 8:1–7. doi: 10.3389/fphys.2017.00428.

Shen, Ying Qiang, Ana Guerra-Librero, Beatriz I. Fernandez-Gil, Javier Florido, Sergio García-López, Laura Martinez-Ruiz, Miguel Mendivil-Perez, et al. 2018. 'Combination of Melatonin and Rapamycin for Head and Neck Cancer Therapy: Suppression of AKT/MTOR Pathway Activation, and Activation of Mitophagy and Apoptosis via Mitochondrial Function Regulation'. *Journal of Pineal Research* 64:1–18. doi: 10.1111/jpi.12461.

Srinivas, Upadhyayula Sai, Bryce W. Q. Tan, Balamurugan A. Vellayappan, and Anand D. Jeyasekharan. 2019. 'ROS and the DNA Damage Response in Cancer'. *Redox Biology* 25:101084. doi: 10.1016/j.redox.2018.101084

Srinivasan, Venkataramanujan, D. Warren Spence, Seithikurippu R. Pandi-Perumal, Ilya Trakht, and Daniel P. Cardinali. 2008. 'Therapeutic Actions of Melatonin in Cancer: Possible Mechanisms'. *Integrative Cancer Therapies* 7(3):189–203. doi: 10.1177/1534735408322846.

Su, Shih Chi, Ming Ju Hsieh, Wei En Yang, Wen Hung Chung, Russel J. Reiter, and Shun Fa Yang. 2017. 'Cancer Metastasis: Mechanisms of Inhibition by Melatonin'. *Journal of Pineal Research* 62(1):1–11. doi: 10.1111/jpi.12370.

Sullivan, Lucas B., and Navdeep S; Chandel. 2014. 'Mitochondrial

Reactive Oxygen Species and Cancer'. *Cancer & Metabolism* 2:17. doi: 10.1186/2049-3002-2-17.

Sun, Tie Cheng, Xiao Chao Liu, Song He Yang, Ling Li Song, Shan Jie Zhou, Shou Long Deng, Li Tian, et al. 2020. 'Melatonin Inhibits Oxidative Stress and Apoptosis in Cryopreserved Ovarian Tissues via Nrf2/HO-1 Signaling Pathway'. *Frontiers in Molecular Biosciences* 7:1–11. doi: 10.3389/fmolb.2020.00163.

Suofu, Yalikun, Wei Li, Frédéric G. Jean-Alphonse, Jiaoying Jia, Nicolas K. Khattar, Jiatong Li, Sergei V. et al. 2017. 'Dual Role of Mitochondria in Producing Melatonin and Driving GPCR Signaling to Block Cytochrome c Release'. *Proceedings of the National Academy of Sciences of the United States of America* 114(38):E7997–8006. doi: 10.1073/pnas.1705768114.

Szatrowski, Ted P., and Carl F. Nathan. 1991. 'Production of Large Amounts of Hydrogen Peroxide by Human Tumor Cells'. *Cancer Research* 51:794–98.

Talib, Wamidh H. 2018. 'Melatonin and Cancer Hallmarks'. *Molecules* 23(3). doi: 10.3390/molecules23030518.

Talib, Wamidh H., Ahmad Riyad Alsayed, Alaa Abuawad, Safa Daoud, and Asma Ismail Mahmod. 2021. 'Melatonin in Cancer Treatment: Current Knowledge and Future Opportunities'. *Molecules* 26(9):2506. doi: 10.3390/molecules26092506.

Tan, Dun-Xian, Lucien Manchester, Eduardo Esteban-Zubero, Zhou Zhou, and Russel Reiter. 2015. 'Melatonin as a Potent and Inducible Endogenous Antioxidant: Synthesis and Metabolism'. *Molecules* 20(10):18886–906. doi: 10.3390/molecules201018886.

Tanida, Satoshi, Tsutomu Mizoshita, Keiji Ozeki, Hironobu Tsukamoto, Takeshi Kamiya, Hiromi Kataoka, Daitoku Sakamuro, and Takashi Joh. 2012. 'Mechanisms of Cisplatin-Induced Apoptosis and of Cisplatin Sensitivity: Potential of BIN1 to Act as a Potent Predictor of Cisplatin Sensitivity in Gastric Cancer Treatment'. *International Journal of Surgical Oncology* 2012. doi: 10.1155/2012/862879.

Tordjman, Sylvie, Sylvie Chokron, Richard Delorme, Annaelle Charrier, Eric Bellissant, Nemat Jaafari, and Claire Fougerou. 2017. 'Melatonin: Pharmacology, Functions and Therapeutic Benefits'. *Current Neuropharmacology* 15:434–43. doi: 10.2174/1570159x14666161228122115.

Vacek, Thomas P., Jonathan C. Vacek, and Suresh C. Tyagi. 2012. 'Mitochondrial Mitophagic Mechanisms of Myocardial Matrix Metabolism and Remodelling'. *Archives of Physiology and Biochemistry* 118(1):31–42. doi: 10.3109/13813455.2011.635660.

Vaupel, Peter, and Gabriele Multhoff. 2021. 'Revisiting the Warburg Effect: Historical Dogma versus

Current Understanding'. *Journal of Physiology* 599(6):1745–57. doi: 10.1113/JP278810.

Vaupel, Peter, Heinz Schmidberger, and Arnulf Mayer. 2019. 'The Warburg Effect: Essential Part of Metabolic Reprogramming and Central Contributor to Cancer Progression'. *International Journal of Radiation Biology* 95(7):912–19. doi: 10.1080/09553002.2019.1589653.

Venegas, Carmen, Jose A. García, Carolina Doerrier, Huayqui Volt, Germaine Escames, Luis C. López, Russel J. Reiter, et al. 2013. 'Analysis of the Daily Changes of Melatonin Receptors in the Rat Liver'. *Journal of Pineal Research* 54:313–21. doi: 10.1111/jpi.12019.

Vriend, Jerry, and Russel J. Reiter. 2016. 'Melatonin and the von Hippel-Lindau/HIF-1 Oxygen Sensing Mechanism: A Review'. *Biochimica et Biophysica Acta - Reviews on Cancer* 1865:176–83. doi: 10.1016/j.bbcan.2016.02.004.

Wallace, Douglas C. 2012. 'Mitochondria and Cancer Douglas'. *Nat Rev, Cancer* 12:685–98. doi: 10.1038/nrc3365.Mitochondria.

Wang, Hao, Xiaoyu Mu, Hua He, and Xiao Dong Zhang. 2018. 'Cancer Radiosensitizers'. *Trends in Pharmacological Sciences* 39(1):24–48. doi: 10.1016/j.tips.2017.11.003.

Wölfler, Albert, Hans Christian Caluba, Peter M. Abuja, Gottfried Dohr, Konrad Schauenstein, and Peter M. Liebmann. 2001. 'Prooxidant Activity of Melatonin Promotes Fas-Induced Cell Death in Human Leukemic Jurkat Cells'. *FEBS Letters* 502:127–31. doi: 10.1016/S0014-5793(01)02680-1.

Xu, Yibin, Ding Xue, Armand Bankhead, and Nouri Neamati. 2020. 'Why All the Fuss about Oxidative Phosphorylation (OXPHOS)?' *Journal of Medicinal Chemistry* 63:14276–307. doi: 10.1021/acs.jmedchem.0c01013.

Yang, Ling, Jianchao Zheng, Rui Xu, Yujie Zhang, Luo Gu, Jing Dong, Yichao Zhu, et al. 2014. 'Melatonin Suppresses Hypoxia-Induced Migration of HUVECs via Inhibition of ERK/Rac1 Activation'. *International Journal of Molecular Sciences* 15:14102–21. doi: 10.3390/ijms150814102.

Yang, Yuhui, Svetlana Karakhanova, Werner Hartwig, Jan G. D'Haese, Pavel P. Philippov, Jens Werner, and Alexandr v. Bazhin. 2016. 'Mitochondria and Mitochondrial ROS in Cancer: Novel Targets for Anticancer Therapy'. *Journal of Cellular Physiology* 231(12):2570–81. doi: 10.1002/jcp.25349.

Zong, Wei-Xing, Joshua D. Rabinowitz, and Eileen White. 2016. 'Mitochondria and Cancer'. *Molecular Cell* 61:667–76. doi: 10.1016/j.molcel.2016.02.011.

Zorov, Dmitry B., Magdalena Juhaszova, and Steven J. Sollott. 2014. 'Mitochondrial Reactive Oxygen Species (ROS) and ROS-Induced ROS Release'. *Physiological Reviews* 94:909–50. doi: 10.1152/physrev.00026.2013.